Zenithal Dependence of the Penetrating Component of Cosmic Radiation.

I. F. QUERCIA and B. RISPOLI

Istituto di Fisica dell'Università - Roma
Istituto Nazionale di Fisica Nucleare - Sezione di Roma

(ricevuto il 10 Gennaio 1953)

Summary (*). — Two experiments are reported, one performed at Cervinia (3 500 m a.s.l.) and one performed at Rome, on the zenithal distribution of penetrating particles and mesons. It is found that the penetrating component at sea level can be represented by the law $I(\theta) = I_0 \cos^n \theta$ with $n = 2.14$ for $E = 500$ MeV whereas at 3 500 m a.s.l. the distribution does not obey this law. At sea level, moreover, the mesonic component with energy between 0.5 an 1.9 GeV follows very closely the law $\cos^{3.06} \theta$.

(*) *Editor's translation.*

1. – Introduction.

Several measurements of the intensity of the penetrating component at sea level have been made in the past. One of the most complete and accurate determinations of zenithal dependence of cosmic radiation at several altitudes was made by GREISEN [1] who found that the zenithal dependence could be expressed by the equation

$$I(\theta) = I_0 \cos^n \theta \, ,$$

[1] K. GREISEN: *Phys. Rev.*, **61**, 212 (1942).

where I_0 is the vertical intensity, θ the zenith angle and n is a constant determined from the experiment; for « penetrating component » (300 MeV for mesons) n was found to be 2.1 while for « total radiation » Greisen found $n = 2.3$ at sea level.

Notwithstanding these accurate measurements some doubts remain on this question. In the past everybody has assumed the penetrating component of cosmic rays to be completely composed of μ-mesons; at the same time several authors defined penetrating particles as the particles with a range greater than 10 or 15 cm of lead while we know that several electrons have penetrations greater than 10 cm of lead.

Probably the greatest source of error is in the assumption that all penetrating particles are mesons. Many authors [2] have shown that at high altitude protons are present together with mesons, although the intensity of protons at sea level, and at mountain altitudes is not yet known.

Recently KRAUSHAAR [3] and ZAR [4] found that zenithal spectrum depends on the type of technique used for the measurement; the exponent n was found by KRAUSHAAR with a coincidence technique to be 2.09 for mesons of momentum greater than 200 MeV/c or for other particles of the same range; with an anticoincidence technique he found n equal to 3.3 for particles with momentum between 200 and 330 MeV/c and he found the same value with delayed coincidences *selecting only mesons* with momentum between 25 and 170 MeV/c. ZAR with similar technique found that n is of the order of 2 in coincidence measurements and of the order of 3 in delayed coincidence or anticoincidence measurements. He found that his results are consistent with the hypothesis that the exponent for zenith angle distribution decreases as the meson energy increases, but statistical errors and also the fact that only two angles were investigated make a satisfactory conclusion impossible.

Moreover VOISIN [5] with a delayed coincidence experiment found an exponent $n = 3.0$ for mesons of momentum between 300 an 510 MeV/c at 30° zenithal angle; on increasing the zenithal angle, however, n decreases (2.26 $\pm$ 0.07 at 60°, 1.71 $\pm$ 0.06 at 80° for mesons of momentum between 300 and 410 and 2.59 $\pm$ 0.08 at 60°, 2.11 $\pm$ 0.06 at 80° between 410 and 510 MeV/c). According to Voisin's experiment zenithal distribution can be expressed by equation:

$$I(\theta) = I_0(1 - a \sin^b \theta) \, ,$$

(2) M. CONVERSI: *Phys. Rev.*, **76**, 444, 849, 851 (1949); T. C. MERKLE, E. L. GOLDWASSER and R. B. BRODE: *Phys. Rev.*, **79**, 926 (1950); E. L. GOLDWASSER and T. C. MERKLE: *Phys. Rev.*, **83**, 43 (1951).

(3) W. L. KRAUSHAAR: *Phys. Rev.*, **76**, 1045 (1949).

(4) J. L. ZAR: *Phys. Rev.*, **83**, 761 (1951).

(5) A. G. VOISIN: *Phys. Rev.*, **84**, 850 (1951).

where $a \simeq 1$ and $b = 1.47 \pm 0.12$ in the momentum range 300-410 MeV/c and $b = 1.61 \pm 0.15$ in the momentum range 410-510 MeV/c.

In addition it has been found recently in photographic plate work ([6]) that the zenithal distribution of mesons of energy greater than 40 MeV at 2 000 m above sea level can be roughly expressed by the law: $\cos^{3.5}\theta$.

For the reasons previously explained we think it is of some interest to compare the results of our measurements performed at « Laboratorio della Testa Grigia » (L.T.G., Cervinia, 3 500 m above sea level, 40° 50′ North geographical latitude) in 1951, with those performed in Rome in 1952.

2. – Apparatus.

The apparatus used at L.T.G. consisted of two winding magnetic circuits, one placed over the other, in which by means of a direct current, it was possible to create a magnetic field. A telescope of three 4×50 cm² counters A, B, C defines a solid angle through the two magnetic circuits as shown in fig. 1. Anticoincidence counters prevent spurious counts due to lateral showers. The apparatus could rotate about an horizontal axis. This apparatus has been used for positive excess measurements ([7]) but we shall now refer to data collected for the total component (positive + negative) in the vertical direction, at 45°, 60° both in the North-South and in the East-West planes.

Fig. 1.

The total thickness of iron was 40 cm which corresponds to about 500 MeV for mesons, but three-fold coincidences (ABC) recorded also other penetrating particles such as protons; *we will refer to the total radiation penetrating* 40 cm *of iron as* « T ».

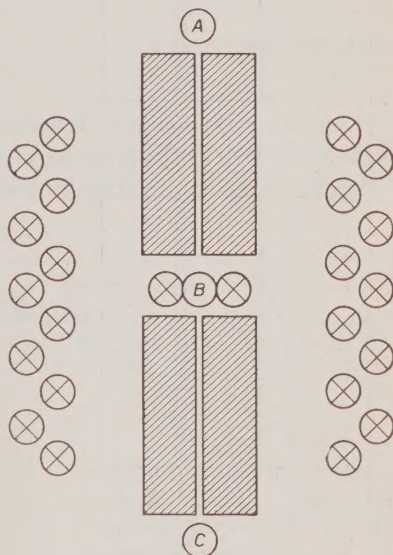With the experiment in Rome the geometry of the counters was changed and

---

([6]) G. BARONI, G. CORTINI, A. MILONE, L. SCARSI and G. VANDERHAEGHE: *Nuovo Cimento*, **9**, 867 (1952).

([7]) I. F. QUERCIA, B. RISPOLI and S. SCIUTI: *Nuovo Cimento*, **7**, 899 (1950).
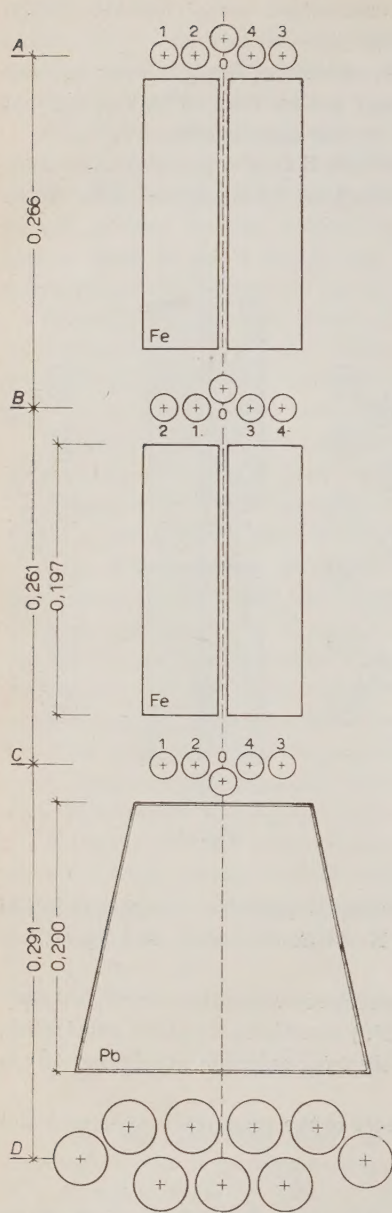
Fig. 2.

in addition a set of counters D was placed under 20 cm lead (fig. 2). The « central counters » $A_0A_2A_4$; $B_0B_1B_3$; $C_0C_2C_4$ were connected to a three-fold coincidence circuit « T_3 » and a four-fold coincidence « T_4 » was formed with counters D. An electronic device was so arranged that no counts were recorded if more than one counter of each set A, B, C was discharged. The cut off energy for « T_3 » results of 500 MeV and for « T_4 » of 800 MeV for me-sons. Moreover three-fold coincidences $(A_1B_1C_1)$; $(A_2B_2C_2)$; $(A_3B_3C_3)$; $(A_4B_4C_4)$ are mixed together and recorded as « M_3 ». « M_3 » in coincidence with the set of D counters (^{8}) is recorded as « M_4 ». It should be noted that M-coin-cidences refer only to mesons because protons of the same range have a mi-nimum energy of 1.8 GeV, so that the magnetic field is inefficient to curve their paths. For this reason we refer to these counts as « M », or meson-component.

3. – Experimental Results.

In table I we report the ratios $T(\theta)/T(0^\circ)$ as function of zenithal angle in East-West plane at L.T.G. and at Rome (^{9}). These data have been obtained by averaging the results obtained in the eastern and the western directions.

(^{8}) A more detailed description of ap-paratus will be given elsewhere.

(^{9}) It must be noted that the ratio $T(\theta)/T(0^\circ)$ is a quite good approximation for the ratio between the corresponding absolute intensities. The error involved is of the order of 0.4%.

TABLE I. – *Relative intensity of total penetrating component in East-West plane* $(T(\theta)/T_0)$.

Altitude m a.s.l.	Energy (MeV) range for mesons		15°	30°	45°	60°
50	« T_3 »	> 500	0.915 ± 0.008	0.716 ± 0.007	0.502 ± 0.004	0.227 ± 0.002
	« T_4 »	> 800	0.892 ± 0.008	0.708 ± 0.007	0.510 ± 0.003	0.241 ± 0.002
	« $T_3 - T_4$ »	$500 < E \leqslant 800$	1.050 ± 0.020	0.771 ± 0.015	0.423 ± 0.009	0.133 ± 0.003
3500	« T_3 »	> 500	—	—	0.541 ± 0.003	0.209 ± 0.001

Data of table I and fig. 3 show that integral zenithal spectra at sea level for particles which have range greater than 40 cm Fe (500 MeV for mesons) and for particles whose range is greater than 40 cm Fe + 20 cm Pb (800 MeV for mesons) are in a very good agreement with the law:

$$I(\theta) = I_0 \cos^n \theta ,$$

where n is found to be 2.14 for the former case and 2.09 for the latter case.

On the contrary the differential spectrum of particles whose range is equal to that of mesons lying between 500 and 800 MeV at the sea level and the integral spectrum at 3500 m are not in agreement with a $\cos^n \theta$ law, as one can see from fig. 3 where as abscissa we

Fig. 3.

× T_3 at s. l.
+ $T_3 - T_4$ at s. l.
⊙ T_3 at 3500 m a. s. l.

have plotted log sec θ and as ordinate log $T(\theta)/T(0)$. Dotted lines represent $\cos^2 \theta$ and $\cos^3 \theta$. We can say that n is a function of zenithal angle and the average value is 2.40 for integral spectrum at 3500 m and 3.06 for differential component in Rome.

In table II and in fig. 4 we report the ratios $M(\theta)/M(0°)$ which refer only to mesons recorded in the East-West plane at sea level.

From fig. 4 one can see that the exponent n seems to decrease with increasing zenithal angle with an average value 2.55 (2.61 and 2.49 respectively for the two ranges of energy).
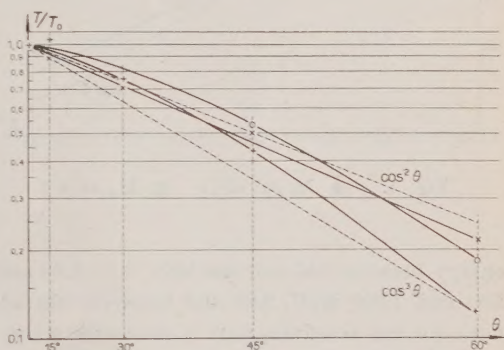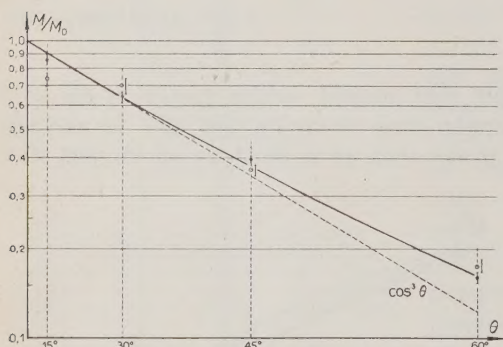
TABLE II. – *Intensity of meson component in East-West plane at sea level* $(M(\theta)/M_0)$.

	Energy range	15°	30°	45°	60°
« M_3 »	$500 < E < 1\,900$	0.77 ± 0.02	0.58 ± 0.02	0.365 ± 0.012	0.163 ± 0.006
« M_4 »	$800 < E < 1\,900$	0.740 ± 0.031	0.700 ± 0.030	0.377 ± 0.017	0.184 ± 0.008

In table III we report the results obtained in North-South plane; unfortunately the data collected are not so complete as the preceding ones, but they do not show any significant difference.

Fig. 4. – M_3 at s.l.; ⊙ M_4 at s. l.

Present results are in very good agreement with measurements of ZAR and KRAUSHAAR for the T component. For M component we have found an exponent n lower than theirs but if we interpret most of the T component stopped in 20 cm of lead as meson component we have for mesons with energy between 500 and 800 MeV, $n = 3.06$ and for mesons with energy between 500 and 1 900 MeV, 2.61 and between 800 and 1 900 MeV, 2.49. From these data we can conclude that n decreases when energy of mesons increases and so Kraushaar's value 3.3 for mesons with momentum between 25 and 170 MeV is not in disagreement with the present work. In a next work we shall attempt an interpretation of present data.

TABLE III.   *Intensity of T and M component as function of θ in North-South plane.*

	Altitude m a.s.l.	Energy (MeV) range for mesons	30°	45°	60°
$T(\theta)/T_0$	50	$\geqslant 500$	0.745 ± 0.007	0.522 ± 0.002	—
		$\geqslant 800$	0.736 ± 0.006	0.512 ± 0.003	—
		$500 \leqslant E \leqslant 800$	0.801 ± 0.015	0.477 ± 0.007	—
	3 500	$\geqslant 500$	—	0.551 ± 0.004	0.228 ± 0.002
	50	$500 < E < 1\,900$	0.641 ± 0.030	0.374 ± 0.010	—
		$800 < E < 1\,900$	0.602 ± 0.030	0.353 ± 0.010	—

RIASSUNTO

Vengono riportati due esperimenti, uno eseguito a Cervinia (3 500 m s.l.m.) ed uno a Roma sulla distribuzione zenitale delle particelle penetranti e dei mesoni. Si trova che la penetrante al livello del mare può essere rappresentata dalla legge $I(\theta) = I_0 \cos^n \theta$ con $n = 2{,}14$ per $E = 500$ MeV, mentre a 3 500 m la distribuzione non segue tale legge. Al livello del mare, inoltre, la componente mesonica con energia compresa fra 0,5 e 1,9 GeV ha un andamento assai prossimo a $\cos^{3,06} \theta$.

Sulla componente elettronica della radiazione cosmica nell'atmosfera derivante dal decadimento dei neutretti.

D. CADORIN

Istituto di Fisica dell'Università - Padova
Istituto Nazionale di Fisica Nucleare - Sezione di Padova

Riassunto. — Si calcola il contributo alla componente elettronica della radiazione cosmica generato, lungo l'atmosfera, dal decadimento del mesone π^0 in due fotoni, usando le equazioni di diffusione con una sorgente di fotoni il cui andamento in funzione dell'energia è stato desunto dai dati sperimentali del gruppo di Bristol, e la cui variazione con la quota è regolata da un cammino di assorbimento di 130 g·cm⁻². L'integrazione delle equazioni di diffusione si fa con un metodo di approssimazioni successive tenendo conto sia della perdita di energia per ionizzazione sia della variazione delle sezioni d'urto di produzione di coppie e di bremsstrahlung con l'energia. Si normalizza il risultato sullo spettro integrale della componente elettronica totale quale risulta dai più recenti risultati sperimentali e si determina il rapporto dei mesoni neutri a quelli carichi ottenendo $\pi^0/\pi^{\pm} = 0,53$. Dal confronto dei valori assoluti così ottenuti con quelli forniti dal gruppo di Bristol, si conclude con la compatibilità dei due dati entro i limiti delle notevoli incertezze relative alla conoscenza di alcuni processi necessaria a detto confronto.

1. – Introduzione.

È noto che per rendere conto della componente elettronica totale della radiazione cosmica nell'atmosfera, occorre postulare la esistenza, oltre a quella degli elettroni di knock-on e di decadimento delle particelle μ, anche di un'altra sorgente [1] che, con la scoperta della disintegrazione del mesone π^0, è stata individuata nello spettro dei fotoni che da esso derivano.

---

[1] B. Rossi: *Phys. Rev.*, **61**, 121 (1942).

Calcoli per verificare tale ipotesi sono stati fatti da BUDINI [2] e da CAL-DIROLA [3]. Entrambi questi Autori ottengono la sorgente di fotoni da considerazioni di ordine teorico sul meccanismo di produzione di mesoni neutri da parte di nucleoni primari, e nel calcolo della cascata elettrofotonica che deriva dai fotoni di disintegrazione dei π^0 introducono delle semplificazioni alquanto grossolane per le basse energie, dove adottano lo schema di ARLEY [4] che tien conto delle sole perdite di energia per ionizzazione ed assume per tutte le sezioni d'urto la loro forma asintotica, o le trascura per valori dell'energia minori di quella critica.

Col presente lavoro intendiamo riprendere tale calcolo considerando anzitutto la cascata elettrofotonica che nasce da una sorgente di fotoni di cui abbiamo desunto l'andamento dai dati sperimentali più attendibili; si evitano così tutte le ipotesi sui meccanismi di collisione dei nucleoni; inoltre si cerca di tenere conto in modo più accurato di tutti quei fattori che influenzano l'evolversi della cascata, sia non trascurando mai le perdite di energia per ionizzazione, sia prendendo in considerazione la variazione delle varie sezioni d'urto con l'energia.

2. – Sorgente di fotoni e sezioni d'urto.

Precisiamo qui i dati del nostro calcolo. Assumiamo per la sorgente di fotoni la forma

$$(1) \qquad \Sigma(W, t) = NS(W) \exp [\lambda_0 t] ,$$

dove N è una costante di normalizzazione, W l'energia dei fotoni misurata in GeV, $S(W)$ lo spettro energetico che è stato desunto dai dati sperimentali ottenuti mediante lastre nucleari dal gruppo di Bristol [5] e così approssimato:

$$S(W) = \begin{cases} W^{-2,8} & \text{per } W \geqslant 1 \text{ GeV} , \\ W^{-1,9} & 0,2 \leqslant W \leqslant 1 , \\ 4,26 \ W^{-1} & 0,075 \leqslant W \leqslant 0,2 , \\ 1,65 \cdot 10^3 \ W^{1,3} & 0,01 \leqslant W \leqslant 0,075 . \end{cases}$$

L'andamento di $S(W)$ per $W \geqslant 1$ GeV, che non è dato nel lavoro sopra citato, è stato uniformato su quello della sorgente dei mesoni π carichi che

[2] P. BUDINI: *Nuovo Cimento*, 7, 868 (1950).
[3] P. CALDIROLA e P. GULMANELLI: *Nuovo Cimento*, 8, 229 (1951).
[4] N. ARLEY: *Proc. Phys. Soc.*, A 168, 519 (1938).
[5] A. G. CARLSON, I. E. HOOPER e D. T. KING: *Phil. Mag.*, 41, 701 (1950).

deriva dai dati di SANDS corretti alle alte energie in base all'andamento dello spettro delle particelle μ sottoterra.

Infine l'andamento con la quota, rappresentato dall'esponenziale nella (1), è stato scelto assumendo un cammino di assorbimento di 130 g·cm⁻² pari a quello della componente nucleonica di media energia, tra 1 e 10 GeV [6], ($\lambda_0 = -0,33$); t è misurato in unità di radiazione che in aria risulta di 43 g·cm⁻².

Per comodità, nei calcoli che seguiranno abbiamo posto:

$$(1')\quad \begin{cases} S_0(W) = S(W) & \text{per}\quad W \geqslant 1 \text{ GeV}, \\ S_1(W) = S(W) & \text{per}\quad W \geqslant 0,2, \\ S_2(W) = S(W) & \text{per}\quad W \geqslant 0,075, \\ S_3(W) = S(W) & \text{per}\quad W \geqslant 0,01. \end{cases}$$

Le varie sezioni d'urto per unità di radiazione, per le quali abbiamo usato le notazioni di ROSSI e GREISEN [7], sono state approssimate nel seguente modo: sezione d'urto differenziale di bremsstrahlung

$$(2)\quad \varphi(U, W)\frac{\mathrm{d}W}{U} = \begin{cases} \varphi_0\left(\dfrac{W}{U}\right)\dfrac{\mathrm{d}W}{U} = \left[h\,\dfrac{U}{W} - h + \dfrac{W}{U}\right]\dfrac{\mathrm{d}W}{U} & \text{per}\quad U \geqslant 0,2 \text{ GeV}, \\[3mm] \chi\left(U, \dfrac{W}{U}\right)\dfrac{\mathrm{d}W}{U} = \left[h\,\dfrac{U}{W} - h + f\left(\dfrac{U}{\mu_e}\right)\right]\dfrac{\mathrm{d}W}{U} & \text{per}\quad U < 0,2, \end{cases}$$

dove U è l'energia totale dell'elettrone misurata in GeV ed

$$f\left(\frac{U}{\mu_e}\right) = 0,2 \ln \frac{U}{\mu_e} - 0,6$$

è una funzione che abbiamo introdotto per tenere conto della variazione della sezione d'urto con l'energia dell'elettrone;

sezione d'urto differenziale di produzione di coppie

$$(3)\quad \psi(W, U)\frac{\mathrm{d}U}{W} = \begin{cases} \psi_0\left(\dfrac{U}{W}\right)\dfrac{\mathrm{d}U}{W} = \left[h\left(\dfrac{U}{W}\right)^2 - h\,\dfrac{U}{W} + 1\right]\dfrac{\mathrm{d}U}{W} & \text{per}\quad W \geqslant 0,2 \text{ GeV}, \\[3mm] \sigma(W)\dfrac{\mathrm{d}U}{W} = b\left(14 \ln \dfrac{2W}{\mu_e} - \dfrac{109}{3}\right)\dfrac{\mathrm{d}U}{W} & \text{per}\quad W < 0,2; \end{cases}$$

in entrambi i casi $b = 0,012$ ed $h = 4/3 + 2b = 1,357$.

---

[6] J. G. WILSON: *Progress in Cosmic Ray Physics* (Amsterdam, 1952), p. 317.
[7] B. ROSSI e K. GREISEN: *Rev. Mod. Phys.*, **13**, 240 (1941).

Abbiamo assunto costante. la perdita di energia per ionizzazione ed uguale a

$$\beta = 0,1 \text{ GeV per unità di radiazione .}$$

Per le sezioni d'urto totali di produzione di coppie e Compton, infine, dato che il minimo nel caso dell'aria non è molto profondo, abbiamo posto

$$\sigma_p \div \sigma_c = \sigma_0 = 0,773 .$$

Inoltre, poichè nel nostro calcolo avremo sempre a che fare con energie $\geqslant 0,01$ GeV, abbiamo trascurato l'energia

Fig. 1. - Confronto fra la espressione approssimata (– – –) della sezione d'urto differenziale di bremsstrahlung per unità di radiazione e l'espressione esatta (———).
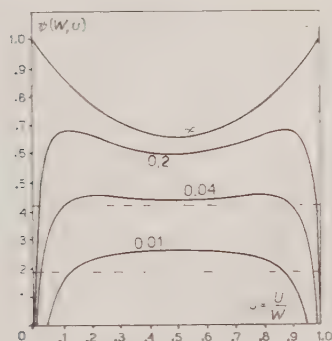

Fig. 2. – Confronto fra la espressione approssimata (– – –) della sezione d'urto differenziale di produzione di coppie per unità di radiazione e l'espressione esatta (———).
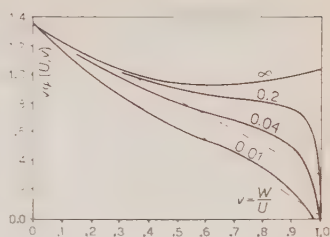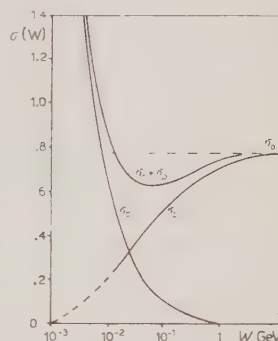

Fig. 3. – Sezioni d'urto totale di produzione di coppie e Compton per unità di radiazione.

μ_c di riposo dell'elettrone rispetto a quella cinetica E e cioè abbiamo posto $U \cong E$.

Il confronto fra le effettive sezioni d'urto e quelle semplificate che abbiamo adottato risulta dalle fig. 1, 2, 3.

3. – Equazioni di diffusione.

Indicando con $\pi(E, t) \, dE \, dt$ e $\gamma(W, t) \, dW \, dt$ rispettivamente gli spettri differenziali degli elettroni e dei fotoni, ed attenendoci alle precedenti notazioni

ed approssimazioni, le equazioni di diffusione si scrivono:

$$
(4) \quad \frac{\partial \pi(E, t)}{\partial t} = 2 \int_{E}^{\infty} \gamma(W, t)\,\psi(W, E)\,\frac{dW}{W} - \int_{0}^{E} \pi(E, t)\varphi(E, W)\,\frac{dW}{E} +
$$

$$
+ \int_{\lambda}^{\infty} \pi(E', t)\varphi(E', E'-E)\,\frac{dE'}{E'} + \beta\,\frac{\partial \pi(E, t)}{\partial E} ,
$$

$$
\frac{\partial \gamma(W, t)}{\partial t} = \int_{W}^{\infty} \pi(E, t)\varphi(E, W)\,\frac{dE}{E} - \sigma_0\gamma(W, t) + \Sigma(W, t) ,
$$

con le condizioni iniziali:

$$
(5) \qquad \pi(E, 0) = 0 , \qquad \gamma(W, 0) = 0 .
$$

Abbiamo integrato questo sistema per approssimazioni successive e precisamente abbiamo assunto per approssimazione zero e per $E, W \geqslant 1$ GeV, la soluzione della (4) con $\beta = 0$, che rappresenta il caso in cui le perdite di energia per ionizzazione sono trascurabili; gli spettri che così si ottengono sono gli stessi dati da BUDINI [3] per energie maggiori di quella critica degli elettroni in aria. Abbiamo ricavato l'approssimazione successiva considerando il sistema (4) per energie $E, W \geqslant 0,2$ GeV e risolvendo prima l'equazione in γ, ponendo al posto di π la approssimazione zero π_0; la prima approssimazione γ_1 così ottenuta si è quindi posta nell'equazione in π al posto della γ. In modo analogo abbiamo proceduto per le successive approssimazioni: la seconda per $E, W \geqslant 0,075$ GeV e la terza per $E, W \geqslant 0,01$ GeV, come si vedrà meglio nella descrizione più dettagliata seguente.

Approssimazione zero (valida per $E, W \geqslant 1$ GeV).

Ponendo nella (4) $\beta = 0$ si ottengono soluzioni del tipo

$$
(6) \qquad \begin{cases} \pi(E, t) = N p(t) S_0(E) , \\[2mm] \gamma_0(W, t) = N g(t) S_0(W) , \end{cases}
$$

con le funzioni $p(t)$ e $g(t)$ che devono soddisfare al sistema

$$
\begin{cases} \dfrac{dp(t)}{dt} = -p(t) + B g(t) , \\[3mm] \dfrac{dg(t)}{dt} = C p(t) - g(t) + \exp[\lambda_0 t] , \end{cases}
$$

la cui integrazione, con le condizioni iniziali

$$p(0) \quad 0 . \quad g(0) \quad 0 .$$

direttamente ricavate dalle (5) e (6), si fa nel modo consueto ottenendo

$$p(t) = \sum_{0}^{2} p_i \exp [\lambda_i t] ,$$

$$g(t) = \sum_{0}^{2} g_i \exp [\lambda_i t] ,$$

dove

$$p_0 = \frac{B}{(\lambda_1 - \lambda_0)(\lambda_2 - \lambda_0)} . \quad p_1 = \frac{B}{(\lambda_1 \cdot \lambda_2)(\lambda_1 - \lambda_0)} , \quad p_2 = \frac{B}{(\lambda_2 \quad \lambda_1)(\lambda_2 - \lambda_0)} .$$

$$g_0 = \frac{A + \lambda_0}{(\lambda_1 - \lambda_0)(\lambda_2 - \lambda_0)} , \quad g_1 = \frac{A + \lambda_1}{(\lambda_1 - \lambda_2)(\lambda_1 - \lambda_0)} , \quad g_2 = \frac{A + \lambda_2}{(\lambda_2 - \lambda_1)(\lambda_2 - \lambda_0)} ;$$

con le lettere A, B, C, λ_1, λ_2 abbiamo indicato i valori che assumono le funzioni $A(s)$, $B(s)$, $C(s)$, $\lambda_1(s)$, $\lambda_2(s)$ riportate nel citato lavoro di ROSSI e GREISEN per $s = 1,8$.

Prima approssimazione (valida per E, $W > 0,2$ GeV).

Seguendo il metodo sopra descritto abbiamo ricavato gli spettri differenziali π_1 e γ_1 risolvendo prima l'equazione in γ, in cui per la π si è posto la π_0 di cui abbiamo esteso la validità anche per $E < 1$ GeV, e scrivendo, per la (1'),

$$\Sigma(W, t) = N S_1(W) \exp [\lambda_0 t] .$$

Si ha allora

$$\frac{\partial \gamma_1(W, t)}{\partial t} = N C p(t) S_0(W) - \sigma_0 \gamma_1(W, t) + N S_1(W) \exp [\lambda_0 t] ,$$

il cui integrale generale, con la condizione iniziale $\gamma_1(W, 0) = 0$, è dato dalla

(7) $$\gamma_1(W, t) = N \big[k(t) S_1(W) + m(t) H_1(W) \big] ,$$

ove

$$k(t) = \frac{\exp[\lambda_0 t] - \exp[-\sigma_0 t]}{\sigma_0 + \lambda_0},$$

$$m(t) = \sum_0^2 {}_i p_i \frac{\exp[\lambda_i t] - \exp[-\sigma_0 t]}{\sigma_0 + \lambda_i},$$

$$H_1(W) = \int_W^\infty \frac{\pi_0(E, t)}{N p(t)} \varphi(E, W) \frac{\mathrm{d}E}{E} = C W^{-2,8}.$$

Si vede immediatamente che $k(t) + m(t) = g(t)$ e quindi lo spettro $\gamma_1(W, t)$ si riduce a $\gamma_0(W, t)$ per $W \geqslant 1$ GeV. Osserviamo che questo spettro fotonico tiene conto della variazione della forma della sorgente con l'energia ma non della perdita di energia per ionizzazione; questo si farà nelle approssimazioni successive.

Poniamo ora γ_1 al posto di γ nella equazione in π e facciamo la posizione [8]:

$$(8) \qquad \frac{\pi_1(E', t)}{\pi(E, t)} = \left(\frac{E}{E'}\right)^{s_1(E, t)+1},$$

ove $s_1(E, t)$ è una funzione di E e t i cui valori vanno da 1,8 per $E \geqslant 1$ GeV e t qualunque, ad un valore compreso fra 0,9 ed 1,8 per $0,2 \leqslant E \leqslant 1$ GeV. In mancanza di indicazioni più precise, e che potrebbero essere ottenute solo conoscendo già la soluzione $\pi_1(E, t)$, abbiamo posto:

$$s_1(E, t) = \begin{cases} 0,63\, E + 1,17 & 0,2 \leqslant E \leqslant 1 \text{ GeV}, \\ 1,8 & E \geqslant 1, \end{cases}$$

cioè abbiamo scelto per s_1 una espressione lineare in E ed indipendente da t e tale che per $E = 0,2$ GeV essa abbia un valore medio fra gli estremi 1,8 e 0,9.

Con la posizione (8) l'equazione in π_1 diventa:

$$(9) \qquad \frac{\partial \pi_1(E, t)}{\partial t} - \beta \frac{\partial \pi_1(E, t)}{\partial E} + A_1(E)\pi_1(E, t) = 2 \int_E^\infty \gamma(W, t)\psi(W, E) \frac{\mathrm{d}W}{W},$$

dove con $A_1(E)$ abbiamo indicato la funzione

$$A_1(E) = \int_0^E \varphi(W, E) \frac{\mathrm{d}W}{E} - \int_E^\infty \left(\frac{E}{E'}\right)^{s_1} \varphi(E', E' - E) \frac{\mathrm{d}E'}{E'},$$

[8] N. DALLAPORTA e E. CLEMENTEL: *Nuovo Cimento*, **3**, 235 (1946).

che è la $A\big[s_1(E)\big]$ di Rossi e Greisen [7]: nei calcoli l'abbiamo approssimata con la espressione

$$A_1(E) = \begin{cases} 0{,}3\,E + 1{,}16 & 0{,}2 \leqslant E \leqslant 1 \text{ GeV}, \\ 1{,}46, & E \geqslant 1. \end{cases}$$

Per integrare la (9) facciamo il cambiamento di variabili seguente

$$(10) \qquad \begin{cases} E = \eta - \beta\tau, \\ t = \tau, \end{cases}$$

per cui essa diventa

$$\frac{\partial \overline{\pi}_1(\eta, \tau)}{\partial \tau} + A_1(\eta - \beta\tau)\overline{\pi}_1(\eta, \tau) = 2\int_{\eta-\beta\tau}^{\infty} \gamma_1(W, \tau)\psi(W, \eta - \beta\tau)\frac{\mathrm{d}W}{W},$$

con la condizione iniziale $\overline{\pi}_1(\eta, 0) = 0$, ed il suo integrale generale è allora:

$$\overline{\pi}_1(\eta, \tau) = 2\int_0^{\tau} \mathrm{d}\zeta \exp\left[\int_{\tau}^{\zeta} A_1(\eta - \beta\xi)\,\mathrm{d}\xi\right]\int_{\eta-\beta\zeta}^{\infty} \gamma_1(W, \zeta)\psi(W, \eta - \beta\zeta)\frac{\mathrm{d}W}{W}.$$

Tornando, dopo alcuni passaggi, alle notazioni in E e t tramite le (10), la espressione definitiva dello spettro differenziale di prima approssimazione π_1 risulta data da

$$\pi_1(E, t) = \frac{2}{\beta}\int_{E}^{E+\beta t} \mathrm{d}\varepsilon \exp\left[\frac{1}{\beta}\int_{\varepsilon}^{E} A_1(\varepsilon')\,\mathrm{d}\varepsilon'\right]\int_{\varepsilon}^{\infty} \gamma_1\left(W, \frac{E+\beta t - \varepsilon}{\beta}\right)\psi(W, \varepsilon)\frac{\mathrm{d}W}{W}.$$

Ponendo in questa al posto di γ_1 la (7), si ottiene una espressione non integrabile in termini finiti, che abbiamo calcolato numericamente. Il risultato (fig. 4) mostra in particolare che $\pi_1(1, t)$ è inferiore a $\pi_0(1, t)$ di circa 18%, il che rappresenta l'effetto a quella energia della perdita di energia per ionizzazione; per $E \cong 2$ GeV le due approssimazioni π_1 e π_0 praticamente coincidono.

Abbiamo approssimato lo spettro π_1, per poterlo usare nelle approssimazioni successive, con la espressione analitica seguente

$$(11) \qquad \pi_1(E, t) = N p(t) \begin{cases} E^{-2,8} & E \geqslant 2 \text{ GeV}, \\ 0{,}812\,E^{-2.5}, & 0{,}5 \leqslant E \leqslant 2, \\ 0{,}707\,E^{-2,3} & 0{,}2 \leqslant E \leqslant 0{,}5, \end{cases}$$
$$(t \geqslant 6),$$

che rispetto ai valori calcolati numericamente è affetta da un errore massimo del 7%, finchè $t < 6$: per valori inferiori di t non è possibile approssimarlo con variabili E e t separate senza introdurre degli errori troppo forti.

Seconda approssimazione (valida per E, $W > 0,075$ GeV).

Seguendo il solito metodo, integriamo l'equazione in γ del sistema (4) con le espressioni (2) e (3) per le sezioni d'urto ponendo al posto di π la (11), ed estendendo anche all'intervallo $0,075 \leqslant E \leqslant 0,2$ GeV l'andamento in $-2,3$.

Si ha allora, come dai calcoli della precedente approssimazione,

$$(12) \qquad \gamma_2(W, t) = N\big[k(t)S_2(W) + m(t)H_2(W)\big] \,,$$

con

$$H_2(W) = \int\limits_W^\infty \frac{\pi_1(E, t)}{N p(t)} \, \varphi(E, \, W) \frac{\mathrm{d}E}{E} \,.$$

Questo spettro γ_2 tiene conto della perdita di energia per ionizzazione in quanto dipende da π_1: per tale ragione per $W \geqslant 0,2$ GeV esso dà dei valori minori dello spettro γ_1 nello stesso intervallo.

Analogamente alla (8) poniamo ora:

$$\frac{\pi_2(E', t)}{\pi_2(E, t)} = \left(\frac{E}{E'}\right)^{s_2(E, \, t) + 1} \,,$$

dove la $s_2(E, t)$, assunta indipendente da t, è tale che per $E \geqslant 0,2$ GeV essa assume i valori dati dagli esponenti dello spettro π_1, che sono noti, e per $E = 0,075$ GeV un valore medio fra 0 e 0,9. Con questa ipotesi abbiamo calcolato numericamente la funzione

$$A_2\big[s_2(E, t)\big] = \int\limits_0^E \varphi(E, \, W) \frac{\mathrm{d}W}{E} - \int\limits_E^\infty \left(\frac{E}{E'}\right)^{s_2} \varphi(E', \, E' - E) \frac{\mathrm{d}E'}{E'} \,.$$

che è stata approssimata colla forma analitica più semplice

$$A_2(E) = \begin{cases} 1{,}46 & E \geqslant 2 \ \text{GeV} \,, \\[2mm] \dfrac{E}{0{,}65 \ E + 0{,}07} & 0{,}075 < E \leqslant 2 \,. \end{cases}$$

Allora l'equazione in π_2 si scrive

$$\frac{\partial \pi_2(E,\,t)}{\partial t} - \beta \cdot \frac{\partial \pi_2(E,\,t)}{\partial E} + A_2(E)\pi_2(E,\,t) = 2 \int\limits_{E}^{\infty} \gamma_2(W,\,t)\psi(W,\,E)\,\frac{\mathrm{d}W}{W}\ .$$

e la sua soluzione, ottenuta analogamente a quella del caso precedente, risulta

$$\pi_2(E,\,t) = \frac{2}{\beta} \int\limits_{E}^{E+\beta t} \mathrm{d}\varepsilon \exp\left[\frac{1}{\beta}\int\limits_{\varepsilon}^{E} A_2(\varepsilon')\,\mathrm{d}\varepsilon'\right] \int\limits_{\varepsilon}^{\infty} \gamma_2\left(W,\,\frac{E+\beta t-\varepsilon}{\beta}\right)\psi(W,\,\varepsilon)\,\frac{\mathrm{d}W}{W}\ .$$

Ponendo in questa la espressione (12) di γ_2, abbiamo calcolato numericamente $\pi_2(E,\,t)$. Si trova che $\pi_2(0,5,\,t) \simeq \pi_1(0,5,\,t)$ mentre per valori di $E < 0,5$ GeV si ha sempre $\pi_2 < \pi_1$ (fig. 4).

Nella approssimazione seguente abbiamo rappresentato la $\pi_2(E,\,t)$ con la espressione analitica

$$(13) \qquad \pi_2(E,\,t) = N p(t) \begin{cases} E^{-2,8} & E \geqslant 2 \ \text{GeV}\,, \\[2mm] 0,812\,E^{-2,5} & 0,5 \leqslant E \leqslant 2\,. \\[2mm] 0,575\,E^{-2} & 0,2 \leqslant E \leqslant 0,5\,, \\[2mm] 0,416\,E^{-1,8} & 0,1 \leqslant E \leqslant 0,2\,, \\[2mm] 0,131\,E^{-1,3} & 0,075 \leqslant E \leqslant 0,1\,, \end{cases}$$

che rispetto ai valori calcolati numericamente è affetta da un errore massimo del 6%.

Terza approssimazione (valida per $E,\,W \geqslant 0,01$ GeV).

Calcoliamo anche qui dapprima lo spettro fotonico integrando la equazione in γ col porre al posto di π lo spettro π_2 nella forma analitica (13) (a differenza dei casi precedenti però poniamo ora $\pi_2(E < 0,075,\,t) =$ costante per il fatto che la sorgente in questo intervallo diminuisce ed il seguire l'andamento della (13) condurrebbe a dei valori in eccesso).

Abbiamo quindi

$$\gamma_3(W,\,t) = N\big[k(t)S_3(W) + m(t)H_3(W)\big]\,,$$

con

$$H_3(W) = \int\limits_{W}^{\infty} \frac{\pi_2(E,\,t)}{N p(t)}\,q(E,\,W)\,\frac{\mathrm{d}E}{E}\ .$$
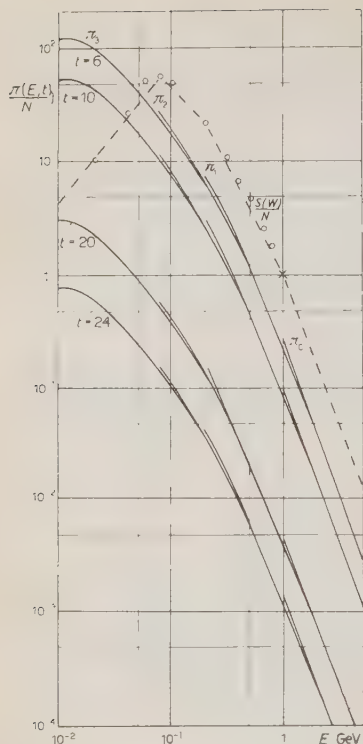
Fig. 4. – Spettro elettronico differenziale nelle varie approssimazioni e spettro energetico della sorgente di fotoni.

Facciamo ancora la posizione

$$\frac{\pi_3(E', t)}{\pi_3(E, t)} = \left(\frac{E}{E'}\right)^{s_3(E, t)+1},$$

e scegliamo per s_3 una espressione dipendente solo da E e tale che per $E = 0,01$ essa assuma il valore 0 e per $E > 0,075$ i valori che si ottengono con la (13).

La funzione $A_3(E)$ risulta poi espressa dalla

$$A_3[s_3(E, t)] =$$

$$= \int\limits_0^E \varphi(E, W) \frac{dW}{E} - \int\limits_E^\infty \left(\frac{E}{E'}\right)^{s_3} \varphi(E', E' - E) \frac{dE'}{E'},$$

e la equazione in π_3

$$\frac{\partial \pi_3(E, t)}{\partial t} - \beta \frac{\partial \pi_3(E, t)}{\partial E} + A_3(E)\pi_3(E, t) =$$

$$= 2\int\limits_E^\infty \gamma_3(W, t)\psi(W, E) \frac{dW}{W},$$

la cui soluzione

$$\pi_3(E, t) = \frac{2}{\beta} \int\limits_E^{E+\beta t} d\varepsilon \exp\left[\frac{1}{\beta} \int\limits_\varepsilon^E A_3(\varepsilon') d\varepsilon'\right] \int\limits_\varepsilon^\infty \gamma_3\left(W, \frac{E + \beta t - \varepsilon}{\beta}\right) \psi(W, \varepsilon) \frac{dW}{W},$$

dà lo spettro elettronico finale. Esso è stato tabulato per vari valori di t: si trova che $\pi_3(0,2, t) \simeq \pi_2(0,2, t)$.

Nella fig. 4 abbiamo riportato gli andamenti delle varie approssimazioni π_0, π_1, π_2, π_3 per alcuni valori di t.

4. – Spettro integrale e normalizzazione.

Partendo dai dati di $\pi_3(E, t)$ abbiamo calcolato numericamente lo spettro integrale $\Pi(t)/N$ degli elettroni per valori di $E > 0,01$ GeV e per varie quote; i risultati sono riportati nella tab. I.

TABELLA I.

t	6	10	20	24
$\Pi(t)/N$	6,31	2.59	0,130	$3,6 \cdot 10^{-2}$

Possiamo ora ottenere il valore della costante N di normalizzazione confrontando lo spettro integrale $\Pi(t, N)$ dato dalla precedente tabella, con lo spettro integrale sperimentale $\Pi(t)$ degli elettroni di decadimento dei neutretti alle varie quote.

Abbiamo ricavato quest'ultimo nel seguente modo: dalla componente elettronica, ottenuta per sottrazione dalla componente totale delle componenti mesonica e protonica totali secondo i più recenti dati sperimentali [*], abbiamo tolto:

a) gli elettroni di decadimento delle particelle μ. Questo dato è stato desunto dal recente lavoro di STROFFOLINI [10]:

b) gli elettroni di knock-on, dedotti dai dati di JÁNOSSY [11], e di ROSSI e KLAPMANN [12] per il valore al livello del mare, e per le quote più alte seguendo l'andamento dei mesoni veloci.

Rimane in tal modo il solo contributo degli elettroni di decadimento dei π^2, che confrontato coi valori della tab. I permette di determinare la costante di normalizzazione N.

La tab. II riassume l'insieme dei dati.

TABELLA II.

t		Compon. elettronica	(a)	(b)	$\Pi(t)$	$\dfrac{\Pi(t)}{N}$	N
n.r.	g·cm⁻²	10^{-4}	10^{-4}	10^{-4}	10^{-4}		10^{-2}
10	430	700	110	19,5	570,5	2,59	2,20
16	690	160	32,5	10,5	117	0,43 [¹]	2,72
20	860	62	18	7,4	36.6	0,13	2,82
24	1 033	24,5	10	5,5	9	0,036	2.50

Il valore [¹] è stato ottenuto per interpolazione grafica dai dati della tab. I.

[*] G. PUPPI: in corso di pubblicazione sul *Suppl. al Nuovo Cimento*.

[10] R. STROFFOLINI: *Nuovo Cimento*, **10**, 300 (1953).

[11] L. JÁNOSSY: *Cosmic Rays* (Oxford, 1948), p. 243.

[12] B. ROSSI e S. KLAPMAN: *Phys. Rev.*, **61**, 414 (1942).

Come si vede i valori ottenuti per N, mediante gli spettri sperimentali alle varie quote, risultano abbastanza concordi con un valore medio di

$$N \simeq 2,6 \cdot 10^{-2} \ .$$

5. – Rapporto $\pi^0/\pi^{\pm}$.

La normalizzazione dello spettro calcolata nel modo precedente ci consente di ottenere una determinazione sperimentale del rapporto $\pi^0/\pi^{\pm}$.

Consideriamo lo spettro di decadimento dei π^0, sorgente dei fotoni, integrato su tutta l'atmosfera:

$$(14) \quad G_\gamma(W)\,\mathrm{d}W = \mathrm{d}W \int\limits_0^{24} \Sigma(W,t)\,\mathrm{d}t = 7,73 \cdot 10^{-2}\,W^{-2,8}\,\mathrm{d}W, \qquad (W \geqslant 1 \ \text{GeV}).$$

Se ora assumiamo il seguente schema di decadimento del mesone neutro:

$$\pi^0 \to 2\gamma \ ,$$

e ammettiamo, in prima approssimazione, che l'energia dei fotoni generati sia quella media, cioè metà di quella del mesone neutro, lo spettro dei π^0 risulta:

$$(15) \qquad\qquad G_{\pi^0}(W)\,\mathrm{d}W = \frac{1}{4}\,G_\gamma\!\left(\frac{W}{2}\right)\mathrm{d}W \ ,$$

cioè, per la (14),

$$G_{\pi^0}(W)\,\mathrm{d}W = 1,35 \cdot 10^{-1}\,W^{-2,8}\,\mathrm{d}W \ , \qquad (W \geqslant 2 \ \text{GeV}).$$

Lo spettro dei mesoni carichi a sua volta si può ottenere da quello delle particelle μ secondo la relazione ben nota:

$$G_{\pi^{\pm}}(W)\,\mathrm{d}W = G_\mu\!\left(\frac{W}{1,25}\right)\frac{\mathrm{d}W}{1,25} \ ,$$

e se assumiamo per lo spettro delle particelle μ quello di Sands, corretto alle alte energie in base ai dati della componente μ sottoterra e integrato su tutta l'atmosfera, otteniamo per i mesoni π carichi lo spettro [9]

$$G_{\pi^{\pm}}(W)\,\mathrm{d}W = 2,55 \cdot 10^{-1}\,W^{-2,8}\,\mathrm{d}W, \qquad (W \geqslant 2 \ \text{GeV}),$$

e da questo, facendo il rapporto:

$$(16) \qquad \frac{\pi^0}{\pi^{\pm}} = \frac{G_{\pi^0}(W)\,dW}{G_{\pi^{\pm}}(W)\,dW} = 0.53 \; .$$

Il valore trovato per il rapporto mesoni neutri e mesoni carichi risulta in accordo soddisfacente con i più recenti dati sperimentali in proposito: per citarne qualcuno:

CARLSON e coll. [5] danno 0.45 ± 0.10, BRADT e coll. [13] 0.39 ± 0.13, SALVINI e coll. [14] 0.36, LOVATI e coll. [15] 0.42, GREGORY e coll. [16] 0.3. Questo ultimo però si riferisce al rapporto fra mesoni neutri e particelle penetranti e quindi rappresenta un limite inferiore del rapporto in questione.

6. – Confronto con i dati sperimentali del gruppo di Bristol.

Può essere interessante, per finire, tentare un confronto dei dati finora raccolti con quelli forniti dai lavori con lastre nucleari dal gruppo di Bristol.

Consideriamo dapprima lo spettro integrale della sorgente di fotoni, definito tramite la (15),

$$\Pi^0(\eta_0, t_0)\,dt = \frac{dt}{4} \int_{\eta_0}^{\infty} \Sigma\left(\frac{W}{2}, t_0\right) dW \; ,$$

ove η_0 è uguale a 0.25 GeV e t_0 a 50.43 u.r., il primo essendo il limite inferiore dei dati sperimentali forniti dal gruppo di Bristol ed il secondo la quota a cui gli stessi sono stati misurati. I calcoli danno

$$(17) \qquad \Pi^0(\eta_0, t_0) = 4.2 \cdot 10^{-5} \cdot \frac{\varrho}{43} = 1.29 \cdot 10^{-5} \quad \text{mesoni neutri con energia}$$

$\geqslant 0.25$ GeV a 50 g·cm⁻² per cm³·s·sterad .

con ϱ_a densità dell'aria standard $\simeq 1.29 \cdot 10^{-3}$ g·cm⁻³.

Dal lavoro di CAMERINI e coll. [17] invece si ha uno spettro differenziale di

---

[13] H. L. BRADT, H. F. KLAPON e B. PETERS: *Helv. Phys. Acta.* **23**, 24 (1950).

[14] G. SALVINI e Y. KIM: *Phys. Rev.*, **86**, 592 (1952).

[15] A. LOVATI, A. MURA, G. TAGLIAFERRI e S. TERRANI: *Nuovo Cimento*, **9**, 946 (1952).

[16] B. P. GREGORY e J. H. TINLOT: *Phys. Rev.*, **81**, 675 (1951).

[17] U. CAMERINI, P. H. FOWLER, W. O. LOCK e H. MUIRHEAD: *Phil. Mag.*, **41**, 413 (1950).

mesoni carichi emessi da stelle ottenuto da misure su lastre nucleari esposte in pallone a 50 g·cm⁻². Da tale spettro differenziale, che è definito da 0,25 GeV a 1,4 GeV e che abbiamo approssimato con la espressione analitica

$$\pi^{\pm}(W, t_0) = 2{,}13 \cdot 10^{-1} \begin{cases} W^{-1} \quad \text{per} \quad W \leqslant 1 \text{ GeV}, & \text{mesoni carichi per GeV} \\ & \text{d'intervallo per stella in} \\ W^{-2{,}8} \quad \text{per} \quad W \geqslant 1 \text{ GeV}, & \text{emulsione a 50 g·cm}^{-2}, \end{cases}$$

abbiamo calcolato l'intensità integrale da 0,25 GeV in su:

$$\Pi^{\pm}(\eta_0, t_0) = 4{,}13 \cdot 10^{-1} \quad \text{mesoni carichi di energia} \geqslant 0{,}25 \text{ GeV}$$
$$\text{per stella in emulsione a 50 g·cm}^{-2}.$$

Da questo, usando del rapporto $\pi^0/\pi^{\pm} = 0{,}45$ dato da CARLSON e coll. [5], otteniamo

(18)
$$\Pi^0(\eta_0, t_0) = 1{,}86 \cdot 10^{-1} \quad \text{mesoni neutri di energia} \geqslant 0{,}25 \text{ GeV}$$
$$\text{per stella in emulsione a 50 g·cm}^{-2}.$$

Per avere un dato confrontabile con la (17) dobbiamo moltiplicare la (18) per il numero ν_a di stelle prodotte in un cm³ di aria al secondo. I dati sperimentali si riferiscono generalmente al numero di stelle prodotte in un cm³ di emulsione al giorno; d'altra parte il rapporto fra il numero di stelle prodotte in aria e quello di emulsione ν_e si può calcolare con la:

$$\frac{\nu_a}{\nu_e} = \frac{\sum_i n_{ia}\sigma_{ia}}{\sum_j n_{je}\,\sigma_{je}},$$

ove n_i e σ_i indicano rispettivamente il numero di nuclei per cm³ e le sezioni d'urto di produzione di stelle dei vari elementi che compongono l'aria e l'emulsione. Assumendo $\nu_e = (2{,}1 \cdot 10^3/8{,}64 \cdot 10^4) = 2{,}43 \cdot 10^{-2}$ [18] e per le σ_i i valori delle sezioni d'urto geometriche [19], si ottiene

$$\nu_a = \nu_e \, 5{,}3 \cdot 10^{-4} = 1{,}29 \cdot 10^{-5}.$$

Dividiamo ancora per 2π e facciamo l'ipotesi che il numero di mesoni uscenti

[18] M. CECCARELLI: comunicazione privata.

[19] J. J. LORD: *Phys. Rev.*, **81**, 901 (1951).

da stelle in aria sia lo stesso di quelli uscenti da stelle in emulsione; otteniamo

(19) $\Pi^0(\nu_0, t_0) = 1{,}86 \cdot 10^{-1} \cdot 1{,}29 \cdot 10^{-5} \cdot \dfrac{1}{2\pi} = 0{,}38 \cdot 10^{-6}$ mesoni neutri di energia $\geq 0{,}25$ GeV a 50 g·cm⁻² per cm³·s·sterad .

Il disaccordo non eccessivo tra il valore così ricavato e quello che abbiamo calcolato con la (17), può molto probabilmente ascriversi alle ipotesi grossolanamente approssimate, data la attuale insufficienza dei dati ad esse relativi, introdotte nell'ultimo ragionamento: in particolare quelle riguardanti la distribuzione angolare dei mesoni π⁰ prodotti, il rapporto delle sezioni d'urto di produzione di stelle e del numero medio di mesoni per stella in aria ed in emulsione.

Riteniamo perciò che il limite di incertezza introdotto dalle precedenti ipotesi sia attualmente abbastanza grande da non consentire di attribuire un valore significativo alla differenza nei fattori numerici delle (17) e (19) nè di poter concludere, da tale disaccordo, sulla probabilità di esistenza di un'altra sorgente della componente elettrofotonica non contemplata nel precedente quadro.

SUMMARY

The contribution from the π⁰ meson decay into two photons to the electronic component of the cosmic radiation, in passing through the atmosphere, is calculated; the diffusion equations are used with a generating function for the photons whose energy dependance is taken from the experimental data of the Bristol group, and whose variation with the altitude is derived from an absorption length of 130 g·cm⁻². The diffusion equations are integrated by a method of successive approximations, taking into account both the ionization energy loss and the variation of the cross sections for pairs and bremsstrahlung with energy. The results are normalized on the integral spectra of the total electronic component taken from the more recent experimental data and a ratio $\pi^0/\pi^\pm = 0{,}53$ of neutral to charged mesons is obtained. The absolute values of the intensity obtained in this way are not inconsistent with those given by the Bristol group, within the wide limits of the incertainties actually existing in the knowledge of some processes used in the comparison.

Theoretical Resonance Curves in the Gyro-Interaction of Electromagnetic Waves in the Ionosphere.

F. H. HIBBERD

Department of Physics, University of Sydney, Australia

Summary. — In a recent communication Dr. Motzo has considered the gyro-interaction of radio waves in the ionosphere when the disturbing wave is incident vertically. She concludes that for this case one would expect to observe always a single maximum in the index of interaction as the frequency of the disturbing wave is varied through the gyro-frequency. It is possible to show that with larger approximations in the calculations either single or double maxima may occur and that there is little difference in the general shape of the resonance curves resulting from vertically incident and obliquely incident disturbing waves. A qualitative outline is given of the theory of gyro-interaction of V. A. Bailey.

1. – Introduction.

In a recent communication M. Motzo [1] has given theoretical curves for the index of interaction of radio waves in the ionosphere when the disturbing gyro-wave is incident vertically. These curves purport to show that for vertical incidence, using data appropriate to Naples, only a single maximum is to be expected in the magnitude of the transferred modulation as the frequency of the disturbing wave is varied about the gyro-frequency. It will be recalled that the original curves drawn by Bailey [2], for a vertical magnetic field and a wave incident at 45°, show that if the wanted wave is reflected at a level below some 3 to 4 km above the bottom of the E-layer a single maximum is to be expected, whereas two maxima, separated by a minimum

---

[1] M. Motzo: *Nuovo Cimento*, **9**, 213 (1952).

[2] V. A. Bailey: *Phil. Mag.*, **26**, 425 (1938).

which is very close to the gyro-frequency, result if the wanted wave is reflected at a higher level. Both single and double maxima have been observed experimentally by CUTOLO [3] and by BAILEY [4] and their respective co-workers. The conclusion that for a certain direction of incidence of the disturbing wave the interaction curve has always a single maximum is unexpected and therefore the question has been examined in greater detail.

2. – The resonance curves for the index of interaction.

In the absence of specification of the wanted wave one cannot estimate the amount of modulation impressed on it. The interaction potentiality of a given disturbing wave can, however, still be calculated. It is expressed in terms of the index of interaction. This index is the quantity $N \nu w$, where N is the electron concentration, ν is the electron collision frequency and w is the mean work done by the disturbing wave on an electron in the interval between collisions.

On general grounds, providing there is a resonance in the absorption of a gyro-wave (*), one would always expect both single and double maxima in the index of interaction. Further, the direction of propagation relative to the direction of the magnetic field is more important than the question of oblique or vertical incidence. Accordingly, with the same data as MOTZO's, for vertical incidence at Naples, the curves representing the index of interaction have been recalculated.

The expressions and data used in the computations are given here again for reference. The mean work $\bar{w}$ done by the disturbing wave on an electron per collision with the gas molecules is given by

$$ w = \tau a_s Z^2 \frac{\frac{1}{2} \sin^2 q}{\nu^2 - \sigma^2 - \nu^2 p' \varepsilon} $$

where $\tau = e^2/m = 2.53 \cdot 10^8$ (e.u.s.)^2/gm;

  $Z =$ R.M.S. value of the electric field of the wave at the point of incidence, estimated by MOTZO as 2.2 mV/m for an 800 watt transmitter;

  $\varphi =$ angle between the electric vector of the wave and the direction of the earth's magnetic field; taken here as 60°;

(3) M. CUTOLO, M. CARLEVARO and M. GHERGHI: *Alta Freq.*, **15**, 111 (1946); M. CUTOLO and R. FERRERO: *Nature*, **163**, 58 (1949); M. CUTOLO: *Nature*, **166**, 98 (1950).

(4) V. A. BAILEY, R. A. SMITH, K. LANDECKER, A. J. HIGGS, and F. H. HIBBERD: *Nature*, **169**, 911 (1952).

(*) For the values of N, ν and Ω corresponding to the lower E-layer, resonance in the absorption of the extraordinary component of a gyro-wave always occurs.

ν = frequency of collisions of electrons with gas molecules;

$\sigma = \omega - \Omega$, where:

ω = angular frequency of the disturbing wave;

Ω = local gyromagnetic angular frequency of the electrons, taken here as 7.387×10^6 (equivalent to 225 m);

$\varepsilon = \sigma/\Omega$; i.e. $\omega = (1 + \varepsilon)\Omega$.

The quantity p' in the expressions for $\bar{w}$ is given by

$$p' = \frac{\text{tg}^3\,\theta - \cot^2\varphi}{\text{tg}^2\,\theta + 2} - \frac{\tau N(1 + \cos^2\theta)}{2\nu^2}$$

where θ = angle between the direction of propagation of the disturbing wave and the earth's magnetic field; taken here as 30°;

N = electron concentration.

Both ν and N vary with height and it is assumed that they vary in the following manner:


Fig. 1. – Graphs of Index of Interaction $N\nu\bar{w}$ against frequency (in terms of ε) of disturbing gyro wave. The dotted line indicates the gyrofrequency. The curves are for various heights above the lower boundary of the E-layer.

$$\nu = \nu_0 \exp[-ay]$$
$$N = N_0 \exp[by]$$

where y is measured in cm upwards from the lower boundary of the E-layer, taken as a height of 90 km, and ν_0 and N_0 are the values at this base level. The values adopted in these expressions are $\nu_0 = 1.1 \cdot 10^6$, $a = 10^{-6}$, $N_0 = 1.00$ per cm³, $b = 10^{-5}$.

The quantity a_s measures the attenuation of the disturbing wave and is given by the relation

$$\log_e a_s = -2\int_0^s k\,ds =$$
$$= -0.0566\,(\text{tg}\,\alpha - \cot\alpha)\int_0^y \frac{N\nu}{\nu^2 + \sigma^2}\,dy,$$

where k = absorption coefficient of the wave,

s = length of the ray-trajectory in the ionosphere, up to the point considered;

and $\text{tg}\,\alpha = \cos\theta$.

The results of these calculations are represented by means of the curves shown in fig. 1.
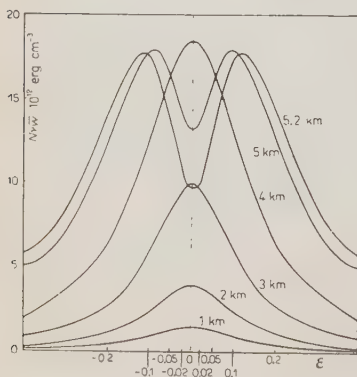
It is thus seen that when the curves given by MOTZO are revised they become very similar to those originally given by BAILEY for oblique incidence. It then appears that the transition from a single to a double hump, as the height of reflection of the wanted wave increases, will always occur, whatever the angle of incidence of the disturbing wave. Further, the asymmetry about the gyro-frequency is not very great.

Although any set of curves such as that shown in fig. 1 is applicable only to a given locality and direction of propagation, it is believed that these revised curves will be of value in connection with the researches in gyro-interaction which are proceeding in Italy. It should be noted, however, that the curves depend on the values adopted for b, the constant which specifies the distribution of the electron density, and for ν, the electron collision frequency, in the lower part of the E-layer. Also there are approximations in the theory of BAILEY (^{2}), though current investigations indicate that the corresponding errors are not serious.

3. – Theory of gyro-interaction.

It is useful now to outline the basic physical ideas of BAILEY's theory (^{2}), (^{5}) of gyro-interaction. From this it will be seen that in general one would always expect to find either single or double maxima, according to the height at which the wanted wave is reflected.

When energy from a wave (the disturbing wave) is absorbed in a region of the ionosphere, the mean energy of agitation of the electrons is increased and this in turn increases the electron collision frequency. This will change the absorbing capacity of that region of the ionosphere. When the amplitude of the disturbing wave is modulated there will be a resulting modulation of the absorbing capacity of the ionosphere. Should a second wave (the wanted wave) suffer absorption in the disturbed region this wave will have impressed upon it a modulation whose fundamental frequency is the same as that of the modulation of the disturbing wave. When the wanted wave is not specified one can determine only the effect which a given disturbing wave will produce in the ionosphere. This is best described in terms of the amount of energy absorbed from the disturbing wave. For this purpose BAILEY has chosen the quantity $N\nu\overline{w}$ and has termed it the « index of interaction ». From the definitions it will be seen that this quantity represents the mean energy absorbed by the electrons per unit volume per second. BAILEY has shown that $N\nu\overline{w}$ $2k\overline{T}$, where k is the absorption coefficient of the disturbing wave

(^{5}) V. A. BAILEY: *Phil. Mag.*, **23**, 929 (1937).

and $\overline{U}$ is the mean value of its energy flux; this is in agreement with the interpretation of $Nv\overline{w}$ given here.

A considerable increase in the amount of transferred modulation may result when the carrier frequency of the disturbing wave is varied through the gyro-frequency. This is because the extraordinary component of a wave suffers greatly increased absorption at the gyro-frequency. The absorption of the extraordinary component of a gyro-wave is so much greater than that of the ordinary component that only the effect of the extraordinary component need be considered. At any given height in the E-layer, $\overline{w}$ is determined by the strength of the disturbing wave at that height, and by the fraction of the wave energy that is absorbed. With increasing heights in the layer, measured from the lower boundary, the fraction of the wave energy that is absorbed increases rapidly but the wave itself becomes weaker. For a given disturbing wave frequency, the index of interaction $Nv\overline{w}$ attains a maximum value at a definite height, as shown by each curve in fig. 2.

The absorption of the extraordinary component has a rather sharp maximum at the gyro-frequency and so the absorption of a wave on the gyro-frequency is much greater than that of a wave whose frequency is a few percent less or greater than the gyro-frequency. Thus the index of interaction attains its maximum value at a smaller depth of penetration for a wave whose frequency is equal (or, more strictly, almost equal) to the giro-frequency than it does for a wave whose frequency is slightly removed from the gyro-frequency. This is illustrated in fig. 2, in wich are drawn the curves corresponding to the gyro-frequency ($\varepsilon = 0$) and to positive values of ε. The curves for negative values of ε are very similar to those for positive ε and are omitted for clarity. At levels not far above the lower boundary of the E-layer, the index of interaction is a maximum for the gyro-frequency, whereas at higher levels the index may be less for the gyro-frequency (because the wave has
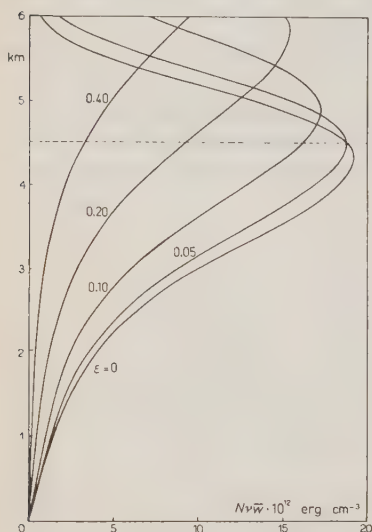

Fig. 2. – Graphs of the Index of Interaction against height inside the E-layer. The disturbing wave frequency corresponding to each curve is indicated by the adjacent value of ε. The curves show that the height, at which a maximum in the index of interaction occurs, increases as the wave frequency departs from the gyro-frequency.

become so weak) than for frequencies a little less or a little greater than the gyro-frequency. Thus, as shown in fig. 1, the curves representing the index of interaction have a single hump at levels just inside the lower E-layer and this single hump changes over to a double hump at higher levels. In fig. 2, the region below the dotted horizontal line corresponds to the single hump, the region above the line corresponds to the double hump. Whether one obtains experimentally the single or the double maxima in the depth of transferred modulation depends on the height at which the wanted wave suffers its greatest absorption. CUTOLO [6] has actually observed a transition from the one type to the other as he varied the carrier frequency, and hence the height of reflection, of the wanted wave.

[6] M. CUTOLO: *Nuovo Cimento*, **9**, 391 (1952).

RIASSUNTO

In un recente articolo della Dott.ssa MOTZO è stata considerata la girointerazione di onde nella ionosfera nel caso di un'onda disturbatrice con incidenza verticale, e si è dimostrata l'esistenza di un solo massimo dell'indice di interazione allorchè si varia la frequenza disturbatrice intorno alla frequenza giromagnetica. Si è pensato allora di fare ulteriori approssimazioni nei calcoli e pertanto si dimostra come è possibile così ottenere due curve; una con un solo massimo e una con due massimi. Inoltre si dimostra che l'andamento generale delle curve di risonanza è lo stesso sia per incidenza verticale che per incidenza obliqua dell'onda disturbatrice. Si dà un breve riassunto delle linee fondamentali della teoria della girointerazione di V. A. BAILEY.

Misure di velocità delle onde elastiche nei solidi a temperatura elevata.

P. G. Bordoni e M. Nuovo

Istituto Nazionale di Ultracustica « O. M. Corbino » - Roma

(ricevuto il 17 Gennaio 1953)

Riassunto. — Si è misurata, con un metodo elettroacustico, la velocità delle onde elastiche estensionali in cinque metalli puri (Pb, Sn, Bi, Al, Cd). In base ai dati sperimentali si è calcolata la derivata logaritmica della velocità rispetto alla temperatura, confrontandone poi le variazioni con quelle del coefficiente di dilatazione termica relativo agli stessi metalli.

1. – Scopo del lavoro.

Le attuali conoscenze sulla struttura dei metalli permettono di attribuire le variazioni nella velocità di propagazione delle onde elastiche con la temperatura a due gruppi di cause ben distinti tra di loro:

1) agli effetti di rilassamento, dovuto, per esempio, al movimento delle dislocazioni nell'interno dei grani cristallini, agli scambi di calore tra i grani stessi, ai mutui scorrimenti del loro contorno, alla eventuale presenza di impurità, e così via;

2) alle variazioni nelle dimensioni medie del reticolo cristallino, prodotte dai cambiamenti di temperatura.

I dati sperimentali di cui attualmente si dispone, riguardano prevalentemente il primo gruppo; le misure relative alle variazioni di velocità in un ampio campo di temperature sono invece assai più scarse, e riesce inoltre difficile collegarle tra di loro, essendo state in gran parte eseguite senza preoccuparsi di una possibile interpretazione fisica [1].

---

[1] Cfr. ad esempio: W. Köster: *Zeits. f. Metallkunde*, **39**, 1 (1948).

Si è quindi ritenuto che un'indagine sistematica sulla dipendenza della velocità dalla temperatura, specialmente nei pressi del punto di fusione, eseguita con la notevole precisione consentita dai metodi elettroacustici di cui attualmente si dispone, ed in condizioni sperimentali particolarmente semplici e chiaramente specificate, potesse fornire un utile contributo alla conoscenza della struttura fisica dei metalli.

Nella presente nota sono raccolti i primi risultati ottenuti in tale indagine, i quali sembrano avere una portata più generale di quella che ci si potrebbe attendere, dato il ristretto gruppo di metalli al quale si riferiscono. Essi mostrano infatti la possibilità di ricavare una legge generale di dipendenza della velocità dalla temperatura, analoga a quella relativa alla dilatazione termica e valida per temperature non troppo vicine a quella di fusione. Nei pressi di quest'ultima, i dati sperimentali suggeriscono invece la possibilità di una trattazione teorica della dipendenza delle proprietà elastiche dalla temperatura basata sulla teoria formale dei fenomeni di rilassamento.

2. – Metodo di misura.

I valori della velocità di propagazione delle onde estensionali (*) sono ottenuti mettendo in vibrazione delle sbarrette cilindriche, prive di ogni sensibile vincolo esterno, e determinandone la frequenza di risonanza fondamentale ν_0. La velocità di propagazione c, per una sbarra infinitamente sottile, è data dalla formula (2)

$$(1) \qquad c = \sqrt{\frac{E}{\varrho}} = 2\nu_0 l \left[1 + \frac{\pi^2}{16} \frac{\sigma^2 d^2}{l^2} \right].$$

dove: E = modulo di Young; ϱ = densità del materiale; l = lunghezza della sbarretta; d = diametro della sbarretta; σ = coefficiente di Poisson.

Prima di ogni serie di misure le sbarrette vengono sottoposte ad un rinvenimento per quanto è possibile completo, in modo da eliminare gran parte delle imperfezioni nel reticolo cristallino, dovute alle lavorazioni precedenti.

Per ridurre al minimo i vincoli esterni le sbarrette, disposte verticalmente, sono sostenute da tre punte di acciaio del diametro di 1 mm, disposte a 120° tra di loro, e contenute nel piano nodale passante per il punto di mezzo della sbarretta. Tali punte penetrano in fori di diametro leggermente superiore, in

---

(*) È sembrato opportuno usare tale espressione per mettere in evidenza il carattere di *estensione semplice* della sollecitazione, alla quale, fuori dell'asse della sbarretta *non* corrispondono spostamenti puramente longitudinali.

(2) LORD RAYLEIGH: *Theory of sound* (London, 1937) 2ª ediz. vol. I, pag. 252.

modo che il contatto con la sbarretta avvenga soltanto su di una porzione della parete laterale dei fori stessi, e sia assicurato unicamente dal peso della sbarretta. Si controlla che tale tipo di sostegno non ha alcuna influenza apprezzabile sul valore di ν_0, in quanto quest'ultima frequenza rimane inalterata anche se le punte non appartengono esattamente al piano nodale.

Durante le misure la sbarretta ed il suo sostegno sono collocati nella muffola cilindrica di un forno elettrico; la regolazione di temperatura, effettuata mediante termometri a mercurio provvisti di un contatto mobile, riduce le oscillazioni di meno di un grado; la misura della temperatura è fatta con termocoppie ferro-costantana, tarate in corrispondenza dei punti di fusione di alcuni dei metalli su cui sono eseguite le misure (Sn, Bi, Cd, Pb, Zn); il raggiungimento dell'equilibrio termico tra la sbarretta e l'aria che la circonda è indicato dalla costanza ([3]) nel tempo della ν_0.

Le misure a bassa temperatura sono invece eseguite collocando la sbarretta ed il suo sostegno, racchiusi in un recipiente a tenuta, in una miscela di alcool etilico ed anidride carbonica solida, contenuta in un thermos e seguendo le

TABELLA I. – *Caratteristiche dei materiali.*

Metallo	Provenienza	Lavorazione prima del rinvenimento	Lunghezza mm	Diametro mm	Freq. di risonanza a 20 °C cps	Densità a 20 °C g·cm⁻³	Temperatura di fusione °K	Temperatura di Debye °K
Piombo	I.G.F. Merck T.P.	Fusione e tornitura	49,0	10,0	13 813	11,35	600,4	88
Stagno	C. Erba (T.P.)	Fusione e tornitura	55,0	10,0	24 545	7,28	504,9	160
Bismuto	I.G.F. Merck (purissimo)	Fusione e tornitura	72,0	10,0	13 872	9,80	544,3	100
Alluminio	Ist. Metalli Leggeri (99,7%)	Fusione e tornitura	99,0	10,0	25 483	2,69	932,7	398
Cadmio	I.G.F. Merck (in sbarre) T.P.	Fusione e tornitura	140,0	10,0	9 000	8,642	593,9	172

([3]) Tale costanza indica inoltre l'assenza di fenomeni di rinvenimento, durante i quali, come è stato precedentemente segnalato, la ν_0 aumenta anche se la temperatura si mantiene costante.

lentissime variazioni di velocità e di temperatura che si hanno durante la fase di riscaldamento.

L'apparecchiatura elettroacustica per l'eccitazione e la misura delle vibrazioni, è sostanzialmente quella stessa dettagliatamente descritta in una nota precedente [4] e già adoperata in diverse altre ricerche. Sarà quindi sufficiente ricordare che essa consente la determinazione di v_0 con un errore relativo non superiore a $1 \div 2 \cdot 10^{-3}$, e con valori della deformazione dell'ordine di 10^{-8}.

3. – Misure effettuate ed interpretazione dei risultati.

La Tab. I indica i materiali su cui sono state effettuate le misure, la loro provenienza, il processo di lavorazione subito prima del rinvenimento, le dimensioni delle sbarrette e le rispettive frequenze. Per comodità si sono anche

TABELLA II. - *Valori sperimentali della velocità di propagazione di onde estensionali.*

Piombo Merck		Stagno C. Erba		Bismuto Merck		Alluminio Ist. Metalli Legg. 99,7%		Cadmio Merck	
T °K	c m/s^{-1}	T °K	c m/s^{-1}	T °K	c m/s^{-1}	T °K	c m/s^{-1}	T °K	c m/s^{-1}
238	1 398	289	2 700	201	2 044	245	5 121	298	2 520
246	1 393	323	2 650	218	2 036	259	5 092	339	2 475
250	1 389	348	2 603	243	2 022	272	5 071	368	2 441
285	1 385	372	2 563	255	2 012	289	5 050	409	2 396
268	1 376	393	2 519	275	2 003	303	5 035	432	2 334
270	1 372	425	2 429	287	2 000	318	5 011	464	2247
287	1 361	448	2 325	317	1 982	335	4996	—	—
304	1 345	474	2 164	318	1 979	361	4 957	—	—
320	1 331	492	2 018	344	1 963	368	4 947	—	—
345	1 310	—	—	350	1 958	389	4 922	—	—
374	1 287	—	—	369	1 946	391	4 917	—	—
399	1 265	—	—	377	1 934	419	4 888	—	—
425	1 243	—	—	390	1 924	454	4 836	—	—
451	1 222	—	—	414	1 896	463	4 826	—	—
464	1 208	—	—	416	1 900	481	4 797	—	—
478	1 198	—	—	443	1 874	491	4 777	—	—
487	1 188	—	—	470	1 849	520	4 740	—	—
519	1 153	—	—	497	1 821	552	4 685	—	—
557	1 086	—	—	520	1 788	578	4 629	—	—
—	—	—	—	531	1 773	602	4 586	—	—
—	—	—	—	—	—	628	4 540	—	—
—	—	—	—	—	—	649	4 508	—	—

[4] Cfr. P. G. BORDONI: *Nuovo Cimento*, **4**, 177 (1947); *Ric. Scient.*, **8**, 103 (1948).

riportati i valori della temperatura di fusione, di quella di Debye e della densità a temperatura ambiente.

I risultati delle misure effettuate sono raccolti nella tab. II. Le curve $c(t)$ che da essi possono essere ricavate, non si prestano però ad istituire un confronto fisicamente significativo tra il comportamento dei diversi metalli; sembra invece preferibile considerare anzichè i valori assoluti di T e di c o, come altri ha fatto, di dc/dT, i rapporti di tali grandezze rispettivamente alla temperatura di fusione T_f ed alla velocità limite c_0 cui tende c quando la T si avvicina allo zero assoluto.

Per evitare le notevoli difficoltà sperimentali inerenti alla determinazione di c_0, basta osservare che sussiste l'identità

$$(2) \qquad -\frac{\partial \log \dfrac{c}{c_0}}{\partial T} = -\frac{\partial \log c}{\partial T} = \beta \,,$$

la quale mostra che la derivata logaritmica della curva sperimentale $c(T)$ ha un significato più generale della curva stessa. Infatti il coefficiente β definito
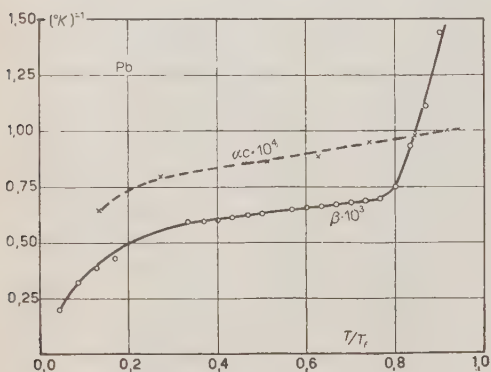

Fig. 1. – Variazioni con la temperatura di β e di α_c per il Piombo, in funzione del rapporto della temperatura assoluta alla temperatura di fusione.

dalla (2) ha per la velocità un ufficio analogo a quello che il coefficiente di dilatazione $\alpha_c = (\partial \log V/\partial T)$ ha per il volume: come α_c consente di paragonare tra loro le dilatazioni di corpi aventi volumi differenti, così β permette il confronto tra le variazioni di c anche per metalli che abbiano valori assoluti della velocità molto diversi tra di loro. Naturalmente, trattandosi di una derivata grafica o numerica, la $\beta(T/T_f)$ è affetta da errori alquanto maggiori di quelli relativi alla curva sperimentale $c(T)$, ma l'elevata precisione delle misure contiene tali errori nei limiti perfettamente accettabili di qualche unità per cento.

Nella fig. 1 sono riportati, in funzione di T/T_f, i valori di β e, a scopo di confronto, anche quelli del coefficiente di dilatazione cubica [5].

---

[5] Cfr. FDK. L. UFFELMANN: *Phil. Mag.*, **10**, 633 (1930); oppure P. HIDNERT, W. T. SWEENEY: *U.S. National Bureau of Standards Journ. of Rs.*, **9**, 703 (1932).

Alle basse e medie ([6]) temperature le due curve hanno un andamento del tutto simile: in particolare si nota in entrambe un tratto abbastanza esteso, corrispondente a $0.2 < T/T_f < 0.75$ nel quale le variazioni sono sensibilmente lineari, e le curve si avvicinano molto a delle rette orizzontali. Invece per $T/T_f > 0.75$ la pendenza della curva $\beta(T/T_f)$ aumenta fortemente, e tale comportamento non trova alcun riscontro in quello della $\alpha_c(T/T_f)$, la cui pendenza si mantiene quasi costante.

Per lo stagno (fig. 2) i valori di β e di α_c che si posseggono ([7]) sono relativi ad un campo di temperature assai più ristretto, e comunque tutto al disopra del punto di trasformazione dalla forma tetragonale a quella cubica (291 °K). Tali valori sono tuttavia sufficienti ad indicare anche per lo stagno l'esistenza di un intervallo di temperatura, limitato superiormente da $T/T_f = 0.75$, nel
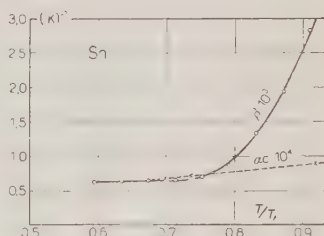

Fig. 2. – Variazioni con la temperatura di β e di α_c per lo Stagno, in funzione del rapporto della temperatura assoluta alla temperatura di fusione.

quale le curve $\alpha_c(T/T_f)$ e $\beta(T/T_f)$ hanno un andamento molto simile e sensibilmente rettilineo, con piccola inclinazione rispetto all'asse delle ascisse. Invece per $T/T_f > 0.75$ la pendenza della curva β aumenta, anche in questo caso, molto più fortemente di quella della curva relativa alla dilatazione termica. Lo stesso andamento si riscontra pure nel Bismuto (fig. 3) per il quale i dati sulla dilatazione termica sono tuttavia troppo incerti, per consentire un efficace confronto.
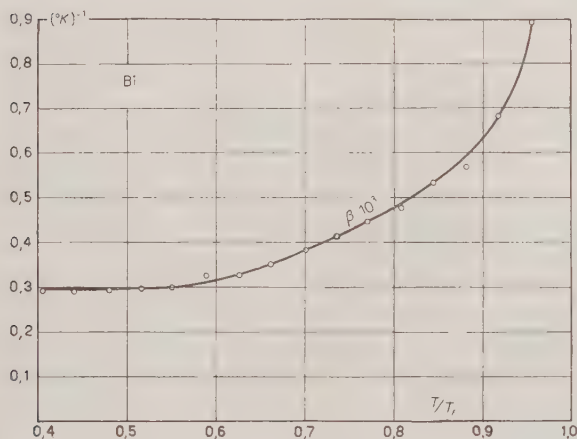

Fig. 3. – Variazioni con la temperatura di β per il Bismuto, in funzione del rapporto della temperatura assoluta alla temperatura di fusione.

([6]) I valori relativi alle basse temperature sono desunti da una ricerca precedente: cfr. P. G. BORDONI: *Elastic behaviour of some face-centered metals at very low temperatures* (in corso di pubblicazione).

([7]) Per i valori di α_c cfr. il primo lavoro citato nella nota ([5]).

Più complicato appare invece l'andamento delle curve relative all'Alluminio ed al Cadmio (figg. 4, 5). In entrambe si nota innanzi tutto la presenza di un massimo abbastanza acuto, dovuto probabilmente a qualche fenomeno di ri-
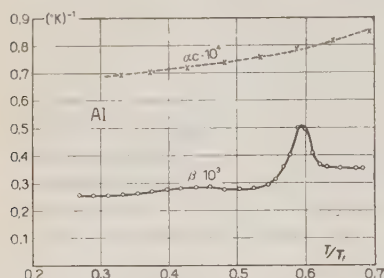

Fig. 4. – Variazioni con la temperatura di β e di α_c per l'Alluminio, in funzione del rapporto della temperatura assoluta alla temperatura di fusione.

lassamento. Infatti considerazioni teoriche abbastanza semplici [8], mostrano che le curve $c(\nu)$ e $c(T)$ possiedono un punto di flesso corrispondente rispettivamente a quei valori della frequenza, o della temperatura, per i quali il periodo di oscillazione della sbarretta, assume un valore prossimo al tempo caratteristico di rilassamento. Le derivate, semplici o logaritmiche, di tali curve rispetto a ν oppure a T, debbono quindi presentare, in corrispondenza al flesso, dei massimi, come quelli che si osservano nelle figg. 4 e 5.

Alle temperature in cui l'effetto di rilassamento non è sensibile ($T < 0.5\,T_f$, per l'Alluminio; $T < 0.65\,T_f$, per il Cadmio) le curve α_c e β hanno sensibilmente lo stesso andamento [9] in entrambi i metalli.

In definitiva il confronto tra le diverse curve che caratterizzano le variazioni relative di velocità e le corrispondenti curve che caratterizzano invece le dilatazioni termiche, rivela, nonostante la presenza di accidentali fenomeni di rilassamento, l'esistenza di una sostanziale similitudine nel comportamento dei diversi metalli riguardo alle variazioni di velocità ed alle dilatazioni termiche, almeno per temperature minori di $0.7\,T_f$. Dal punto di vista teorico tale similitudine appare perfettamente giustificata dal fatto che le variazioni di volume e di velocità sono entrambe dovute ad una stessa causa, e cioè alla non-linearità delle
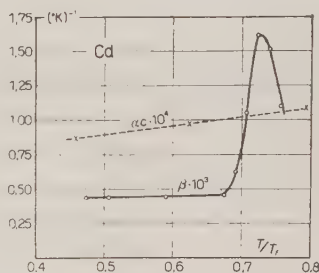

Fig. 5. – Variazioni con la temperatura di β e di α_c per il Cadmio, in funzione del rapporto della temperatura assoluta alla temperatura di fusione.

città sono entrambe dovute ad una stessa causa, e cioè alla non-linearità delle

---

[8] Cfr. ad esempio: C. ZENER: *Elasticity and anelasticity of solids* (Chicago, 1948); oppure: P. G. BORDONI: *Nuovo Cimento*, **7**, 144 (1950).

[9] Per i valori di α relativi all'Alluminio cfr.: *Tables annuelles internationales de constantes et données numériques* (Paris (1931-1934), **11**, 1, n. 4, 2. Per il Cadmio cfr.: *International Critical Tables* (New York, 1933), **1**, 459.

relazioni che legano — in media — le azioni interatomiche alle dimensioni del reticolo.

I risultati sperimentali ottenuti suggeriscono quindi la possibilità di ricavare dalla equazione di stato dei solidi, analogamente a quanto già si è fatto per α_c [10] una relazione teorica che dia β in funzione della temperatura. Non sembra però che una tale relazione possa giustificare anche lo scostamento della curva $\beta(T/T_f)$ dalla $\alpha_c(T/T_f)$ che si verifica nei pressi del punto di fusione. Infatti T_f non compare direttamente nell'equazione di stato, e d'altra parte le ipotesi semplificative poste a base di quest'ultima, divengono sempre meno valide man mano che cresce la temperatura.

Sembra piuttosto che il forte aumento della pendenza che si riscontra nella curva $\beta(T/T_f)$ quando ci si avvicina al punto di fusione indichi l'esistenza di qualche fenomeno di rilassamento, il cui massimo, alle frequenze considerate può anche corrispondere a temperature maggiori di T_f.

4. – Conclusioni.

Le misure di velocità delle onde elastiche eseguite in funzione della temperatura ed a frequenze comprese tra 5 kHz e 25 kHz su Pb, Sn, Bi, Al, Cd, mostrano che:

1) Le curve che danno $-\partial \log c/\partial T$ in funzione di T/T_f hanno sostanzialmente lo stesso andamento per tutti i metalli considerati, nonostante la presenza, nei provini di Al e di Cd, di fenomeni di rilassamento il cui effetto è d'altronde sensibile soltanto in un ristretto intervallo di temperatura.

2) Tali curve possiedono un tratto intermedio, abbastanza esteso, che appare sensibilmente rettilineo e poco inclinato sull'asse delle ascisse.

3) Per ognuno dei metalli considerati e per $T < 0,7\, T_f$, la curva che dà $-\partial \log c/\partial T$ ha inoltre lo stesso andamento di quella che caratterizza $\partial \log V/\partial T$.

4) Quando ci si avvicina alla temperatura di fusione la pendenza della curva $\partial \log c/\partial T$ aumenta fortemente, mentre nulla di simile si verifica nella $\partial \log V/\partial T$.

[10] Cfr. ad esempio: J. C. SLATER: *Introduction to chemical physics* (New York, 1939), p. 219.

SUMMARY

The velocity c of extensional waves has been determined as a function of temperature T for five pure metals (Pb, Sn. Bi, Al and Cd). The vibration frequency had its lowest value for Cadium (9000 cps at 20 °C) and the highest one for Aluminium (25 483 cps at 20 °C); the strain was of the order of 10^{-8}. From the experimental data the coefficient $\beta = -\partial \log c/\partial T$ has been computed, and the curves $\beta(T/T_c)$ traced T_c being the melting point temperature. From the inspection of the above curves, and their comparison with the corresponding ones for the thermal expansion coefficient $\alpha_c = \partial \log V/\partial T$ suggest the following conclusions: 1) For the five metals investigated the $\beta(T/T_c)$ curves look substantially alike, notwithstanding some relaxation phenomena, which occur in the Aluminium and Cadmium samples. 2) All these curves in an intermediate temperature range are straight lines and in the same range β keep almost constant. 3) For every metal among the five considered, and for $T < 0.7\,T_c$ the β and α_c-curves are rather similar to one another. 4) When T gets near the melting point value the β curve becomes more and more steep, while nothing of the kind happens in the α_c-curve.

Diffrazione dei raggi X nei liquidi.

F. Cennamo

Istituto di Fisica Sperimentale dell'Università - Napoli

Riassunto. — Si descrive il metodo sperimentale seguito per la misura dell'intensità dei raggi X diffratti dai liquidi e si riportano i risultati relativi al benzolo ed al cicloesanolo.

Allorquando un fascetto monocromatico di raggi X attraversa un liquido, l'intensità dei raggi da questo diffratti presenta uno o più massimi in corrispondenza di particolari valori degli angoli di diffusione che dipendono sia dal liquido che dalla lunghezza d'onda della radiazione impiegata: interponendo una lastra fotografica normalmente al percorso del fascetto che attraversa il liquido si ottengono anelli di diffrazione più o meno sfumati.

Questo comportamento mostra che nella sostanza allo stato liquido resta indubbiamente una regolarità ed infatti la distanza tra le molecole di una sostanza allo stato liquido calcolata per diffrazione dei raggi X, e la distanza tra le molecole della stessa sostanza allo stato solido determinata col metodo delle polveri sono tanto vicine che in prima approssimazione si possono considerare le stesse.

Diverse teorie sono state proposte per spiegare la diffrazione dei raggi X prodotta dai liquidi (Keesom e de Smedt [1], C. V. Raman e K. R. Ramanathan [2], Debye [3], P. Zernike e J. A. Prins [4], H. Menke [5], G. W. Stewart [6], ecc.), ma qualunque possa essere l'interpretazione è evidente che

[1] W. H. Keesom e J. de Smedt: *Proc. Acad. Amsterdam*, **27**, 112 (1923).
[2] C. V. Raman e K. R. Ramanathan: *Nature*. **3**. 185 (1923).
[3] P. Debye: *Phys. Zeits.*, **28**, 135 (1927).
[4] P. Zernike e J. A. Prins: *Zeits. f. Phys.*, **41**, 184 (1927).
[5] H. Menke: *Phys. Rev.*, **33**, 593 (1932).
[6] G. W. Stewart: *Phys. Rev.*, **32**. 153 (1928).

la presenza di anelli di diffrazione nei liquidi sta ad indicare la presenza di piani reticolari e quindi di raggruppamenti regolari dovuti alla permanenza di forze intermolecolari più deboli, ma della stessa natura di quelle esistenti allo stato solido. In alcune note precedentemente pubblicate [7] noi abbiamo riportato l'andamento delle intensità dei raggi X diffratti da alcune sostanze allo stato liquido sia al variare della temperatura sia al variare della concen-trazione in alcuni miscugli: ci proponiamo ora di descrivere il metodo seguito in queste misure.
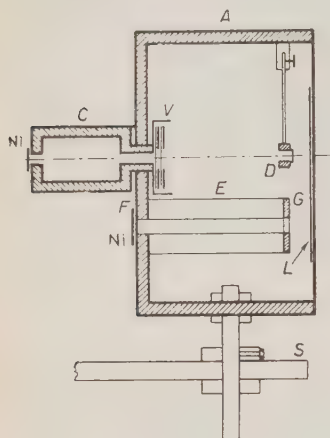

Fig. 1.

Il dispositivo sperimentale utilizzato è illustrato in fig. 1: la scatola A, a pareti di piombo dello spessore di 7 mm, rigidamente fissata al tubo a raggi X a mezzo del so-stegno S, presenta nella sua parete anteriore un collimatore costituito da un tubo cilin-drico cavo di piombo sulle cui basi è prati-cato, in corrispondenza dell'asse, un foro del diametro di 1 mm. Un terzo foro, in asse coi precedenti, è praticato sulla parete della sca-tola ed è, dalla parte rivolta verso la va-schetta contenente il liquido da analizzare, opportunamente svasato. Il fascetto di raggi X, così delimitato, dopo aver attra-versato il liquido posto nella vaschetta V, giunge sulla lastra fotografica L; lungo il percorso però incontra un di-schetto di piombo D del diametro di 4 mm e dello spessore di 3 mm con al centro un foro di 2 mm, chiuso da una laminetta di piombo di spessore opportuno: la intensità del fascetto incidente è così ridotta in modo che l'an-nerimento da essa prodotto risulti uguale all'incirca a 0,6-0,7 e cioè perfetta-mente misurabile.

Al disotto del cilindro C sulla parete anteriore della scatola una fenditura orizzontale F, lunga 15 mm ed alta 5 mm si prolunga nell'interno in un tubo E a pareti molto spesse della stessa sezione.

Lungo E, il cui asse è opportunamente inclinato rispetto al tubo a raggi X, passa quindi un fascetto di raggi X, ridotto in intensità da una laminetta di piombo di spessore opportuno e da un filtro di nichel dello stesso spessore di quello utilizzato per rendere monocromatico il fascetto che attraversa il colli-matore.

[7] F. CENNAMO: *Rend. Acc. Lincei*, **9**, 339 (1950); **10**. 310 (1951), **10**. 475 (1951); **12**, 294 (1952).

Una spessa lamina di piombo G, nella quale sono incise sette fenditure, posta all'estremo del tubo E, permette l'uscita di sette fascetti di uguale intensità: l'uguaglianza delle intensità dei fascetti emergenti dalle fenditure è stata sempre assicurata dal fatto che i rispettivi annerimenti prodotti sulla lastra fotografica, misurati al microfotometro, risultano uguali.

Disponendo invece lungo queste fenditure delle laminette di piombo di spessore diverso, i fascetti emergenti dalla lamina G risulteranno di diversa intensità e quindi in corrispondenza sulla lastra fotografica produrranno delle tracce con annerimenti diversi. Noi ci siamo avvalsi di queste marche per costruire una curva di taratura la quale consentisse di

Fig. 2.

trasformare la distribuzione degli annerimenti prodotti dai raggi diffratti dal liquido sulla lastra fotografica in distribuzione d'intensità, ed allo scopo abbiamo proceduto nel seguente modo.

Com'è noto, i raggi X, per quanto riguarda la loro azione fotografica, solo apparentemente sono simili alle radiazioni visibili ed a quelle ultraviolette: l'esame microscopico di uno strato sensibile esposto all'azione dei raggi X mostra, a differenza della luce visibile, che i raggi X producono attraverso l'intero spessore dello strato sensibile un'uguale distribuzione di granuli di argento depositato: variando l'intensità del fascetto incidente varia il numero di granuli di argento depositati per unità di volume, ferma restando la uniformità di distribuzione per l'intero spessore dell'emulsione. Pertanto una lastra fotografica, esposta all'azione dei raggi X, esaminata per trasparenza si comporta come una lamina a spessore costante ma con coefficiente di assorbimento variabile da punto a punto a seconda della intensità del fascetto di raggi X che ha colpito ciascun punto della lastra.

Indicando con D_0 la deviazione segnata dal galvanometro del microfotometro per un punto non colpito dall'azione dei raggi X, e con D la deviazione misurata invece in corrispondenza di un punto colpito dall'azione delle radiazioni, l'annerimento S è definito dall'espressione seguente:

(1)
$$S = \log_{10} \frac{D_0}{D} .$$

L'annerimento S così definito varia in funzione del tempo di esposizione t, dell'intensità I del fascetto incidente e della lunghezza d'onda λ della radiazione, per cui si può scrivere:
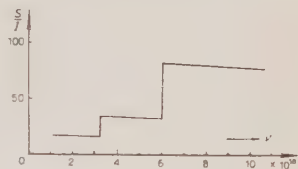
(2)
$$S = f(I, t, \lambda) .$$

A parità di I e t, l'annerimento è una funzione piuttosto complessa di λ come si può osservare nella fig. 2 riportata dal lavoro di R. BERTHOLD ed R. GLOCKER ([8]): S decresce con legge lineare molto lentamente per frequenze crescenti sino a $\nu = 3{,}23 \cdot 10^{18}$, aumenta bruscamente in corrispondenza di tale frequenza, decresce con la stessa legge nell'intervallo di frequenze $3{,}23\text{-}6{,}00 \cdot 10^{18}$, subisce in corrispondenza di tale frequenza un ulteriore aumento brusco ed
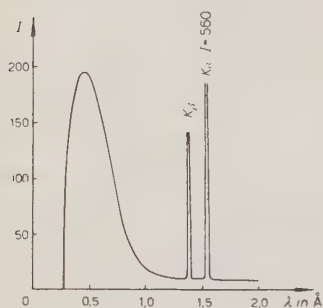

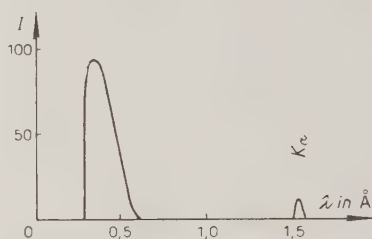Fig. 3.   Fig. 4.

infine decresce con l'aumentare della frequenza sempre con legge lineare molto prossima a quella relativa ai due intervalli precedenti.

Le brusche variazioni sono dovute all'assorbimento selettivo del bromo e dell'argento dell'emulsione e si manifestano in corrispondenza del passaggio da lunghezze d'onde superiori a lunghezze d'onda inferiori a quelle corrispondenti ai rispettivi massimi di assorbimento di queste due sostanze.

Poichè, come si è fatto osservare, la diminuzione di S colle lunghezze d'onda è, per ciascuno dei tre intervalli considerati, molto piccola, l'annerimento si può, per lo meno in prima approssimazione, in ciascuno di questi tre intervalli considerare indipendente da λ, ed inoltre, determinato per uno dei tre intervalli spettrali l'andamento della funzione $S = f(I, t)$ si potrà ricavare quello relativo agli altri due intervalli moltiplicando le intensità corrispondenti ai diversi annerimenti per un coefficiente numerico facilmente ricavabile dalla fig. 2.

A tali criteri ci siamo ispirati nella determinazione delle curve di taratura delle lastre a mezzo delle marche precedentemente descritte.

Lo spettro di un ordinario tubo a raggi X con anticatodo di rame contiene, oltre alle radiazioni CuK_γ e CuK_β caratteristiche anche delle radiazioni con λ più piccole, ed il filtro di nichel, che con lo spessore da noi adoperato rende

([8]) R. BERTHOLD e R. GLOCKER: *Zeits. f. Phys.*, **31**. 261 (1925).

sufficientemente monocromatico il fascio agli effetti della diffrazione dei liquidi, eliminando la CuK$_\beta$ lascia passare, ed in buona parte, anche queste radiazioni.

In fig. 3 si è riportata la distribuzione spettrale dei raggi X emessi da un anticatodo di Cu per una tensione applicata agli elettrodi di 44 kV [9]; nella fig. 4 invece è riportata la stessa distribuzione spettrale filtrata però attraverso una lamina di nichel dello spessore di 10^{-2} cm da noi utilizzata. Il successivo filtro di piombo, usato per la costruzione delle marche, riduce del tutto la intensità della radiazione CuK$_\beta$ e molto poco quella delle radiazioni dure e ciò in dipendenza del fatto che la curva di assorbimento del piombo presenta valori molto elevati per $\lambda = 1,4$ Å ed un massimo molto meno accentuato per $\lambda = 0,7$ Å.

L'annerimento delle marche di controllo si può quindi considerare prodotto da radiazioni le cui lunghezze d'onda sono comprese nell'intervallo spettrale: $\lambda = 0,5\text{-}0,2$ Å.

Com'è noto, l'intensità del fondo continuo emesso da un anticatodo varia proporzionalmente al quadrato della tensione applicata al tubo, mentre l'intensità della radiazione monocromatica caratteristica varia all'incirca proporzionalmente a $(V - V_0)^{3,2}$, in cui V_0 è la tensione di eccitazione della radiazione monocromatica: mantenendo quindi costante sia la tensione applicata che la corrente che passa nell'ampolla si può ritenere che resti costante la distribuzione spettrale emessa dall'anticatodo e quindi quella relativa alle piccole λ trasmessa attraverso i due filtri.

Poichè nell'intervallo spettrale innanzi citato S si può considerare indipendente da λ, potremo, in queste condizioni, ritenere l'annerimento solo funzione di I e di t e precisamente si può porre:

$$(2) \qquad S = I \cdot t^p ,$$

essendo p un coefficiente numerico che tende ad 1 per piccole intensità

Però per determinare il valore dell'intensità I_i del fascio emergente dalla i-esima fenditura non è evidentemente possibile avvalersi della relazione:

$$I_i = I_0 \exp\left[-\mu x_i\right] ,$$

nella quale I_0 rappresenta l'intensità del fascio incidente su ciascuna delle sette fenditure, μ il coefficiente di assorbimento del piombo, x_i lo spessore di piombo attraversato, sia perchè, come si è detto, il fascio non è monocromatico e quindi essendo $\mu = f(x, \lambda)$ i calcoli sarebbero piuttosto laboriosi e sia perchè la parte assorbita dallo schermo:

$$I_{a, i} = I_0(1 - \exp\left[-\mu x_i\right]),$$

[9] J. BOUMAN: *Selected Topics in X-Ray Crystallography* (Amsterdam, 1951), p. 116.

è, com'è noto, in parte riemessa sotto forma di radiazioni secondarie (radia-
zioni di fluorescenza, radiazione diffusa senza cambiamento di lunghezza d'onda,
effetto Compton) e queste radiazioni secondarie apportano anche un loro con-
tributo, sia pure modesto, all'annerimento della lastra fotografica che risulta
pertanto maggiore di quello che si avrebbe, a parità
dell'intensità del raggio trasmesso, in loro assenza.
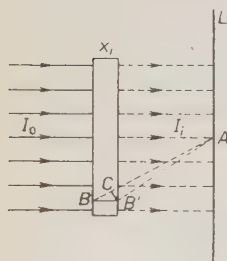
Fig. 5.

In altre parole, su di un punto A della lastra foto-
grafica L (fig. 5), oltre al raggio con intensità I_i tra-
smesso attraverso lo spessore x_i della laminetta di
piombo, giungeranno anche le radiazioni parassite
secondarie riemesse a causa dell'assorbimento attra-
verso lo schermo e provenienti da tutti i punti di questo.

Abbiamo pertanto preferito procedere alla taratura
delle marche per via sperimentale ed allo scopo sono
state eseguite, sulla stessa lastra, fotografie dei sette
fascetti emergenti dallo schermo G con tempi di posa
diversi avendo cura che durante l'esposizione le condizioni di funzionamento
del tubo restassero rigorosamente costanti in modo da poter considerare tali sia
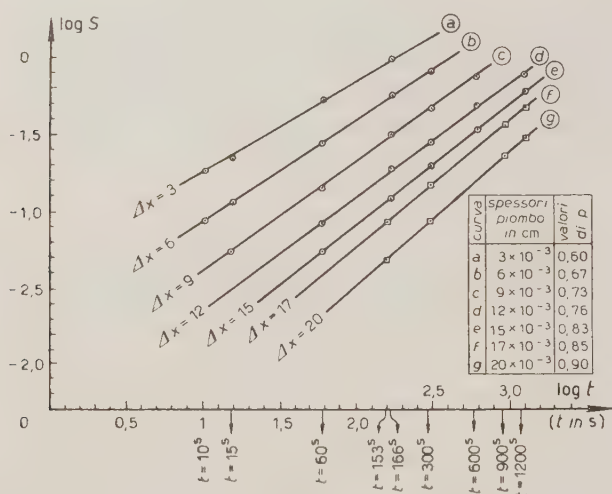
Fig. 6.

la composizione che l'intensità di ciascun fascetto.

Riportando (fig. 6) sull'asse delle ordinate i logaritmi degli annerimenti
prodotti da ciascuna fenditura e su quelle delle ascisse i logaritmi dei corri-

spondenti tempi di posa si sono ottenute, in accordo con la relazione:

$$\log S = p \log t + \text{costante}$$

delle rette.

I coefficienti angolari di queste rette danno i valori di p corrispondenti a ciascuno degli spessori di piombo attraversati.

In fig. 7 è riportato l'andamento di p in funzione di Δx: con l'aumentare di Δx e quindi col diminuire dell'intensità del fascetto incidente sulla lastra, p tende al valore unitario.
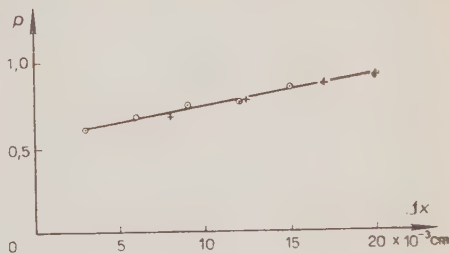
Determinati i valori di p e quindi delle espressioni t^p, si riportano (fig. 8) sull'asse delle ordinate gli annerimenti S e su

Fig. 7.

quelle delle ascisse i corrispondenti valori t^p e per ciascuna marca si ottiene una retta il cui coefficiente angolare esprime, in base alla (2), il valore della
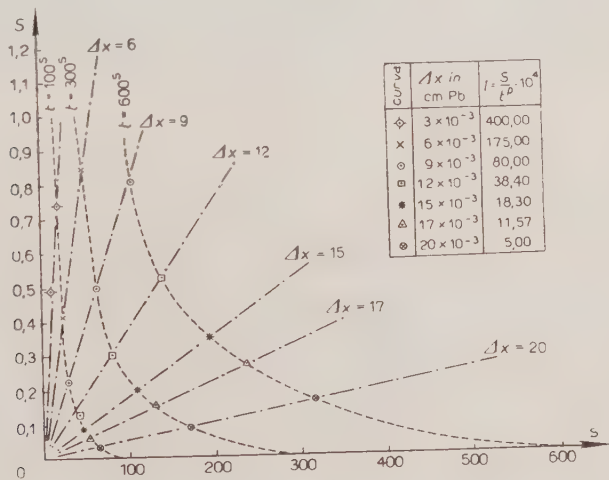
Fig. 8.

intensità del fascetto trasmesso attraverso la marca in esame.

Nella fig. 9 sono riportati i risultati relativi a diverse marche d'intensità ottenuti con lastre diverse, sempre nelle stesse condizioni di funzionamento del tubo, ma con tempi di posa diversi: si ottengono, riportando sull'asse delle

ascisse gli spessori di piombo attraversati e sulle ordinate i logaritmi naturali dei rapporti $S/t^p = I$, delle rette tra loro parallele, il cui coefficiente angolare, col segno cambiato, rappresenta il coefficiente angolare di cui si è innanzi parlato. Tale coefficiente è risultato uguale a $K = 252$ cm^{-1}.

Se si tien conto del fatto che le sostanze attraversate sono il piombo ed il nichel, che le radiazioni trasmesse sono comprese tra $\lambda = 0.28$ Å e $\lambda = 0.50$ Å
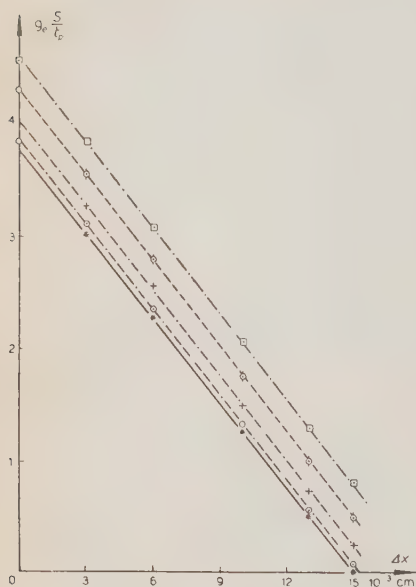
Fig. 9.
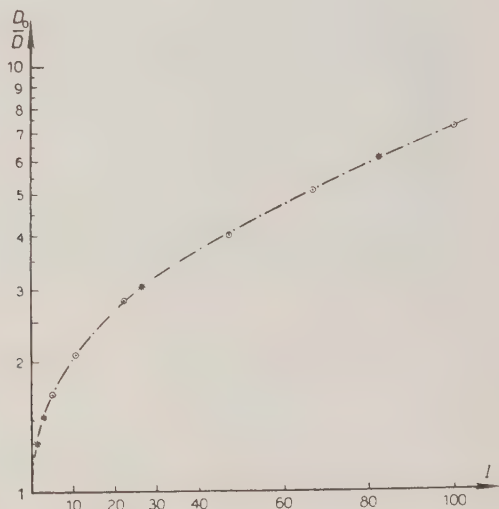
Fig. 10.

e che in quest'intervallo per il piombo è, in media $\mu_1 = 340$ cm^{-1} e per il nichel si ha $\mu_2 = 90$ cm^{-1}, il valore di K ottenuto è abbastanza vicino a quello $K' = 280$ cm^{-1} che si ottiene dalla relazione:

$$K' = \frac{\mu_1 x_1 + \mu_2 x_2}{x_1 + x_2}.$$

nella quale x_1 ed x_2 rappresentano rispettivamente gli effettivi spessori di piombo e di nichel attraversati. Il valore sperimentale di K, inferiore a quello così ottenuto, può giustificarsi pensando all'influenza delle radiazioni secondarie di cui si è innanzi parlato.

Poichè, anche nelle stesse condizioni di funzionamento del tubo, l'annerimento delle marche può variare da lastra a lastra e per variazioni nel tempo

di posa e per le variate condizioni di sviluppo, si deve, al fine di rendere confrontabili i risultati ottenuti con lastre diverse, nell'assegnare il valore dell'intensità relativa alla marca più intensa, determinarne il valore I_1 per interpolazione della curva annerimenti-intensità relativa ad una lastra della stessa
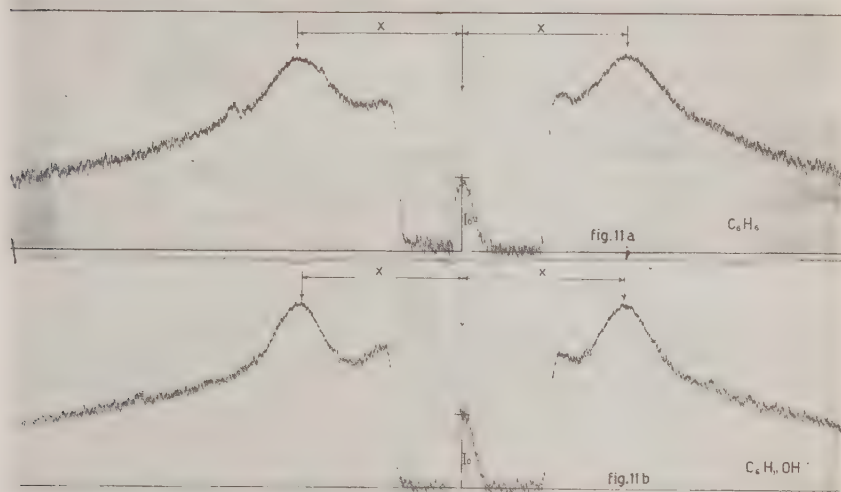
Fig. 11.

serie e poi stabilire quello da assegnare alle altre marche di controllo dalla relazione:

$$I_i = I_0 \exp \left[- kx_i\right].$$

Nella fig. 10 è riportata la curva di taratura delle lastre Ferrania tipo U, relative ad una serie di fotografie.

Nelle fig. 11 a) e b) sono riportate le microfotometrie degli anelli di diffrazione ottenuti per il benzene e per il cicloesanolo: la vaschetta nella quale era posto il liquido in esame era a pareti di mica, per cui sulla lastra fotografica oltre all'anello di diffrazione prodotto dal liquido compaiono in parte a questo sovrapposti i Laue prodotti dalla mica che però, come del resto appare dalle fig. 11 possono, nell'eseguire la microfotometria dell'alone, facilmente evitarsi, scegliendo una direzione opportuna.

Nella fig. 12 sono riportate le distribuzioni d'intensità delle stesse sostanze in funzione degli angoli di diffrazione espressi in radianti; i valori ottenuti per le intensità nelle varie direzioni sono stati moltiplicati per l'espressione $I/\cos^3 \theta$.

Questo fattore di correzione è stato introdotto allo scopo di poter confrontare i valori ottenuti per le intensità relativamente a punti diversi della lastra fotografica i quali, essendo quest'ultima piana, capitavano a distanze dal punto nel quale era posto il liquido colpito dal fascetto di raggi X diverse fra loro.

Infine nella fig. 13 sono riportate le bande di diffrazione caratteristiche delle due sostanze, le quali sono state ottenute sottraendo il continuo che si estende
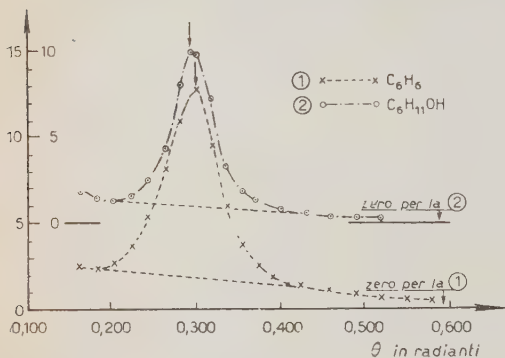
Fig. 12.
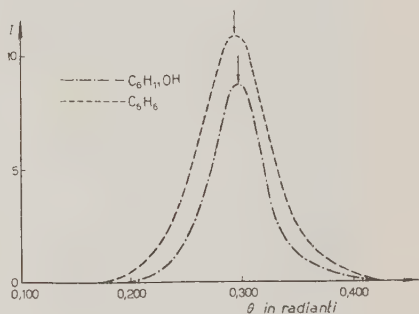
Fig. 13.

da 0,2 a 0,6 radianti. I massimi di diffrazione sono di poco spostati tra loro, però la larghezza delle due bande di diffrazione, misurata in corrispondenza dell'intensità $I' = \frac{1}{2} I_m$ è notevolmente diversa: per il cicloesanolo si ha, come del resto appare dal confronto delle microfotometrie, una banda di diffrazione molto più stretta.

Le due distribuzioni d'intensità relative a queste due bande di diffrazione verranno utilizzate in un prossimo lavoro in corso di pubblicazione.

- -

SUMMARY (*)

The experimental method is reported emploied in determining the intensity of X rays diffracted by liquids and results are given referring to benzene and cyclo-hexanol.

———— ————

(*) *Editor's translation.*

Cascades in the Gamma-Ray Spectrum of $^{214}_{84}$Po.

F. Demichelis and R. Malvano

Istituto di Fisica Sperimentale del Politecnico - Torino

Summary. — Coincidence absorption measurements have been conducted on the γ-ray spectrum of $^{214}_{84}$Po. We have proved the existence of a strong γ-ray cascade of 1,120-1,761 MeV respectively. On the basis of our results the two level schemes suggested by E. Rutherford and J. Surugue have been compared.

1. – Introduction.

The study of the decay spectrum of natural radioactive nuclides, initiated long before the discovery of artificial radioactivity, has not yet given a knowledge of the β and γ spectra of natural nuclides as complete as for nearly all the artificial ones.

The incompleteness of the data about those spectra is not caused by the lack of systematic studies on the subject but by the great spectral complexity of the nuclides belonging to the natural radioactive series.

We wished to extend the experimental knowledge of the case of γ-ray cascades, which are useful in the studies of nuclear levels. Taking also into account certain already well know intuitions [1] [2], we have settled our attention on the case of $^{214}_{83}$Bi(RaC), of the $^{226}_{88}$Ra series, which presents a very complicated decay spectrum.

It decays (half-life $T = 19,7$ min) $99,96\%$ into $^{214}_{84}$Po, thus emitting β particles, and $0,04\%$ into $^{210}_{81}$Tl, emitting α-particles [3].

[1] E. Rutherford, W. B. Lewis and B. V. Bowden: *Proc. Roy. Soc.*, A **142**, 347 (1933).

[2] J. Surugue: *Journ. de Phys. et le Radium*, (8), **7**, 145 (1946).

[3] F. Rasetti: *Elements of Nuclear Physics* (London, 1937), p. 37.

$^{214}_{84}$Po, making electromagnetic transitions from the excited to the ground state, emits many γ-rays of different wave lengths and intensities.

Our aim in this research is to study the γ transitions of $^{214}_{84}$Po and in particular to verify experimentally the existence of possible γ-ray cascades.

In order to make the subject clearer we set forth more elaborate data about spectroscopy of the γ-rays and of long range α particles emitted by $^{214}_{84}$Po, both of fundamental importance in our problem.

2. – γ-ray spectrum of $^{214}_{84}$Po.

The information usually given concerns the energies and the number of quanta emitted by $^{226}_{88}$Ra, and its equilibrium decay products; in this case for each α particle emitted by $^{226}_{88}$Ra we have in the average a disintegration of every nuclide of the $^{226}_{88}$Ra series.

The data of Table I, obtained from the results given in various papers [4] have been acquired experimentally in different ways, i.e. measuring, by means of a β spectrograph:

— the energy of the Compton electrons produced in the interaction of γ-rays with matter and emitted at a certain angle with the direction of the incident γ-ray;

— the energy of the internal conversion positrons which originate in the interaction of γ-rays, having energy > 1 MeV, with the Coulomb field near the nucleus;

— the energy of the internal conversion electrons, which are pulled off from the electronic cloud quite close to the nucleus due to the interaction of the γ-rays.

The above results have been partly confirmed and improved by M. MLA-DENOVIC and A. HEDGRAM [5] in very recent measurements; incidentally we may observe that with the procedure and the improvement of the measurements, the γ-ray spectrum of $^{222}_{88}$Ra and its equilibrium decay products become more and more complicated, because new energy rays are discovered, fortunately of very small intensity.

We can state, therefore, that the essential feature of this spectrum is now well defined.

―――― ― ―- -

[4] C. D. ELLIS and G. H. ASTON: *Proc. Roy. Soc.*, A **129**, 180 (1930); C. D. ELLIS: *Proc. Roy. Soc.*, A **143**, 350 (1935); G. D. LATYSHEV: *Rev. Mod. Phys.*, **19**, 132 (1947); W. BOTHE: *Zeits. f. Phys.*, **96**, 607 (1935).

[5] M. MLADENOVIC and A. HEDGRAM: *Proceedings of the Conference on β and γ Radio-activity* (Amsterdam, 1952); not yed published.

The same cannot be said about the intensity of the γ radiations. As intensity we mean the average quanta per α particle of $^{226}_{88}$Ra.

The inaccuracy about the γ-rays intensities is due partly to purely experimental reasons, which could be avoided by using very strong radioactive sources, and partly to uncertainties of the theories which tend to explain the interaction phenomena.

TABLE I. – *Gamma-ray spectrum of radium and its equilibrium decay products.*

Transition	Average quanta per alpha ray of $^{226}_{88}$Ra		Energy per photon (MeV)	
	(a)	(b)	(a)	(b)
$^{226}_{88}$Ra $\rightarrow$ $^{222}_{86}$Em	0,01	—	0,184	—
$^{214}_{82}$Pb $\rightarrow$ $^{214}_{83}$Bi	0,11	—	0,241	—
	0,26	—	0,294	—
	0,45	—	0,350	—
$^{214}_{83}$Bi $\rightarrow$ $^{214}_{84}$Po	0,03	—	0,426	—
	—	—	0,498	—
	0,66	—	0,607	0,606
	0,06	—	0,766	—
	0,07	—	0,933	—
	0,21	0,20	1,120	1,120
	0,06	0,05	1,238	1,234
	0,06	0,15	1,379	$\begin{cases}1,290\\1,370\end{cases}$
	—	—	—	1,414 (*)
	—	0,06	—	1,520
		0,29		$\begin{cases}1,620\\1,690\end{cases}$
	0,26		1,761	1,761
	—	0,04	—	1,820
	0,07	0,12	2,198	$\begin{cases}2,090\\2,200\end{cases}$
	—	0,04	—	2,420
$^{210}_{84}$Po $\rightarrow$ $^{206}_{82}$Pb	(c) 7·10^{-6}			(c) $\begin{cases}0,202\\0,798\\1,068\end{cases}$

(a) C. D. ELLIS and G. H. ASTON: *Proc. Roy. Soc.*, A **129**, 180 (1930); C. D. ELLIS: *Proc. Roy. Soc.*, A **143**, 350 (1934).

(b) G. D. LATYSHEV: *Rev. Mod. Phys.*, **19**, 132 (1947).

(c) W. BOTHE: *Zeits. f. Phys.*, **96**, 607 (1935).

(*) In the spectrum of the internal conversion electrons there is a line corresponding to a 1,414 MeV photon that however is not found in the γ-ray spectrum. This is a well-established case of non-radiative nuclear transition where the transference of energy to the electrons takes place through direct interaction.

We can thus understand why, in Table I, there are such discordant values for the intensities according to the different experimental methods and the different experimenters.

On the other hand it must be emphasized that the precise knowledge of the various γ-rays lines is very important in order to get the internal conversion ([6]) and the internal pair formation coefficients ([7]), and thus to establish the type of transition (dipole, quadrupole...,) involved in the γ-ray emission.

3. – $^{214}_{84}$Po long range α particles spectrum.

$^{214}_{84}$Po, emitting α particles, decays into $^{210}_{82}$Pb. The α particles spectrum of $^{214}_{84}$Po has been accurately determined by E. RUTHERFORD ([1]) by range measurements as well as with a magnetic spectrograph method.

The disintegration energy, i.e. the kinetic energy of the α particle plus the recoil energy of the nucleus, the energy excess of the long range α particles above the energy of the normal ones, and the number of α particles per disintegration ([1]) are given in Table II.

TABLE II.

Energy of disintegration (corrected for recoil) (MeV)	Energy excess of excited level above normal level (MeV)	Number of alpha-particles per disintegration $\times 10^{-6}$
7,829	0	10^6
8,437	0,608	0,43
9,112	1,283	(0,45)
9,241	1,412	22
9,493	1,663	0,38
9,673	1,844	1,35
9,844	2,015	0,35
9,968	2,138	1,06
10,097	2,268	0,36
10,269	2,439	1,67
10,342	2,513	0,38
10,526	2,697	1,12
10,709	2,880	0,23

([6]) H. R. HULME: *Proc. Roy. Soc.*, A **138**, 643 (1932); H. M. TAYLOR and N. F. MOTT: *Proc. Roy. Soc.*, A **138**, 665 (1932); H. R. FOWLER: *Proc. Roy. Soc.*, A **129**, 1 (1930).

([7]) J. C. JAEGER and H. R. HULME: *Proc. Roy. Soc.*, A **148**, 708 (1935).

Comparing Table I with Table II it can immediately be deduced that the observed long range α particles are emitted by $^{214}_{84}$Po formed in an excited state by β decay from its parent $^{214}_{83}$Bi nuclide.

From this standpoint the energy of these omogeneous groups of α particles represents the energy of the excited nuclear levels. In an extremely short interval ($< 10^{-11}$ s) the excited nucleus decays into the ground state and the energy excess of the α particles is emitted in the form of electromagnetic radiation, either as a single photon or as successive photons, in which case the excited nucleus passes through one or more transition energy levels.

Fig. 1. – The solid line levels correspond to measured long range α particles; those drawn in dotted and dashed lines have been assumed to exist according to Rutherford's scheme.

Obviously the number of α particles per disintegration is not directly connected with the intensity of the γ-rays emitted by $^{214}_{84}$Po. On the contrary the above two processes compete with each other; and while the emission probability of long range α particles increases with the energy of the α particles, and depends from the angular momentum of the excited state, the probability of emission of the associated γ-ray is connected with the absolute magnitude of dipole or quadrupole electric or magnetic moment of the transition: i.e. it depends on the distribution of charges inside the nucleus itself [8].

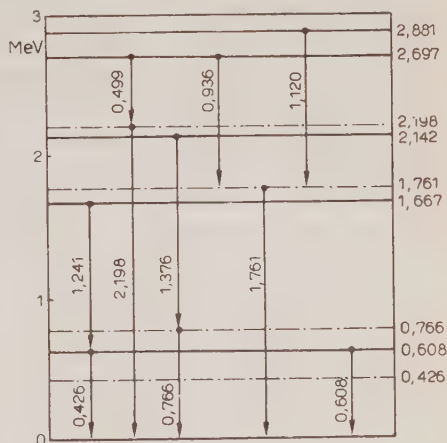Knowing the energies and the intensities of the γ-rays and the
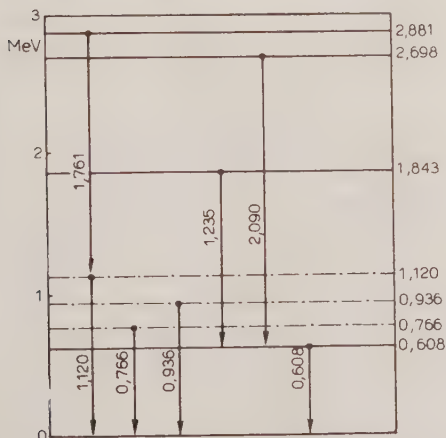
Fig. 2. – The solid line levels correspond to measured long range α particles; those drawn in dotted and dashed lines have been assumed to exist according to Surugue's scheme.

[8] G. GAMOW and C. L. CRITCHFIELD: *Theory of Atomic Nucleus and Nuclear Energy-Sources* (Oxford, 1949).

energies and the number of α particles per disintegration of $^{214}_{84}$Po, it is possible to build up schemes (figg. 1 and 2) [1] [2] of energy levels: these energy level schemes account fairly well for almost all experimental data we have about the α particles and γ-rays energy.

Building up these schemes it was necessary to consider not only direct transitions but more complicated ones between levels where the nucleus looses its excess energy in successive stages; i.e. it was necessary to admit, without experimental proof, the existence of γ-rays cascades, and one or more transition levels not connected with measurable long range α particles.

According to the purpose of our research (§ 1), we tried to *verify experimentally the existence of such cascades* [9]. *In order to test which one of the above schemes were the most acceptable we measured by an absorption method* [10] *the energy of the corresponding γ-rays.*

This was made possible thanks to the new very efficient technique of γ-ray detection.
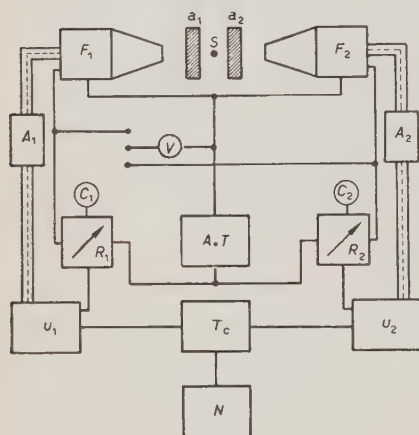
Fig. 3.

4. – Experimental apparatus.

The experimental apparatus used in our research is suitable to determine the absorption curves of two coincident γ-rays giving rise, namely, to a cascade of $^{214}_{84}$Po.

F_1 and F_2 (fig. 3) are two scintillation detectors consisting in 931A photomultipliers, placed so as to « see » the scintillations eventually produced inside NaI(Tl) crystals (*).

The voltage pulses at the output of the photomultipliers F_1 and F_2 are conveniently amplified through A_1 and A_2 and then brought to the grids (input) of two asymmetrical univibrators U_1 and U_2 acting as pulse shapers.

After a process of differentiation, the pulses are applied to the grids of a twin triode T_c, which indicates the possible coincidence of two pulses at its cathode output.

The numerator N records the total number of coincidences; C_1 and C_2 are

[9] F. DEMICHELIS and R. MALVANO: *Nuovo Cimento*, **9**, 1106 (1952).

[10] A. C. G. MITCHELL: *Rev. Mod. Phys.*, **20**, 296 (1948).

(*) Provided by the Physikalisches Synthetische Einkristalle Laboratorium - Kiel (Germany).

two counting rate meter (C.R.M.), which indicate the total counting rate of pulses at the output of the pulse shapers.

The d.c. voltage for the photomultipliers is given by the power supply $A \cdot T$ and measured by means of the electronic voltmeter V with an accuracy of 0.5% (or better).

The photomultiplier voltage is automatically regulated by R_1 and R_2 so that, for the same geometrical and physical conditions of the source and the detectors, the counting rate of the pulses is constant altough other concurring conditions (temperature, voltages on the single dynodes,...) may noticeably change ([11]).

The total voltage at the ends of the photomultipliers is placed at a voltage as high as 940 volt in order that the resolving time of the coincidence apparatus be indipendent from the pulse heights of the photomultipliers ([12]).

The absorbers a_1 and a_2 consist of a set of lead disks of various thickness and the same diameter of about 2 cm; they are placed between the source and the scintillation counters and entirely shield the one from the others.

The solid angles formed by the absorbers with the source and with the counters are very wide; but this fact cannot give rise to any inconvenience because accidental coincidence with Compton photons produced inside the absorbers are very improbable, as one can see by simple computation.

The source S (radium bromide in equilibrium with its decay products) has an activity I of about 35 μc and is contained inside a small glass enclosure.

From Table I we deduce that $^{226}_{88}$Ra, $^{222}_{86}$Em, $^{211}_{82}$Pb, γ-rays have too low energies; while the $^{206}_{82}$Pb γ-rays have too small an intensity to sensibly influence our experimental results, which therefore exclusively concern the $^{214}_{84}$Po.

5. – Measurements and experimental results.

Repeated coincidence measurements have been made with various thicknesss of absorbers.

A first series of measurements (symmetrical arrangement) have been done by placing an equal thickness of absorber in front of each detector and by counting the number of the coincidences for each thickness of lead from $x = x_0 = 0$ to $x = 12$ mm.

The counting rate of pulses from each detector being kept constant by a suitable stabilizer, as before said, if we introduce between source and detector an absorber, the detector counting rate would remain constant and the

([11]) R. Ascoli: *Nuovo Cimento*, **9**, 615 (1952).
([12]) F. Demichelis and R. Malvano: *Nuovo Cimento*, **9**, 1227 (1952).

photomultiplier voltage, and consequently the detector sensitivity, would change.

In order to avoid this inconvenience we act properly on the stabilizer so that we read always the same photomultiplier voltage on the electronic volt-meter.

After all to be sure that the detector sensitivity is always constant, we test at intervals, the constancy of the rate of pulses given by the C.R.M.: C_1 and C_2 with no absorber in front of the detectors.

A second series of measurements (asymmetrical arrangement) have been done placing a constant thickness (2 mm) of lead in front of one detector and a variable thickness from $x = x_0 = 2$ to $x = 16$ mm in front of the other.

The stabilizers R_1 and R_2 are regulated in the same way as before mentioned.

Points of fig. 4(a) and 4(b) represent the experimental data respectively for the symmetrical and asymmetrical arrangements. In both cases the abscissae represent the values of $x - x_0$ and the ordinates represent the ratio between the effective coincidence counting rate N_x for various absorber thicknesses and the effective coincidence counting rate N_{x_0} for minimum absorber
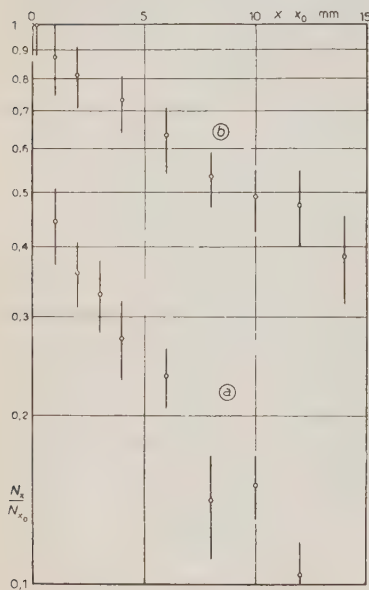
Fig. 4.

thickness. On the other hand the effective coincidence counting rate is given by the total coincidence counting rate, minus the accidental coincidence counting rate N_c.

This number is given by the well know formula

$$N_c = 2\tau N_1 N_2 ,$$

where N_1 and N_2 are the counting rate of pulses read on each of the C.R.M. and τ is the resolving time of the coincidence circuit.

We have measured the value of τ by means of two different sources of radium, each placed so as to radiate only one detector and, in order to be sure that the resolving time τ be indipendent of the γ-ray energy, we have measured this value with various absorber thicknesses from 0 to 16 mm of lead.

The value thus determined was constantly $(1,28 \pm 0,01) \cdot 10^{-7}$ s during all our measurements.

As both N_1 and N_2 are affected by a probable error which is less than 1%, we may determine the accidental coincidence counting rate with an error less than 2%. Taking into account the probable error in the determination of the total coincidence counting rate, the probable errors which affects the experimental points are represented in figg. 4(a) and (b).

Another series of measurements concern the determination of the effective coincidence counting rates against the resolving time τ of the coincidence apparatus. In front of each detector, 2 mm lead absorbers were constantly placed in order to eliminate completely the spurious coincidences caused by Compton photons.

Fig. 5 represents the diagram of the effective coincidence counting rate N and the diagram of the ratio Δ between the accidental coincidence counting rate against the resolving time τ (*). In the diagram

Fig. 5.

are also represented the probable errors which affect the experimental points.
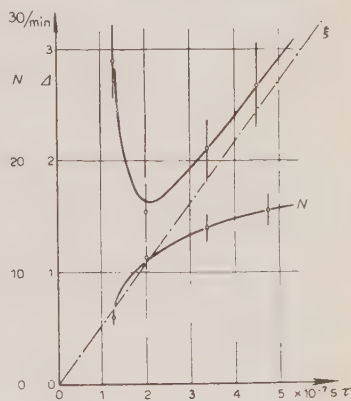
6. – Discussion of the experimental results.

It is well to discuss how to deduce the γ-ray energy of the cascades from the experimental data and how to calculate their total intensity.

As to what concerns the energy of the cascades we can easily see that when a radioactive nuclide decays to the ground state emitting two γ-rays in cascade, the decreasing of the effective coincidence counting rate versus the absorber thickness is given by the following formula

$$N_x = N_{x_0} \exp\left[-(\mu_1 + \mu_2)(x - x_0)\right],$$

in the symmetrical arrangement and by the formula

$$N_x = N_{x_0} \frac{\exp\left[-\mu_1(x - x_0)\right] + \exp\left[-\mu_2(x - x_0)\right]}{2},$$

in the asymmetrical arrangement.

_____

(*) The ratio Δ is conveniently corrected for spurious countings of the photomultiplier [see formulae (4), (5), (6)].

N_x is the coincidence counting rate for lead thickness x and N_{x_0} is the coincidence counting rate for lead thickness x_0; μ_1 and μ_2 are respectively the absorption coefficients of the two rays of the cascade.

On the contrary the preceeding relations become respectively

$$(1) \qquad N_x = N_{x_0} \sum_i p_i \varrho_{i_1} \varrho_{i_2} \exp\left[-(\mu_{i_1} + \mu_{i_2})(x - x_0)\right],$$

$$(2) \qquad N_x = N_{x_0} \sum_i p_i \left[\varrho_{i_1} \frac{\exp\left[-\mu_{i_1}(x - x_0)\right]}{2} + \varrho_{i_2} \frac{\exp\left[-\mu_{i_2}(x - x_0)\right]}{2}\right],$$

if the nuclide decays giving rise to more than one cascade.

The summation index i extends to all the cascades; the coefficient p_i is the intensity of the i-th cascade and ϱ_{i_j} is the efficiency of the counter for the energy of j-th γ-ray belonging to the i-th cascade.

However a practically straight diagram, having as abscissae $x - x_0$ and as ordinates N_x/N_{x_0} represents these formulae. The slope of represented straight lines is directly dependent on the existing cascades.

The solid line of fig. 6(a) fits best the experimental points of the fig. 4(a) when the absorber thickness exceeds 1 mm.

In effect for lead thicknessses below 1 mm we have a very great absorption owing to the existence of many spurious coincidences of backscattered quanta inside the crystal detectors.

The dotted and dashed line is obtained from formula (1) admitting the existence of the 5 cascades of Rutherford's scheme (fig. 1); the intensities p_i (Table I) are those of LATYSHEV (*) the values of μ_{i_j} are obtained from the table of the absorption coefficients of γ-rays in lead; for the values of ϱ_{i_j} see the Appendix.

In the contrary assuming the existence of only the following 3 cascades
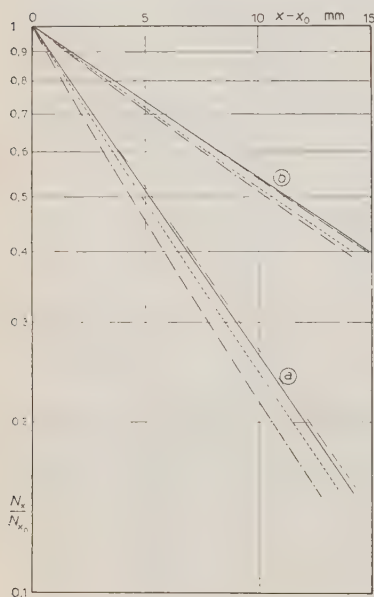
Fig. 6.

(*) We have used the data of LATYSHEV, being almost certainly more precise.

of Rutherford's scheme:

    1) 0,933 MeV, 1,761 MeV;

    2) 1,376 MeV, 0,760 MeV;

    3) 1,120 MeV, 1,761 MeV;

we have the broken line of fig. 6(a).

The dotted line is finally obtained by assuming the existence of the cascades of fig. 2 scheme (SURUGUE).

In fig. 6(b) the different lines have a similar meaning as those in fig. 6(a), but they are derived from equation (2) valid for the asymmetrical arrangement.

Examining both figg. 6(a) and (b) we must conclude that the complete scheme suggested by RUTHERFORD seems absolutely inacceptable; on the contrary the partial scheme consisting only on the three cascades 1), 2) and 3) seems to be in accordance with our experiments. But in this case the two fairly strong 1,241 and 2,198 MeV γ-rays of the two cascades

    4) 1,241 MeV, 0,426 MeV,

    5) 0,499 MeV, 2,198 MeV,

would not have any place, because their energy do not correspond directly to the energy excess of any long range α particles; except if we assume that the hypothetis 1,241 and 2,198 levels have an extremely short life.

The scheme suggested in the work of SURUGUE could be experimentally justified because the dotted lines run very near our experimental lines: however we want to point out that this scheme allows the 1,761 and 1,120 MeV rays to have the same intensities, while this fact does not agree with the experimental data of Table I.

We are dealing now with the total intensity of the cascades.

The accidental coincidence counting rate N_c may be written in the following way

$$(3) \qquad N_c = 2\tau N_1 N_2 =$$
$$= 2\tau[\Omega_1\Omega_2 I^2 \sum_i q_i\varrho_i \sum_j q_j\varrho_j + n_1 n_2 + \sum_i q_i\varrho_i I\Omega_1 n_2 + \sum_j q_j\varrho_j I\Omega_2 n_1],$$

where I is the source disintegration rate, Ω_1 and Ω_2 the solid angles subtended by the detectors, n_1 and n_2 the pulse rates of the detectors without source, q_i, q_j the intensities of each γ-ray and ϱ_i, ϱ_j the detector efficiencies of the receivers for the different energies.

From (3) we get

$$(4) \qquad 2\tau N_1 N_2 - 2\tau n_1 n_2 - 2\tau \sum_i q_i \varrho_i I \Omega_1 n_2 - 2\tau \sum_j q_j \varrho_j I \Omega_2 n_1 =$$
$$= 2\tau \Omega_1 \Omega_2 I^2 \sum_i q_i \varrho_i \sum_j q_j \varrho_j .$$

All terms on the left of (4) are experimentally known; on the other hand the effective coincidence counting rate is given by

$$(5) \qquad N = 2I \Omega_1 \Omega_2 \sum_i p_i \varrho_i \varrho_j .$$

Thus the ratio $\varDelta$ between (4) and (5) becomes

$$(6) \qquad \varDelta = \frac{\tau I \sum_i q_i \varrho_i \sum_j q_j \varrho_j}{\sum_i p_i \varrho_i \varrho_j} .$$

The experimental behaviour of $\varDelta$ versus τ is represented in fig. 5. The slope of the asymptote ξ to the line indicates the values of the ratio $\varDelta$.

$\sum_i q_i \varrho_i \sum_j q_j \varrho_j$ is experimentally known (see the Appendix); hence we can derive $\sum_i p_i \varrho_i \varrho_j$ whose value results $0{,}50 \pm 0{,}05$.

ϱ_i and ϱ_j being known we have in conclusion for

$$\sum_i p_i \varrho_i \varrho_j$$

the complete scheme of RUTHERFORD 0,56

the partial scheme of RUTHERFORD 0,53

the scheme of SURUGUE 0,41

We can deduce from the above results the existence of a strong cascade of 1,761 and 1,120 MeV γ-rays respectively and we can consider more plausible the partial scheme suggested by Rutherford both for the energies and for the intensities; anyway by means only of absorption measurements we cannot exclude the validity of the scheme suggested by Surugue (*).

(*) *Note added in the proofs.* -- We regret that the conclusions deduced by A. H. WAPSTRA (*Academisch Proefschrift* (Amsterdan, 1953)) on the basis of $\beta - \gamma$ coincidence measurements are not in agreement with our results.

7. – Aknowledgements.

This research has been developed in the Physical Laboratory of the Politecnico (Torino) and we want to express our deep gratitude to Prof. E. PERUCCA, Director of the Institute, for his advise and encouragement.

This work could be developed thanks the help of Prof. E. CONTE of the Radiological Institute of the Ospedale Mauriziano (Torino), of the Proff. C. CALOSI, T. H. CLARK, R. M. FANO, E. FUBINI, F. GIORDANI; through their help we could obtain the photomultipliers necessary to this research.

<p align="center">APPENDIX</p>

To interpret the experimental results we had to know the dependence of the γ-ray detection efficiency [13] from the energy of the incident γ-rays.

In order to resolve this problem we compared the experimental absorption curve (line S of fig. 7) of the γ-rays emitted by our radium source with the theoretical absorption curve, drawn on the assumption of constant efficiency (line T).
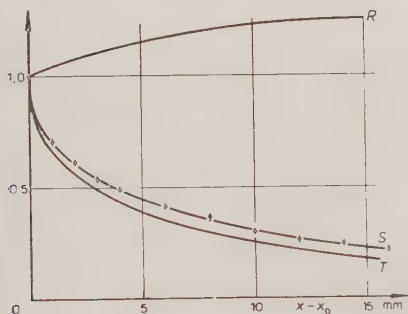
Fig. 7.
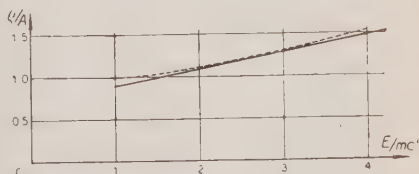
Fig. 8.

Line R represents the ratio S/T between the value of the ordinates of lines S and T. Assuming, in the first approximation, that the energy dependence of the detector efficiency be of the simple type

$$(7) \qquad \varrho = A \left[a_0 + a_1 \frac{E}{mc^2} \right],$$

from the experimentally known ratio S/T and the intensities of each γ-ray we can determine the coefficients a_0 and a_1.

[13] J. V. DUNWORTH: *Rev. Sc. Instr.*, **11**, 1677 (1940).

We obtained in this way the solid line of fig. 8. The coefficient A of the equation (7) depends on the geometrical conditions of the receivers.

The dotted line of fig. 8 represents the theoretical variation of the energy absorbed by an NaI(Tl) crystal, versus the energy of the incident photons.

From the solid line of fig. 8 we have deduced the values of ϱ/A necessary to interprete our results [14].

[14] F. NORLING: *Phys. Rev.* **58**. 277, (1940).

RIASSUNTO

Sono state fatte misurazioni di assorbimento in coincidenza sullo spettro γ del $^{214}_{84}$Po. Abbiamo sperimentalmente confermato l'esistenza di una intensa cascata di raggi γ di 1,120 ed 1,761 MeV. Sulla base dei risultati ottenuti si è proceduto ad un confronto tra gli schemi di livelli energetici suggeriti rispettivamente da E. RUTHERFORD e J. SURUGUE.

Application of second quantization methods to the classical statistical mechanics (II).

M. Schönberg

Centre de Physique Nucléaire de l'Université Libre de Bruxelles

(ricevuto il 28 Gennaio 1953)

Summary. — The classical mechanics of indistinguishable particles discussed in I is further developed. The mechanical foundations of thermodynamics are discussed with the classical wave theory and the « quantized » fields in phase space. It is shown that the formalism eliminates automatically the Gibbs paradox. The classical statistics is treated with the Gibbs-von Neumann method and also by a generalized form of the Boltzmann method which allows to take into account the interactions. The introduction of finite cells in phase space leads to formulas similar to those of the quantal statistics for free particles, but no more so for interacting particles. The statistical treatment of the « quantized » field in phase space leads immediately to the canonical grand ensemble. It is shown that the theory of the « quantized » fields in phase space can be derived from the theory of a « non-quantized » field in phase space, in which there are only continuous distributions of matter, by a procedure of « quantization » altogether similar to that of the quantum theory of fields, but not involving the Planck constant, or any other universal constant. The « non-quantized » field in phase space corresponds to a theory less accurate than the classical mechanics and gives an approximation of the same kind as the molecular chaos hypothesis of the kinetic gas theory, it contains both the dynamics and the heat theory of a continuous medium. A new derivation of the Boltzmann equation involving a special kind of time average is given and a similar equation is established for the two particle distribution function.

1. - Introduction.

In the preceding part of this paper (^{1}) we have shown that it is possible to develop in the classical mechanics a wave formalism in phase space which presents many of the features of the quantum wave mechanics. The possibility

---

(^{1}) M. Schönberg: *Nuovo Cimento*, **9**, 1139 (1952). This paper will be indicated by I.

of that treatment results from the fact that the theory of the Hamilton
equations of motion for a dynamical system

$$
(1) \qquad \frac{\mathrm{d}q_l}{\mathrm{d}t} = \frac{\partial H}{\partial p_l} \qquad \frac{\partial p_l}{\partial t} = -\frac{\partial H}{\partial q_l} \,, \qquad\qquad (l = 1, 2, \dots r)
$$

is equivalent to that of the first order partial differential equation

$$
(2) \qquad i\,\frac{\partial f}{\partial t} = Lf \,, \qquad L = \sum_{l=1}^{r} i\left(\frac{\partial H}{\partial q_l}\,\frac{\partial}{\partial p_l} - \frac{\partial H}{\partial p_l}\,\frac{\partial}{\partial q_l}\right),
$$

which becomes the Liouville equation of statistical mechanics when $f(q, p)$ is
a probability density in the phase space of the dynamical system in consi-
deration. The equation (2) being of the first order, the square of the absolute
value of any solution $\Theta(q, p)$ is also a solution. Therefore we may introduce
a wave function $\Theta(q, p)$, in general complex, such that the probability den-
sity be the square of its absolute value:

$$
(3) \qquad f(q, p) = |\Theta(q, p)|^2 \,.
$$

The consideration of the wave function gives some essential new possibilities,
because it is not restricted to have only real and positive values, as the pro-
bability density. Thus, when our dynamical system is formed by n identical
particles and we denote by τ_j the set of coordinates and momenta of the
j-th particle, we can impose to the wave function the symmetry condition

$$
(4) \qquad \mathcal{P}\Theta(\tau_1, \dots, \tau_n) = \Theta(\tau_1, \dots, \tau_n) \,,
$$

$\mathcal{P}$ indicating any permutation of the indices. This leads to a classical form
of the Bose statistics. A classical analogue of the Fermi statistics is obtained
by taking, instead of (4), the following condition

$$
(5) \qquad \mathcal{P}_{\pm}\Theta(\tau_1, \dots, \tau_n) = \pm\,\Theta(\tau_1, \dots, \tau_n) \,,
$$

$\mathcal{P}_r$ and $\mathcal{P}_-$ denoting even and odd permutations, respectively. When no
symmetry conditions are imposed to the wave function, we get the Boltzmann
statistics. From a pure mathematical point of view, we may say that the
classical dynamics of a system of identical indistinguishable particles is equi-
valent to the theory of the symmetrical, or of the anti-symmetrical, solutions
of the corresponding linear partial differential equation of the first order (2).
It is convenient to consider sometimes this more abstract correspondence

rather than that based on the interpretation of the solution of (2) as a probability amplitude, as will be seen.

The « second quantization » formalism gives a unified treatment of the evolution equation (2) and the symmetry conditions (4) or (5). In the case of the Bose statistics, the absorption and emission operators $\psi(\tau)$, $\psi^*(\tau)$ are characterized by the following commutation rules:

$$(6) \qquad \begin{cases} [\psi(\tau), \psi^*(\tau')]_- = \delta(\tau - \tau') \, , \\[2mm] [\psi(\tau), \psi(\tau')]_- = [\psi^*(\tau), \psi^*(\tau')]_- = 0 \, . \end{cases}$$

τ denotes a point in the phase space Ω of a single particle and the bracket $[A, B]_-$ of two operators A and B their commutator:

$$(7) \qquad [A, B]_- = [A, B] = AB - BA \, .$$

In the case of the Fermi statistics, the commutation rules for the absorption and emission operators are:

$$(8) \quad [\psi(\tau), \psi^*(\tau')]_+ = \delta(\tau - \tau') \, , \qquad [\psi(\tau), \psi(\tau')]_+ = [\psi^*(\tau), \psi^*(\tau')]_+ = 0 \, ,$$

$$(9) \qquad [A, B]_+ = AB + BA \, .$$

The differential operator L is replaced by the operator $\mathcal{R}$

$$(10) \qquad \mathcal{R} = \mathcal{R}_{\text{kin}} + \mathcal{R}_{\text{pot}} \, ,$$

$$(11) \qquad \mathcal{R}_{\text{kin}} = \int_\Omega \psi^*(\tau) \frac{\boldsymbol{p}^2}{2m} \psi(\tau) \, d\tau \, ,$$

$$(12) \qquad \mathcal{R}_{\text{pot}} = \frac{i}{2} \int_\Omega \psi^*(\tau) \psi^*(\tau') \left(\frac{\partial \Phi}{\partial \boldsymbol{x}} \cdot \frac{\partial}{\partial \boldsymbol{p}} + \frac{\partial \Phi}{\partial \boldsymbol{x}'} \cdot \frac{\partial}{\partial \boldsymbol{p}'} \right) \psi(\tau') \psi(\tau) \, d\tau \, d\tau' \, ,$$

$\Phi(\boldsymbol{x} - \boldsymbol{x}')$ denoting the potential energy of a couple of particles and m the mass of the constituent particles. The partial differential equation (2) is replaced by the following equation for the wave functional χ:

$$(13) \qquad i \frac{d\chi}{dt} = \mathcal{R}\chi \, .$$

We showed in the preceding paper that the « second quantization » formalism is entirely equivalent to the wave theory of a n-particle system, when the

wave functional χ is an eigenfunctional of the operator for the number of particles N_{op}

$$(14) \qquad N_{op} = \int_{\Omega} \psi^*(\tau)\psi(\tau)\,d\tau\,,$$

corresponding to the eigenvalue n

$$(15) \qquad N_{op}\chi = n\chi\,.$$

The general solutions of (13) do not correspond to determined numbers of particles and may be considered as describing assemblies of systems of identical particles, each system of the assembly having a different number of particles. There is no difficulty whatsoever in extending the « second quantization » formalism to the case of indistinguishable composite constituenss. As a matter of fact, the « second quantization » formalism can even be developed when f is a function of any number of points τ in an abstract space Ω, in which a measure can be introduced suitably, and has an evolution equation of the form

$$(16) \qquad i\,\frac{\partial f}{\partial t} = Kf\,,$$

K being a linear operator. This general « second quantization » formalism will be discussed in a forthcoming paper.

The main objective of the present paper is the application of the classical wave mechanics in phase space and of the corresponding « second quantization » formalism to the statistical thermodynamics. As a consequence of the similarity between the classical and quantal wave mechanics, the von Neumann density operators can be used also in the classical wave mechanics. In section 3 the main results of the quantal form of the Gibbs theory due to von Neumann ([2]), Dirac ([3]) and Klein ([4]) are recalled and put under a form adequate to our purpose. The canonical and microcanonical ensemble are discussed in sections 4 and 5. It is shown that the thermodynamical behaviour of the systems described by the symmetrical and anti-symmetrical solutions of the Liouville equation is the same in equilibrium. It is however possible to obtain a difference in their thermodynamical behaviour in equilibrium by associating

([2]) J. von Neumann: *Göt. Nach.*, 245 (1927).

([3]) P. A. M. Dirac: *Proc. Cam. Phil. Soc.*, **25**, 62 (1929); **26**, 376 (1930); **27**, 240 (1930).

([4]) O. Klein: *Zeits. f. Phys.*, **72**, 767 (1931).

to the von Neumann density matrix theory a suitable division of the phase space of a single particle into finite cells, i.e. by a suitable modification of the density operators describing canonical and microcanonical ensembles. Such a division is not quite consistent with a purely classical treatment, but has the advantage of giving a simple approximation to the quantal theory. It is shown that in the case of systems of non interacting particles the results are the same as in the quantal theory, with a suitable choice of the cell size, but no more so for interacting particles.

The density operator method is applied to the statistical treatment of the « quantized » field in phase space in section 9. The present analysis differs in an essential point from the quantal statistics of the fields developed by SCHEIDEGGER and McKAY ([5]), by taking into account the special kind of non ergodicity of the field arising from the existence of the integral of the motion N_{op}, which was not considered by those authors. The existence of the integral of the motion N_{op}, requires a modification of the definition of the density operator corresponding to the canonical ensemble of fields. The modification of the definition of a canonical ensemble of fields associated with the integral N_{op} has the remarkable consequence of leading automatically to canonical grand ensembles of particles. The canonical grand ensemble thus appears as of a more fundamental nature than the canonical ensemble. Another important difference with respect to the work of SCHEIDEGGER and McKAY lies in the fact that a potential interaction between the particles is included in our treatment.

The main result of the introduction of the indistinguishability in the classical statistical thermodynamics is the automatic elimination of the Gibbs paradox. It is shown that the Gibbs paradox subsists when the classical wave mechanics is used as the basis of the statistical thermodynamics without taking into account the indistinguishability of the particles, as happens in the quantal statistical mechanics. This result is of philosophical interest because it shows that a limitation of the individuality of the particles is required, even in a consistent classical picture, in order to avoid the Gibbs paradox.

The classical wave mechanics affords the basis for a very general extension of the Boltzmann treatment of statistical mechanics based on the division of the phase space into cells. A similar technique can also be applied to the « quantized » fields in phase space, as shown in section 8. It is shown in section 7 that the application of the generalized Boltzmann treatment to the « quantized » field in phase space leads also to a kind of canonical grand ensemble of particles.

([5]) A. E. SCHEIDEGGER and C. D. McKAY: *Phys. Rev.*, **83**, 125 (1951).

The generalized Boltzmann treatment can also be applied to systems of particles in interaction and gives an alternative to the density matrix treatment.

There seems to be a considerable difference between the conceptions of statistical mechanics used in I and in the present paper. In I the wave functions in phase space Θ, or the wave functionals χ, were used as the tools of the statistical mechanics, whereas now the density operators are employed. The difference results from the existence of two essentially different applications of the Gibbsian ensembles:

(a) The use of a probability distribution in the phase space as a means for the analysis of the motions of systems whose initial states are incompletely specified.

(b) The use of ensembles of similar systems to obtain a mechanical foundation for thermodynamics.

The essential difference between (a) and (b) is not clearly seen when probability distributions are employed to describe the ensembles. But it is no more so in the classical wave mechanics. In I we had mainly in view the application (a), whereas now we deal mostly with (b). Strictly speaking, the difference between (a) and (b) may still be overlooked to some extent in the unrealistic case of distinguishable identical particles, but the difference must be always taken into account in the theory of indistinguishable particles, as shown in section **6**. It is shown in sections **4** and **5** that the density operators for the fundamental canonical and microcanonical ensembles are actually formed with mixtures of delta-like wave functions which describe completely specified states, i.e. completely known values of the coordinates and momenta of the particles. The reason why a classical wave formalism separates the two problems (a) and (b) can be understood by taking into account the assumption of the randomness of phases underlying the use of the von Neumann density operators (see for the discussion of this important point in the quantum mechanics the § 84 in *The Principles of Statistical Mechanics* of TOLMAN, Oxford, 1946). There is an important point to be noticed when systems of indistinguishable particles are considered:

The wave function $\Theta(t_0; \tau)$ describes the amount of information regarding the positions and velocities of the particles at the initial time t_0, but it does also define their statistical nature (bosons or fermions), whereas the probability density $|\Theta(t_0; \tau)|^2$ describes only the amount of information regarding positions and velocities. Even when the coordinates and momenta are given exactly at the initial time t_0, it is still necessary to consider a wave function, in order to specify its behaviour under permutations of the particles.

The necessity of the wave functions, even when the initial positions and velocities of the particles are assumed to be exactly known, is a consequence of the central part played by the groups of permutations in the theory of indistinguishable particles. The way in which the wave function comes in in

the description of the motion is discussed in section 2. The imposition of a symmetry condition leads to an identification of a number of different trajectories of a system in its phase space, and also to the exclusion of certain trajectories in the case of fermions. The situation is clarified by the comparison of the usual (incomplete in the case of indistinguishable particles) classical description of the motion by the Hamilton equations and the complete description given by the adequate solution of the Liouville equation with their quantal analogues: the Heisenberg and Schrödinger representations plus symmetry condition for the wave function. The classical Hamilton equations correspond to the q-number Hamilton equations of the quantal Heisenberg representation, which do not include a specification of the statistics of the particles.

It is obvious that the solution of the Hamilton equations allows to get the value of the classical wave function at any time in terms of the wave function at the initial time. But the knowledge of the general symmetrical or anti-symmetrical solution of the Liouville equation is not sufficient to get the general solution of the Hamilton equations. From this point of view the classical mechanics of systems of indistinguishable particles appears as simpler than the usual classical mechanics of distinguishable particles. This simplification has an important bearing in the discussion of the Einstein and Zermelo cycles, as well as in the formulation of the ergodic problem, as shown in section 2.

The introduction of the classical wave functions clarifies the meaning of the unitary transformations in Hilbert space associated with the motion of a classical system, which were introduced by KOOPMAN ([6]). The Koopman Hilbert-space can be taken as that of the classical wave functions. The wave functions of the systems of indistinguishable particles correspond to closed sub-spaces of the Koopman Hilbert-space.

The importance of the introduction of the indistinguishability of the particles is shown in a particularly striking form by the existence of the « quantized » fields in phase space associated with indistinguishable particles. The most powerful tool of the classical statistical theory, the grand canonical ensemble, finds its most natural justification in the theory of the « quantized » fields. Thus it is seen that the field formalism, although apparently more complicated, leads often to the simplest solutions, because of its more powerful methods. Moreover the field formalism throws light on very difficult problems, such as the thermodynamical irreversibility. The work done in recent years in the quantum theory of fields has shown that the S matrix of fields in interaction is different from the unity matrix, so that there is irreversibility. The S matrix

([6]) B. O. KOOPMAN: *Proc. Nat. Acad. USA,* **17**. 315 (1931).

formalism can obviously be applied to the theory of the χ-field in phase space and its S matrix is not the unity matrix, as a consequence of the interaction between the particles. Thereby the behaviour of the χ-field is irreversible. The bearing of this result on the thermodynamical irreversibility will be discussed in a forthcoming paper. We shall now limit ourselves to the remark that the field formalism shows that even the statistical theory of a system of a finite number of indistinguishable particles leads to the statistics of a system with an infinite number of degrees of freedom.

The fact that the classical theory of indistinguishable particles leads to a field formalism similar to that of the quantum theory of fields — the classical particles being « quanta » of the fields in phase space — shows that there is the possibility of developing a kind of super-classical theory in which there are only continuous distributions. This super-classical theory can be obtained by ignoring the non commutability of the ψ and ψ^* and keeping the same equations of motion for the c-numbers ψ_c, ψ_c^* thus obtained. The equations for ψ_c and ψ_c^* can be derived from a variational principle, put under hamiltonian form and « quantized ». This « quantization » is quite similar to the true quantization of a field in ordinary space, the c-number Poisson brackets being replaced by commutators with a suitable numerical factor. Neither the Planck constant nor any other physical constant is involved in that « quantization », which leads to the formalism of the « quantized » field in phase space, i.e. to the exact classical theory of indistinguishable particles. The super-classical field formalism gives a kind of Hartree approximation to the classical wave mechanics, in which the self-forces are not subtracted (see the discussion of the quantal analogue of the super-classical formalism in the Appendix of HEISENBERG's book, *Die Physikalischen Prinzipien der Quantentheorie*, Leipzig, 1930).

The super-classical theory is discussed in sections **12** and **13**. It may be used in some cases to get a convenient treatment of the motion of a continuous medium. The existence of heat is immediately shown by the fact that the kinetic energy of the macroscopic motion is less than that of the microscopic motion. A definition of the entropy similar to that of Gibbs can be obviously introduced but leads to the same difficulty as in the other cases, the total entropy being time independent. This point is quite interesting, because it shows clearly that an incomplete specification of the motion is not sufficient to get an increasing entropy, as often assumed without any satisfactory justification.

The equation for $\varrho_c = \psi_c^* \psi_c$ derived from the super-classical theory coincides with that of the Vlassov formalism [7] for a system of a large number

---

[7] A. A. VLASSOV: *Journ. Exper. Theor. Phys.*, **18**, 840 (1948).

of particles of the same kind with two-body forces. The Vlassov method of introducing the temperature in the case of stationary motions leads to the same value given by the general dynamical definition of local temperature.

In order to clarify the reasons of the unsatisfactory behaviour of the entropy in the super-classical theory we give in section **13** a new derivation of the Boltzmann equation starting from the integro-differential equation relating the one and two particle probability distributions obtained from the Liouville equation (that equation plays a central part in the work of YVON ([8]), BORN and GREEN ([9]) and KIRKWOOD ([10,11]). Our derivation of the Boltzmann equation has some analogy with that of KIRKWOOD ([11]), but is essentially different insofar the time averaging is done in such a way that the three particle collisions do not come in. This results from the fact that our time averaging is not taken along the actual notion of a molecule or pair of molecules, but rather along a virtual motion of a two molecule system. The time averaging along a virtual motion appears as the most natural one, once the integro-differential equation relating the one and two particle distribution functions is written in a convenient form, thus it is seen that the complication of the Kirkwood derivation results from the choice of the method of time averaging. Our proof shows clearly that the time variation of the entropy is due to the time averaging and not to the incomplete specification of the motion of the particles or to the molecular chaos assumption. The continuity equation of the super-classical theory is seen to coincide with the form taken by the integro-differential equation relating the one and two particle probability densities when the hypothesis of molecular chaos is introduced.

The method of time averaging along a virtual motion can also be applied to the integro-differential equation relating the two and three particle distribution functions and gives a new approach to the theory of transport phenomena in cases other than the diluted gas.

2. – The Schrödinger and Heisenberg representations in the classical and quantal wave theories.

Let H_n be the hamiltonian of a system of n identical particles of mass m:

$$(17) \qquad H_n = \sum_{l=1}^{n} \frac{p_l^2}{2m} + \frac{1}{2} \sum_{l=1}^{n} \sum_{l' \neq l} \Phi(\boldsymbol{x}_l - \boldsymbol{x}_{l'}) \,.$$

([8]) J. YVON: *La théorie statistique des fluides* (Paris, 1935).
([9]) M. BORN and H. S. GREEN: *Proc. Roy. Soc.*, A **188**, 10 (1947).
([10]) J. G. KIRKWOOD: *Journ. Chem. Phys.*, **14**, 180 (1946).
([11]) J. G. KIRKWOOD: *Journ. Chem. Phys.*, **15**, 72 (1947).

We shall denote the Liouville operator L of our system by L_n and its wave function by Θ_n. (The notations in this paper will be the same as in I, as far as possible). The unitary operator of the motion is $U_n(t)$:

$$(18) \qquad U_n(t) = \exp\left[-itL_n\right], \qquad \Theta_n(t) = U_n(t)\Theta_n(0).$$

The passage to the Heisenberg representation is a contact transformation determined by $U_n(t)$:

$$(19) \qquad A^{(H)}(t) = U_n^{-1}(t)A^{(S)}U_n(t), \qquad \Theta_n^{(H)} = U_n^{-1}(t)\Theta_n(t) = \Theta_n(0);$$

$A^{(S)}$ and $A^{(H)}(t)$ are the operators which correspond to the same time independent physical A quantity in the Schrödinger and Heisenberg representations, respectively. The equation of motion in the Heisenberg representation is:

$$(20) \qquad i\frac{d}{dt}A^{(H)}(t) = \left[A^{(H)}, L_n\right].$$

Hence we have the Hamilton equations

$$(21) \qquad \frac{d}{dt}x_l^{(H)} = \frac{\partial H_n^{(H)}}{\partial p_l^{(H)}}, \qquad \frac{d}{dt}p_l^{(H)} = -\frac{\partial H_n^{(H)}}{\partial x_l^{(H)}},$$

because

$$(22) \qquad [\boldsymbol{x}_l, L_n]\Theta = i\boldsymbol{x}_l(H_n, \Theta)_n - i(H_n, \boldsymbol{x}_l\Theta)_n = -i(H_n, \boldsymbol{x}_l)_n\Theta = i\frac{\partial H_n}{\partial \boldsymbol{p}_l}\Theta,$$

and

$$(23) \qquad [\boldsymbol{p}_l, L_n]\Theta = -i(H_n, \boldsymbol{p}_l)_n = -i\frac{\partial H_n}{\partial \boldsymbol{x}_l}\Theta,$$

the Poisson bracket being defined in the usual way:

$$(24) \qquad (\Phi, \Psi)_n = \sum_{l=1}^{n}\left(\frac{\partial\Phi}{\partial\boldsymbol{x}_l}\cdot\frac{\partial\Psi}{\partial\boldsymbol{p}_l} - \frac{\partial\Phi}{\partial\boldsymbol{p}_l}\cdot\frac{\partial\Psi}{\partial\boldsymbol{x}_l}\right).$$

The operators for the coordinates and momenta are commutable in the Schrödinger representation of the classical wave formalism, so that the corresponding operators at the same time in the Heisenberg representation will also be com-

mutable. Moreover, since H_r is a function of the x and p, it does commute with these operators. As a consequence of (21) we have:

$$(25) \qquad \left[\frac{\mathrm{d}}{\mathrm{d}t}\, \boldsymbol{x}_i^{(H)}(t),\, \boldsymbol{p}_{i'}^{(H)}(t) \right] = \left[\frac{\partial H_n^{(H)}(t)}{\partial \boldsymbol{p}_i^{(H)}},\, \boldsymbol{p}_{i'}^{(H)}(t) \right] = 0 \,.$$

In a similar way we get:

$$(26) \qquad \left| \frac{\mathrm{d}}{\mathrm{d}t}\, \boldsymbol{p}_i^{(H)}(t),\, \boldsymbol{x}_{i'}(t) \right| - \left[\frac{\mathrm{d}}{\mathrm{d}t}\, \boldsymbol{p}_{i'}^{(H)}(t),\, \boldsymbol{p}_{i'}^{(H)}(t) \right] - \left| \frac{\mathrm{d}}{\mathrm{d}t}\, \boldsymbol{x}_i^{(H)}(t),\, \boldsymbol{x}_{i'}^{(H)}(t) \right| = 0 \,.$$

Therefore the operators for the coordinates and momenta at two times t and $t + \mathrm{d}t$ do commute, and by successive infinitesimal time displacements we see that the same holds for any times t and t'. Since the operators at the time $t = 0$ do coincide in the two representations, it follows that the $x^{(H)}(t)$ and $p^{(H)}(t)$ are diagonal for all the values of t. The Hamilton equations (21) may therefore be replaced by c-number equations, which are essentially the Hamilton equations of the ordinary form of the classical theory.

It results from the preceding considerations that, for the functions of the coordinates and momenta, the Heisenberg representation attached to the wave formalism in phase space is essentially the ordinary form of classical mechanics. It is obvious that, in the Heisenberg representation, the symmetry conditions (4) or (5) do appear under the form

$$(27a) \qquad\qquad \mathcal{P} \Theta_n^{(H)}(x,\, p) = \Theta_n^{(H)}(x,\, p) \,, \qquad\qquad \text{(Bose particles)}$$

or

$$(27b) \qquad\qquad \mathcal{P}_{\pm} \Theta_n^{(H)}(x,\, p) = \pm\, \Theta_n^{(H)}(x,\, p) \,. \qquad\qquad \text{(Fermi particles)}$$

When the coordinates and momenta are given at the time $t = 0$, we must take for bosons

$$(28a) \qquad \Theta(\tau_1, \ldots, \tau_n) = \Theta_n(0;\, \tau_1, \ldots, \tau_n) =$$
$$= \frac{1}{n!} \sum_{\text{permut. } k} \delta\big(\tau_1 - \tau_{k_1}(0)\big) \ldots \delta\big(\tau_n - \tau_{k_n}(0)\big) = \delta_+^{(n)}\big(\tau, \tau(0)\big) \,,$$

and for fermions

$$(28b) \quad \Theta_n^{(H)}(\tau_1, \ldots, \tau_n) = \Theta_n(0;\, \tau_1, \ldots, \tau_n) =$$
$$= \frac{1}{n!} \begin{vmatrix} \delta(\tau_1 - \tau_1(0)) & \delta(\tau_1 - \tau_2(0)) & \ldots & \delta(\tau_1 - \tau_n(0)) \\ \delta(\tau_2 - \tau_1(0)) & \delta(\tau_2 - \tau_2(0)) & \ldots & \delta(\tau_2 - \tau_n(0)) \\ \ldots & \ldots & \ldots & \\ \delta(\tau_n - \tau_1(0)) & \delta(\tau_n - \tau_2(0)) & \ldots & \delta(\tau_n - \tau_n(0)) \end{vmatrix} = \delta_-^{(n)}\big(\tau, \tau(0)\big).$$

The introduction of the wave functions shows at once a characteristic feature of the indistinguishability: The $\Theta_n^{(H)}$ are not, in general, eigenfunctions of the operators for the coordinates and momenta $x_l^{(S)}$ and $p_l^{(S)}$. The $\Theta_n^{(H)}$ are nevertheless eigenfunctions of all the operators of the form $f(\tau_1^{(S)}, ..., \tau_n^{(S)})$, $f(\tau_1, ..., \tau_n)$ being any function of the τ_l invariant for permutations of the τ. This results from the fact that the maximal theoretically possible information is to know that there is a particle at each of the points $\tau_l(0)$, without distinguishing which of the particles is at each of the points. A set of $6n$ independent invariant functions is the following:

$$(29) \quad \begin{cases} \xi_1^{(\alpha)} = \sum_{j=1}^{n} x_j^{(\alpha)} , \quad \xi_2^{(\alpha)} = \frac{1}{2} \sum_{j_1 \neq j_2}^{1,...,n} x_{j_1}^{(\alpha)} x_{j_2}^{(\alpha)} \quad .... \quad \xi_n^{(\alpha)} = x_1^{(\alpha)} x_2^{(\alpha)} .... x_n^{(\alpha)} \\[2mm] \eta_1^{(\alpha)} = \sum_{j=1}^{n} p_j^{(\alpha)} , \quad \eta_2^{(\alpha)} = \frac{1}{2} \sum_{j_1 \neq j_2}^{1,...,n} p_{j_1}^{(\alpha)} p_{j_2}^{(\alpha)} \quad .... \quad \eta_n^{(\alpha)} = p_1^{(\alpha)} p_2^{(\alpha)} .... p_n^{(\alpha)} . \end{cases}$$

The index α denotes a component of a vector. The eigenvalue of the operator $f(\tau_1^{(S)}, ..., \tau_n^{(S)})$ which corresponds to the eigenfunctions $\Theta_n^{(H)}$ is $f(\tau_1(0), ..., \tau_n(0))$. Although there are $6n$ independent functions $\xi_l^{(\alpha)}$, $\eta_l^{(\alpha)}$, it is not sufficient to give the eigenvalues $\xi_l^{(\alpha)}(0)$, $\eta_l^{(\alpha)}(0)$ of the corresponding operators to determine the n points $\tau_l(0)$. Indeed, when the $\xi_l^{(1)}(0)$ are given, the $x_l^{(1)}(0)$ are determined, but for the order, as roots of the equation

$$(30) \quad u_1^n - \xi_1^{(1)}(0) u_1^{n-1} + \xi_2^{(1)}(0) u_1^{n-2} - ... + (-1)^n \xi_n^{(1)}(0) = 0 ,$$

and a similar conclusion holds for the $x_l^{(2)}(0)$ when the $\xi_l^{(2)}(0)$ are given, but no information is thus obtained on the way in which the different coordinates must be coupled. This shows how awkward it is to work with permutation invariants in the phase space wave formalism.

It is easily seen that the solution of the Hamilton equations allows to solve immediately the Liouville equation for the wave function. Indeed, the general solution of the Hamilton equations gives us the coordinates and momenta of the particles, treated as distinguishable, as functions of the time t and of the position and momentum vectors $\boldsymbol{a}_l$, $\boldsymbol{b}_l$ at an arbitrarily chosen initial time t_0:

$$(31) \quad \begin{cases} \boldsymbol{x}_l(t) = \boldsymbol{F}_l(t - t_0; \boldsymbol{a}_1, ..., \boldsymbol{a}_n; \boldsymbol{b}_1, ..., \boldsymbol{b}_n) \\[2mm] \boldsymbol{p}_l(t) = \boldsymbol{G}_l(t - t_0; \boldsymbol{a}_1, ..., \boldsymbol{a}_n; \boldsymbol{b}_1, ..., \boldsymbol{b}_n) . \end{cases}$$

The equation of motion for any function $R(t; \boldsymbol{x}, \boldsymbol{p})$ is:

$$(32) \quad \frac{\mathrm{d}R}{\mathrm{d}t} = \frac{\partial R}{\partial t} + (R, H_n)_n .$$

Hence, when R is a solution of the Liouville equation, we have:

$$(33) \qquad R(t; \boldsymbol{F}(t-t_0; \boldsymbol{a}, \boldsymbol{b}), \boldsymbol{G}(t-t_0; \boldsymbol{a}, \boldsymbol{b})) = R(t_0; \boldsymbol{a}, \boldsymbol{b}) .$$

By applying (33) to the wave function Θ_n we get the solution of the wave equation:

$$(34) \qquad \Theta_n(t; \boldsymbol{x}, \boldsymbol{p}) = \Theta_n(t_0; \boldsymbol{F}(t_0-t; \boldsymbol{x}, \boldsymbol{p}), \boldsymbol{G}(t_0-t; \boldsymbol{x}, \boldsymbol{p})) .$$

Equation (34) shows that $U_n(t)$ is a substitution operator

$$(35) \qquad U_n(t)\Theta(\boldsymbol{x}, \boldsymbol{p}) = \Theta(\boldsymbol{F}(-t; \boldsymbol{x}, \boldsymbol{p}), \boldsymbol{G}(-t; \boldsymbol{x}, \boldsymbol{p})) ,$$

which replaces the $\boldsymbol{x}_l$ by the $\boldsymbol{F}_l(-t; \boldsymbol{x}, \boldsymbol{p})$ and the $\boldsymbol{p}_l$ by the $\boldsymbol{G}_l(-t; \boldsymbol{x}, \boldsymbol{p})$.

The equation (33) is not dependent on the symmetry conditions imposed to the wave function. Let us examine now the effect of the symmetry conditions. The equations

$$(36) \qquad \begin{cases} \boldsymbol{x}_l(t)_{k_1,\dots,k_n} = \boldsymbol{F}_l(t-t_0; \boldsymbol{a}_{k_1}, \dots, \boldsymbol{a}_{k_n}; \boldsymbol{b}_{k_1}, \dots, \boldsymbol{b}_{k_n}) \\ \boldsymbol{p}_l(t)_{k_1,\dots,k_n} = \boldsymbol{G}_l(t-t_0; \boldsymbol{a}_{k_1}, \dots, \boldsymbol{a}_{k_n}; \boldsymbol{b}_{k_1}, \dots, \boldsymbol{b}_{k_n}) . \end{cases}$$

describe the motion of the particles, treated as distinguishable, which corresponds to a permutation of the initial coordinates and momenta. If we assume that Θ_n is symmetrical at the time t_0, we get:

$$(37) \qquad \Theta_n\big(t; \boldsymbol{x}(t)_{k_1,\dots,k_n}, \boldsymbol{p}(t)_{k_1,\dots,k_n}\big) = \Theta_n(t_0; \boldsymbol{a}_{k_1}, \dots, \boldsymbol{a}_{k_n}; \boldsymbol{b}_{k_1}, \dots, \boldsymbol{b}_{k_n}) =$$
$$= \Theta_n(t_0; \boldsymbol{a}_1, \dots, \boldsymbol{a}_n; \boldsymbol{b}_1, \dots, \boldsymbol{b}_n) = \Theta_n\big(t; \boldsymbol{x}(t), \boldsymbol{p}(t)\big) .$$

Hence the trajectories in the phase space of the system corresponding to $\{\boldsymbol{x}(t), \boldsymbol{p}(t)\}$ and to $\{\boldsymbol{x}(t)_{k_1,\dots,k_n}, \boldsymbol{p}(t)_{k_1,\dots,k_n}\}$ do describe the same state of motion of the system of bosons. In the case of fermions we get

$$(38) \qquad \Theta_n\big(t; \boldsymbol{x}(t)_{k_1,\dots,k_n}, \boldsymbol{p}(t)_{k_1,\dots,k_n}\big) = \pm \Theta_n\big(t; \boldsymbol{x}(t), \boldsymbol{p}(t)\big) ,$$

the sign corresponding to the parity of the permutation $\{k_1, k_2, \dots, k_n\}$. The conclusion is the same as in the case of the bosons. Hence, when the particles are indistinguishable the set of trajectories corresponding to the different $\{\boldsymbol{x}(t)_{k_1,\dots,k_n}, \boldsymbol{p}(t)_{k_1,\dots,k_n}\}$ is lumped into a single state of motion. It is obvious by reasons of symmetry that:

$$(39) \qquad \boldsymbol{x}_l(t)_{k_1,\dots,k_n} = \boldsymbol{x}_{k_l}(t) , \qquad \boldsymbol{p}_l(t)_{k_1,\dots,k_n} = \boldsymbol{p}_{k_l}(t) .$$

Hence the symmetry (or anti-symmetry) of the wave function at one instant
of time t_0 ensures the symmetry (or anti-symmetry) for all the values of t, as
a consequence of (37) (or of (38)).

The preceding results show clearly that the consideration of the wave
function is necessary to give a complete dynamical description of a
system of indistinguishable classical particles, even when there is no uncer-
tainty on the initial values of the coordinates and momenta of the particles,
as was emphasized in the Introduction. The situation is similar to that of
the quantal wave mechanics. The quantal equations of motion of the oper-
ators for the coordinates and momenta are also Hamilton equations, they
have exactly the same form of the corresponding classical equations (21), the
only difference consisting in the non commutability of the operators for the
coordinates and momenta. As happens in our classical theory, the Hamilton
equations of the quantal Heisenberg representation do not specify the stati-
stical nature of the identical particles. This is done by the choice of the time
independent wave function of the quantal Heisenberg representation.

There is one aspect of the dynamical behaviour in whose analysis the in-
troduction of the indistinguishability is of fundamental importance: the
quasi-periodicity of the motion on a finite surface of constant energy in phase
space. The duration of a Poincaré cycle must now be defined in terms of the
states of motion, instead of trajectories. Since a state of motion includes in
general n! trajectories in the case of a system of n indistinguishable particles,
the duration of the true cycle will be shorter than in the theory of distinguis-
hable particles. Thus the Einstein point of view is seen to be satisfactory
(see the interesting remarks of BORN: *Natural Philosophy of Cause and Chance*,
Oxford, 1949, appendix VI). The necessity of defining the representative
point in phase space « without regard of the individuality of the particles »
(BORN) has a rigorous justification in the present theory.

In the case of systems of indistinguishable particles, the ergodic problem
is no more the same as in the ordinary classical theory, because now we must
consider time averages in a state of motion and not along a trajectory of the
system in phase space. The time averaging in a state of motion can be split
into two steps: (a) time averaging along each of the trajectories pertaining
to the state of motion; (b) an ordinary average of the time averages along
the different trajectories. It is obvious that the ergodic condition for systems
of indistinguishable particles is less stringent than in the ordinary theory,
especially in the case of systems with a large number of particles. We shall
discuss elsewhere in more detail this important point.

The above results show that the theory of the motion of systems of
indistinguishable particles is simpler than that of systems of the same structure
whose particles are distinguishable. From a very general point of view this
is quite obvious, since in the latter case we must determine all the solutions

of the Liouville equation, whereas in the former case only a part of these solutions are required. It is well known that a n particle system has only $6n$ independent constants of the motion, hence the corresponding Liouville equation has only $6n$ independent solutions. These can not be all symmetrical in the variables of the n particles, because this would imply that all the solutions are symmetrical. It is easily seen that the number of the independent anti-symmetrical constants of the motion is equal to that of the symmetrical constants and thereby less than $6n$. The preceding remarks lead to an important conclusion:

The knowledge of all the symmetrical (or anti-symmetrical) wave functions is not sufficient to obtain the general solution of the Hamilton equations, which depends on the knowledge of $6n$ independent constants of the motion.

3. – The von Neumann density matrix.

The analogue of the Gibbs statistical mechanics in the quantal theory was given by VON NEUMANN ([2]) and DIRAC ([3]). The description of an incompletely known state is given by the density operator R of von Neumann, which satisfies the quantal analogue of the Lionville equation for the classical distribution function

$$(40) \qquad i\hbar \frac{\mathrm{d}R}{\mathrm{d}t} = [H, R] \,.$$

H denoting the quantal hamiltonian operator. If it is only known that at the initial time t_0 the system was in one of the orthogonal states of wave functions φ_a, with the respective probabilities q_a, the initial density operator must be taken as

$$(41) \qquad R(t_0) = \sum_a q_a P_a \,,$$

with

$$(42) \qquad \sum q_a = 1 \,,$$

the P_a being the projection operators corresponding to the states φ_a. There is no loss of generality in assuming that the φ_a are a complete set of orthogonal and normalized functions, since this can always be done by taking some of the q_a equal to 0. In the representation whose basic vectors are the φ_a, the matrix elements of $R(t_0)$ have the simple form:

$$(43) \qquad \langle a' \,|\, R(t_0) \,|\, a'' \rangle = q_{a'} \delta_{a', a''} \,.$$

In the particular case of a completely specified quantal state Ψ, R is a projection operator

$$(44) \qquad R = P_\Psi ,$$

P_Ψ being the projection operator of the state Ψ. Let us consider the particular case of a system of n identical spinless particles and the representation in which their coordinates are diagonal. The matrix elements of R in this representation are:

$$(45) \qquad \langle \boldsymbol{x}_1', \boldsymbol{x}_2', ..., \boldsymbol{x}_n' | R(t) | \boldsymbol{x}_1'', \boldsymbol{x}_2'', ..., \boldsymbol{x}_n'' \rangle \doteq \sum_a q_a \varphi_a(t; \boldsymbol{x}') \varphi_a^*(t, \boldsymbol{x}'') ,$$

$$(46) \qquad \varphi(t) = \exp\left[-\frac{i}{\hbar} (t - t_0)H \right] \varphi_a .$$

The probability of finding the n particles in the elements of volume $\mathrm{d}\boldsymbol{x}_i$ at the time t is $\langle \boldsymbol{x}_1, ..., \boldsymbol{x}_n | R(t) | \boldsymbol{x}_1, ..., \boldsymbol{x}_n \rangle \mathrm{d}\boldsymbol{x}_1 ... \mathrm{d}\boldsymbol{x}_n$.

We shall now consider indistinguishable particles. In order to get the Fermi statistics we would have to take particles with half-integer spin. The introduction of spin variables would represent an unnecessary complication for the goal we have in view. Moreover, since we are dealing wtih a non relativistic theory, there is no inconsistency in imposing the Fermi statistics to spinless particles. We shall thereby use the simpler formalism of spinless particles for the two statistics.

In the von Neumann quantal statistical mechanics, an entropy is attributed to the incompletely specified state described by R:

$$(47) \qquad S_R = - k \operatorname{Tr}(R \log R) .$$

Tr denotes the trace of the operator. The definition (47) is also applicable to a completely specified state and gives to any of such states the entropy 0, as well known. The trace of an operator can be computed in any representation, by using that corresponding to (43) we get:

$$(48) \qquad S_R(t_0) = - k \sum_a \sum_{a'} \langle a | R(t_0) | a' \rangle \langle a' | \log R(t_0) | a \rangle = - k \sum_a q_a \log q_a .$$

We shall now assume that the φ_a are eigenfunctions of H, corresponding to energy levels E_a. In the case of degeneracy we shall have the same value E_a for g_a levels. The expectation value of the energy in the condition described by $R(t_0)$ is:

$$(49) \qquad \langle H \rangle_{t_0} = \operatorname{Tr}(R(t_0)H) = \sum_a q_a E_a .$$

In the present case R is time independent, thereby we may drop the time variable. The most important ensemble of this type is the canonical ensemble:

$$(50) \qquad q_a = \frac{\exp\left[-\dfrac{E_a}{\theta}\right]}{Z} \, , \qquad Z = \sum_a \exp\left[-\frac{E_a}{\theta}\right] ,$$

$$(51) \qquad R_{\mathrm{can}} = \exp\left[\frac{\Psi - H}{\theta}\right] .$$

The parameter Ψ has the following value:

$$(52) \qquad \Psi = -\,\theta \log Z \, .$$

It is well known that the canonical ensemble describes the behaviour of a system in thermal equilibrium with a bath at constant temperature T

$$(53) \qquad \theta = kT \, ,$$

k being the Boltzmann constant. The entropy of the system is S_{can}

$$(54) \qquad S_{\mathrm{can}} = k \log Z + \frac{1}{T} \langle H \rangle_{\mathrm{can}} \, ,$$

$$(55) \qquad \langle H \rangle_{\mathrm{can}} = \frac{1}{Z} \sum_a E_a \exp\left|-\frac{E_a}{kT}\right| ,$$

Ψ is therefore the Helmholtz free energy of the system F:

$$(56) \qquad \Psi = -\,kT \log Z = \langle H \rangle_{\mathrm{can}} - TS_{\mathrm{can}} = F \, .$$

The formalism of the von Neumann density operators becomes more complicated when the wave function of the system fulfills symmetry conditions. The allowed wave functions of the system form a closed sub-space of the Hilbert space of the system without symmetry conditions. Let us denote by $\overset{+}{P}{}^{(n)}$ the projection operator on the closed Hilbert sub-space corresponding to the symmetrical wave functions of a system of n particles and by $\overset{-}{P}{}^{(n)}$ the projection operator on the closed sub-space of the anti-symmetrical wave functions. In the construction of the ensemble the allowed $P_a^{(n)}$ must satisfy the conditions:

$$(57a) \qquad \sum_a \overset{+}{P}{}_a^{(n)} = \overset{+}{P}{}^{(n)} \qquad \left(\overset{+}{P}{}_a^{(n)} \overset{+}{P}{}_{a'}^{(n)} = \delta_{a,a'} \overset{+}{P}{}_a^{(n)} \ \ \overset{+}{P}{}_a^{(n)} \overset{+}{P}{}^{(n)} = \overset{+}{P}{}_a^{(n)} \right) \quad \text{(bosons)} ,$$

$$(57b) \qquad \sum_a \overset{-}{P}{}_a^{(n)} = \overset{-}{P}{}^{(n)} \qquad \left(\overset{-}{P}{}_a^{(n)} \overset{-}{P}{}_{a'}^{(n)} = \delta_{a,a'} \overset{-}{P}{}_a^{(n)} \ \ \overset{-}{P}{}_a^{(n)} \overset{-}{P}{}^{(n)} = \overset{-}{P}{}_a^{(n)} \right) \quad \text{(fermions)} .$$

The density operators of the canonical ensembles in the cases of indistinguishability are

$$(58) \qquad \overset{\pm}{R}^{(n)}_{\mathrm{can}} = \overset{\pm}{P}^{(n)} \exp\left[\frac{\Psi^{(n)}_{\pm} - H_n}{\theta}\right],$$

with

$$(59) \qquad \Psi^{(n)}_{\pm} = -\theta \log Z^{(n)}_{\pm}, \qquad Z^{(n)}_{\pm} = \sum_{E_a} \overset{\pm}{g}_a \exp\left[-\frac{E_a}{\theta}\right],$$

$\overset{+}{g}_a$ and $\overset{-}{g}_a$ being the weights of the energy level E_a for bosons and fermions, respectively. *The difference of the weights renders the free energies different in the various quantal statistics.*

4. – Canonical ensembles in the classical wave formalism.

The introduction of the von Neumann operators in the phase space wave mechanics and in the theory of the « quantized » fields in phase space can obviously be done by applying the rules of the preceding section. From the formal point of view the only differences arise from the necessity of considering continuous spectra of eigenvalues. There are nevertheless some very important differences resulting from the fact that the classical wave functions in phase space describe both completely specified states and incompletely specified ones, such as those corresponding to approximately known initial values of the coordinates and momenta of the particles. In other words, the most significant differences arise from the fact that the pure states of the wave mechanics in phase space are not entirely similar to those of the quantal wave mechanics.

The above difficulty indicates that it is necessary to distinguish between two different applications of the Gibbs methods:

a) The use of a probability distribution in phase space as a means for the analysis of the motion of systems whose states are incompletely specified.

b) The use of ensembles of similar systems in order to obtain a mechanical foundation for thermodynamics.

It is clear that the problem of the analysis of the motion of a mechanical system, whose initial state is incompletely known, is essentially different from that of the foundations of thermodynamics. This difference was not emphasized in Gibbs' book, because of his definition of statistical mechanics as the branch of mechanics dealing with the motions of assemblies of non interacting similar systems. In the *Elementary principles in statistical mechanics*, GIBBS considered different applications of the methods of statistical mechanics,

in the above sense, some of them entirely unrelated to thermodynamics. Later some authors have assumed that the problem of the mechanical foundation of thermodynamics was essentially a particular case of that of the analysis of the motion of a mechanical system whose condition is incompletely specified, because the thermodynamical specification of the state of a body does not include a complete mechanical specification of the condition of its microscopic parts. This point of view is misleading, since the relevant fact is that the thermodynamical laws are not dependent on the complete microscopical specification, so that such a specification is not required, even if it would be known.

The distinction of the two problems (a) and (b) in our theory comes out in a clear cut way as a consequence of the nature of the wave formalism in phase space, in which both completely and incompletely specified conditions are described by wave functions and appear as pure states, whereas an ensemble in the sense (b) is described by a von Neumann density operator.

The density operator $R_{\text{can}}^{(n)}$ of a canonical ensemble of n-particle systems, in the case of distinguishable particles, is

$$(60) \qquad R_{\text{can}}^{(n)} = \exp\left[\frac{\Psi_n - H_n}{\theta}\right]_{\text{op}},$$

as a consequence of (51), or rather of the analogous formula in our classical wave theory, with

$$(61) \qquad \Psi_n = -\theta \log \int \exp\left[-\frac{H_n(\tau_1, ..., \tau_n)}{\theta}\right] d\tau_1 ... d\tau_n,$$

hence

$$(62) \qquad \tau_1', ..., \tau_n' \; R_{\text{can}}^{(n)} \; \tau_1'', ..., \tau_n'' =$$
$$= \exp\left[\frac{\Psi_n - H_n(\tau_1', ..., \tau_n')}{\theta}\right] \delta(\tau_1' - \tau_1'') ... \delta(\tau_n' - \tau_n'').$$

In the present case the density operator $R_{\text{can}}^{(n)}$ is built with the eigenfunctions of the operators x and p (commutable) having continuous spectra. A complete set of orthogonal and normalized eigenfunctions of the operators for the coordinates and momenta of the n-particles is given by the $\delta(\tau_1 - \bar{\tau}_1) ... \delta(\tau_n - \bar{\tau}_n)$:

$$(63) \qquad \begin{cases} x_i^{(\alpha)} \, \delta(\tau_1 - \bar{\tau}_1) ... \delta(\tau_n - \bar{\tau}_n) = \bar{x}_i^{(\alpha)} \, \delta(\tau_1 - \bar{\tau}_1) ... \delta(\tau_n - \bar{\tau}_n) \\ \\ p_i^{(\alpha)} \, \delta(\tau_1 - \bar{\tau}_1) ... \delta(\tau_n - \bar{\tau}_n) = \bar{p}_i^{(\alpha)} \, \delta(\tau_1 - \bar{\tau}_1) ... \delta(\tau_n - \bar{\tau}_n). \end{cases}$$

The normalization of the eigenfunctions corresponds to the well known rule:

$$(64) \qquad \int \mathrm{d}\tau_1 \dots \mathrm{d}\tau_n \{\delta(\tau_1 - \bar{\tau}_1) \dots \delta(\tau_n - \bar{\tau}_n)\} \{\delta(\tau_1 - \bar{\tau}_1') \dots \delta(\tau_n - \bar{\tau}_n')\} =$$
$$= \delta(\bar{\tau}_1 - \bar{\tau}_1') \dots \delta(\bar{\tau}_n - \bar{\tau}_n') .$$

Equation (62) can be written as follows:

$$(65) \qquad \langle \tau_1', \dots, \tau_n' | R_{\mathrm{can}}^{(n)} | \tau_1'', \dots, \tau_n'' \rangle =$$
$$= \int \mathrm{d}\bar{\tau}_1 \dots \mathrm{d}\bar{\tau}_n \exp\left[\frac{\Psi_n - H_n(\bar{\tau})}{\theta}\right] \delta(\tau_1' - \bar{\tau}_1) \dots \delta(\tau_n' - \bar{\tau}_n) \, \delta(\tau_1'' - \bar{\tau}_1) \dots \delta(\tau_n'' - \bar{\tau}) .$$

The right hand side of (65) shows that the mixed state described by $R_{\mathrm{can}}^{(n)}$ is formed with the eigenstates of the coordinates and momenta $\delta(\tau_1 - \bar{\tau}_1) \dots \delta(\tau_n - \bar{\tau}_n)$, the respective proportions being $\exp\left[\dfrac{\Psi_n - H_n(\bar{\tau})}{\theta}\right] \mathrm{d}\bar{\tau}_1 \dots \mathrm{d}\bar{\tau}_n$, hence this is the probability of finding the n particles in the elements of volume $\mathrm{d}_{\bar{\tau}}\bar{\tau}$ of Ω.

Let us consider now the cases of indistinguishability. The corresponding canonical density operators are given by a formula analogous to (58), with phase space projection operators $\overset{\pm}{P}{}^{(n)}$:

$$(66) \qquad \overset{\pm}{R}_{\mathrm{can}}^{(n)} = \overset{\pm}{P}{}^{(n)} \exp\left[\frac{\Psi_{\pm}^{(n)} - H_n(\tau)}{\theta}\right]_{\mathrm{op}} .$$

It is easily seen that

$$(67) \qquad \langle \tau_1', \dots, \tau_n' | \overset{\pm}{P}{}^{(n)} | \tau_1'', \dots, \tau_n'' \rangle = \delta_{\pm}^{(n)}(\tau', \tau'') ,$$

hence:

$$(68) \qquad \langle \tau_1', \dots, \tau_n' | \overset{\pm}{R}_{\mathrm{can}}^{(n)} | \tau_1'', \dots, \tau_n'' \rangle = \exp\left[\frac{\Psi_{\pm}^{(n)} - H_n(\tau')}{\theta}\right] \delta_{\pm}^{(n)}(\tau', \tau'') .$$

We have:

$$(69) \qquad \langle \tau_1', \dots, \tau_n' | \overset{\pm}{R}_{\mathrm{can}}^{(n)} | \tau_1'', \dots, \tau_n'' \rangle =$$
$$= \int \mathrm{d}\bar{\tau}_1 , \dots \mathrm{d}\bar{\tau}_n \exp\left[\frac{\Psi_{\pm}^{(n)} - H_n(\bar{\tau})}{\theta}\right] \delta_{\pm}^{(n)}(\tau', \bar{\tau}) \, \delta_{\pm}^{(n)}(\tau'', \bar{\tau}) ,$$

Equation (69) shows that the $\overset{\pm}{R}_{\mathrm{can}}^{(n)}$ are built with the wave functions $\delta_{\pm}^{(n)}(\tau, \bar{\tau})$ of states of completely known coordinates and momenta, which are analogous to the pure states of the quantum theory. Since permutations of the $\bar{\tau}$ in

the $\delta_{\pm}^{(n)}(\tau, \bar{\tau})$ do not lead to different states, we must use the following normalization:

$$(70) \qquad \frac{1}{n!} \int_{\Omega} \exp\left[\frac{\Psi_{\pm}^{(n)} - H_n(\bar{\tau})}{\theta}\right] d\bar{\tau}_1 \dots d\bar{\tau}_n = 1 .$$

In order to get the thermodynamical interpretation we may use the von Neumann definition of the entropy. The same reasoning of section 3 shows that $\Psi_{\pm}^{(n)}$ is the Helmholtz free energy:

$$(71) \qquad F_{\pm}^{(n)} = \Psi_{\pm}^{(n)} = - kT \log\left[\frac{1}{n!} \int_{\Omega} \exp\left[-\frac{H_n(\bar{\tau})}{kT}\right] d\bar{\tau}_1 \dots d\bar{\tau}_n\right] .$$

This formula differs from (61) only by the divisor $n!$ under the logarithm. It is well known that such a divisor must be introduced to render the free energy an extensive quantity. In the usual form of the classical theory the divisor $n!$ is introduced a posteriori, but in our theory this is not necessary because the formalism leads automatically to the correct value, as a consequence of the indistinguishability of the particles.

The von Neumann definition (47) gives for the entropy of the system of n indistinguishable particles the formula

$$(72) \qquad S_{\pm}^{(n)} = - \frac{k}{n!} \int_{\Omega} \exp\left[\frac{\Psi_{\pm}^{(n)} - H_n(\bar{\tau})}{kT}\right] \frac{\Psi_{\pm}^{(n)} - H_n(\bar{\tau})}{kT} d\bar{\tau}_1 \dots d\bar{\tau}_n ,$$

account being taken of the normalization (70). In the case of distinguishable particles the von Neumann definition gives the ordinary expression of the entropy:

$$(73) \qquad S^{(n)} = - k \int_{\Omega} \exp\left[\frac{\Psi_n - H_n(\bar{\tau})}{kT}\right] \frac{\Psi_n - H_n(\bar{\tau})}{kT} d\bar{\tau}_1 \dots d\bar{\tau}_n .$$

It is easily seen that in the case of a gas of non interacting particles of mass m enclosed in a volume V:

$$(74) \qquad \int_{\Omega} \exp\left[-\frac{H_n(\bar{\tau})}{kT}\right] d\bar{\tau}_1 \dots d\bar{\tau}_n = (2\pi mkT)^{3n/2} V^n .$$

Hence

$$(75) \qquad \Psi_{\pm}^{(n)} = - kT \log \frac{(2\pi mkT)^{3n/2} V^n}{n!} ,$$

and by applying the Stirling formula we get:

$$(76) \qquad S_{\pm}^{(n)} = nk \left[\log \frac{V}{n} + \frac{3}{2} \log (2\pi mkT) + \frac{5}{2} \right].$$

With this expression of the entropy there is no Gibbs paradox.

The results obtained with the von Neumann density operators in our classical wave theory are not so satisfactory as in the quantal statistics, because the entropy still gains an additive constant term by a change of units, as in the ordinary Gibbs theory. This is due to the fact that there is no division of the phase space Ω into finite cells. The introduction of finite cells leads also to a different thermodynamical behaviour of the systems of classical bosons and fermions, as can be expected.

Let us divide the phase space Ω into non overlapping cells ω_λ of volume ω and introduce the functions $f(\tau; \omega_\lambda)$ which are equal to 1 when τ lies inside ω_λ and to 0 when τ lies outside ω_λ. We shall assume that the energy of the system varies little when the n points τ_l move inside the cells of any of the sets $\omega_{\lambda_1}, ..., \omega_{\lambda_n}$. In order to build a density matrix we shall pick up a point τ_l in each of the ω_λ and take

$$\langle \tau_1', ..., \tau_n' | \overset{\pm}{R}_\omega^{(n)} | \tau_1'', ..., \tau_n'' \rangle = \sum_{\lambda_1, ..., \lambda_n} \exp \left[\frac{\Psi_{\pm, \omega}^{(n)} - H_n(\tau_{\lambda_1}, ..., \tau_{\lambda_n})}{\theta} \right].$$

$$(77) \qquad \cdot D_\pm(\tau_1', ..., \tau_n'; \omega_{\lambda_1}, ..., \omega_{\lambda_n}) D_\pm(\tau_1'', ..., \tau_n''; \omega_{\lambda_1}, ..., \omega_{\lambda_n}),$$

with

$$(78) \quad D_+(\tau_1, ..., \tau_n; \omega_{\lambda_1}, ..., \omega_{\lambda_n}) = (n! \, \omega^n)^{-1/2} (s_1! \, ... \, s_r!)^{-1/2} \sum_{\text{permut. } k} f(\tau_{k_1}; \omega_{\lambda_1}) ... f(\tau_{k_n}; \omega_{\lambda_n}),$$

r being the number of the distinct λ, $(s_1, s_2, ..., s_r)$ their multiplicities and

$$(79) \quad D_-(\tau_1, ..., \tau_n; \omega_{\lambda_1}, ..., \omega_{\lambda_n}) = (n! \, \omega^n)^{-1/2} \begin{vmatrix} f(\tau_1; \omega_{\lambda_1}) & f(\tau_1; \omega_{\lambda_2}) & .... f(\tau_1; \omega_{\lambda_n}) \\ f(\tau_2; \omega_{\lambda_1}) & f(\tau_2; \omega_{\lambda_2}) & .... f(\tau_2; \omega_{\lambda_n}) \\ \vdots & \vdots & \vdots \\ f(\tau_n; \omega_{\lambda_1}) & f(\tau_n; \omega_{\lambda_2}) & .... f(\tau_n; \omega_{\lambda_n}) \end{vmatrix}.$$

The $\Psi_{\pm, \omega}^{(n)}$ are determined by the normalization of the probabilities:

$$(80) \qquad \frac{1}{n!} \sum_{\lambda_1, ..., \lambda_n} g_\pm(\lambda_1, ..., \lambda_n) \exp \left[\frac{\Psi_{\pm, \omega}^{(n)} - H_n(\tau_{\lambda_1}, ..., \tau_{\lambda_n})}{\theta} \right] = 1,$$

$$(81a) \qquad g_+(\lambda_1, ..., \lambda_n) = s_1! \, s_2! \, ... \, s_r!$$

$$(81b) \qquad g_-(\lambda_1, ..., \lambda_n) = \begin{cases} 1 & \text{for} \quad r = n \\ 0 & \text{for} \quad r < n, \end{cases}$$

$n!/g_+(\lambda_1, ..., \lambda_n)$ is simply the number of times that $D_+(\tau_1', ..., \tau_n'; \omega_{\lambda_1}, ..., \omega_{\lambda_n})$ appears in the right hand side of (77). It follows from (80) that:

$$(82) \qquad \exp\left[-\frac{\Psi^{(n)}_{\pm, \omega}}{\theta}\right] = \frac{1}{n!} \sum_{\lambda_1 ... \lambda_n} g_\pm(\lambda_1, ..., \lambda_n) \exp\left[-\frac{H_n(\tau_{\lambda_1}, ..., \tau_{\lambda_n})}{\theta}\right].$$

The sum in the right hand side of (82) is larger in the case of bosons than in the case of fermions. When the particles do not interact, $\Psi^{(n)}_{\pm, \omega}$ can be easily evaluated with the saddle-point method (see SCHRÖDINGER: *Statistical Thermodynamics*, chapter VII, Cambridge, 1948):

$$(83) \qquad \Psi^{(n)}_{\pm, \omega} = \theta\left[n \log \zeta_\pm \pm \sum_\lambda \log\left\{1 \mp \zeta_\pm \exp\left[-\frac{p_\lambda^2}{2m\theta}\right]\right\}\right],$$

$\zeta_\pm$ is determined by the equation:

$$(84) \qquad n = \sum_\lambda \frac{\ddots}{\exp\left|\frac{p_\lambda^2}{2m\theta}\right|} = \cdot\cdot$$

Thus in the case of a gas of non interacting particles we get the well known quantal values of the free energy, with the only difference of the weight introduced by the spin, provided the volume of the cells ω is taken as h^3.

The division of the phase space Ω into finite cells corresponds to the Boltzmann approach to statistical mechanics. The above results show that in the case of free particles the Boltzmann finite cell method applied to our classical theory of indistinguishable particles gives results similar to those of the quantal theory, with the choice $\omega = h^3$. In more complicated cases the introduction of finite cells will not, in general, lead to the quantal results, even when $\omega = h^3$.

By using the density operators $R^{(n)}_\omega$ we can also get formulas for the average values of the occupation numbers of the different cells ω_λ which are similar to those of the quantal statistics of systems of non interacting particles. For instance, in the case of a system of n free bosons the probability of finding the set of occupation numbers $n_{\lambda_1}, n_{\lambda_2}, ...$ with $\sum_\lambda n_\lambda = n$

is $\exp\left[\dfrac{\Psi^{(n)}_{+, \omega} - \sum_\lambda n_\lambda p_\lambda^2/2m}{\theta}\right]$. Hence the average value of n_{λ_1} is

$$(85) \qquad \langle n_{\lambda_1}\rangle_+ == \sum_{n_{\lambda_1}, n_{\lambda_2}...}' n_{\lambda_1} \exp\left[\frac{\Psi^{(n)}_{+, \omega} - \sum_\lambda n_\lambda p_\lambda^2/2m}{\theta}\right],$$

$\sum'$ denoting that the condition $\sum_\lambda n_\lambda = n$ is satisfied. It follows from (85) and (82) that

$$(86) \qquad \langle n_{\lambda_1} \rangle_+ = \frac{\partial \Psi_{+,\omega}^{(n)}}{\partial \varepsilon_{\lambda_1}} = \frac{1}{\dfrac{1}{\zeta_+} \exp\left[\dfrac{\varepsilon_{\lambda_1}}{\theta}\right] - 1} \,, \qquad \left(\varepsilon_{\lambda_1} = \frac{p_{\lambda_1}^2}{2m} \right).$$

In a similar way we get:

$$(87) \qquad \langle n_{\lambda_1} \rangle_- = \frac{1}{\dfrac{1}{\zeta} \exp\left[\dfrac{\varepsilon_{\lambda_1}}{\theta}\right] + 1} \,.$$

The values of the $\zeta_\pm$ depend obviously on the choice of ω.

5. – The microcanonical ensembles in the classical wave mechanics.

The microcanonical distribution is the most fundamental tool of the classical statistical mechanics because it describes the thermodynamical behaviour of an isolated system. The average values taken in a microcanonical distribution are also important because of the theorem of ORNSTEIN ([12]) and KROÒ ([13]) which shows that the average value of a quantity in the microcanonical distribution will coincide with its time average whenever the time average be the same for all the trajectories lying on a surface of constant energy in phase space (see the very interesting discussion of the microcanonical distribution given by P. HERTZ in *Statistische Mechanik*, vol. I, part 2, of the WEBER-GANS *Repertorium der Physik*, Leipzig, 1916).

The matrix elements of the density operator $R_{\text{mic}}^{(n)}$ of the microcanonical ensemble corresponding to an energy interval $E - E + \Delta E$ are:

$$(88) \qquad \langle \tau_1', ..., \tau_n' | R_{\text{mic}}^{(n)} | \tau_1'', ..., \tau_n'' \rangle =$$
$$= C^{(n)} \int_E^{E+\Delta E} \mathrm{d}\bar{\tau}_1 ... \mathrm{d}\bar{\tau}_n \, \delta(\tau_1' - \bar{\tau}_1) ... \delta(\tau_n' - \bar{\tau}_n) \, \delta(\tau_1'' - \bar{\tau}_1) ... \delta(\tau_n'' - \bar{\tau}_n) \,.$$

In the cases of indistinguishability $R_{\text{mic}}^{(n)}$ is replaced by $\overset{\pm}{R}_{\text{mic}}^{(n)}$:

$$(89) \qquad \langle \tau_1', ..., \tau_n' | \overset{\pm}{R}_{\text{mic}}^{(n)} | \tau_1'', ..., \tau_n'' \rangle = C_\pm^{(n)} \int_E^{E+\Delta E} \mathrm{d}\bar{\tau}_1 ... \mathrm{d}\bar{\tau}_n \, \delta_\pm^{(n)}(\tau', \bar{\tau}) \, \delta_\pm^{(n)}(\tau'', \bar{\tau}) \,.$$

([12]) L. S. ORNSTEIN: *K. Akad. Wetens. Amsterdam*, 818 (1911).

([13]) J. KROÒ: *Bul. Acad. Sci. Cracovie*, 563 (1913).

The C are determined by the relations:

$$(90) \qquad C^{(n)} \int_{E}^{E+\Delta E} d\bar{\tau}_1 \dots d\bar{\tau}_n = 1 \; ,$$

$$(91) \qquad \frac{1}{n!} \, C_{\pm}^{(n)} \int_{E}^{E+\Delta E} d\bar{\tau}_1 \dots d\bar{\tau}_n = 1 \; .$$

The von Neumann definition of the entropy gives:

$$(92) \qquad S_{\mathrm{mic}}^{(n)} = - \, k C^{(n)} \log C^{(n)} \int_{E}^{E+\Delta E} d\bar{\tau}_1 \dots d\bar{\tau}_n = - \, k \log C^{(n)} \; ,$$

$$(93) \qquad S_{\pm,\mathrm{mic}}^{(n)} = - \frac{k}{n!} \, C_{\pm}^{(n)} \log C_{\pm}^{(n)} \int_{E}^{E+\Delta E} d\bar{\tau}_1 \dots d\bar{\tau}_n = - \, k \log C_{\pm}^{(n)} \; .$$

It is easily seen that in the case of non interacting particles:

$$(94) \qquad \log \int_{E}^{E+\Delta E} d\bar{\tau}_1 \dots d\bar{\tau}_n = n \left[\log V + \log (2\pi m E)^{3/2} - \frac{3}{2} \left(\log \frac{3n}{2} - 1 \right) \right] + \log \frac{\Delta E}{E} \; .$$

Hence we have:

$$(95) \qquad S_{\pm,\mathrm{mic}}^{(n)} = nk \left[\log (2\pi m E)^{3/2} + \log \frac{V}{n} + \frac{5}{2} - \frac{3}{2} \log \frac{3n}{2} \right] + k \log \frac{\Delta E}{E} \; .$$

The temperature can be determined by the well known thermodynamical formula:

$$(96) \qquad \left(\frac{\partial S}{\partial E} \right)_V = \frac{1}{T} \; .$$

The last term in the right hand side of (95) may be neglected and we get:

$$(97) \qquad E = \frac{3n}{2} \, kT \; .$$

$$(98) \qquad S_{\pm,\mathrm{mic}}^{(n)} = nk \left[\log (2\pi m k T)^{3/2} + \log \frac{V}{n} + \frac{5}{2} \right] \; .$$

This is the same expression obtained with the canonical ensemble.

In order to get a different thermodynamical behaviour in equilibrium for the classical bosons and fermions it is necessary to introduce finite cells in Ω, as in the case of the canonical ensembles. It is worthwhile to remark that the density operators of the microcanonical distributions are built with $\delta(\tau_1 - \bar{\tau}_1) \ldots \delta(\tau_n - \bar{\tau}_n)$ or $\delta_\pm^{(n)}(\tau, \bar{\tau})$ which describe states analogous to the pure states of quantum theory, as happens also in the case of the canonical ensembles. The finite cells can be introduced as follows:

$$\langle \tau_1', \ldots, \tau_n' | \overset{\pm}{R}_{\omega,\mathrm{mic}}^{(n)} | \tau_1'', \ldots, \tau_n'' \rangle = C_{\pm,\omega}^{(n)} \sum_{\lambda_1, \ldots, \lambda_n} G\big(H_n(\tau_{\lambda_1}, \ldots, \tau_{\lambda_n}) - E\big) \cdot$$

$$(99) \qquad \cdot D_\pm(\tau_1', \ldots, \tau_n'; \omega_{\lambda_1}, \ldots, \omega_{\lambda_n}) D_\pm(\tau_1'', \ldots, \tau_n''; \omega_{\lambda_1}, \ldots, \omega_{\lambda_n}),$$

$$(100) \qquad G(x - E) = \begin{cases} 1 & E \leqslant x \leqslant E + \Delta E, \\ 0 & x < E, \quad x > E + \Delta E. \end{cases}$$

The entropies of the ensembles (99) are:

$$(101) \quad S_{\pm,\omega}^{(n)} =$$

$$= -\frac{k}{n!} C_{\pm,\omega}^{(n)} \sum_{\lambda_1, \ldots, \lambda_n} g_\pm(\lambda_1, \ldots, \lambda_n) G\big(H_n(\tau_{\lambda_1}, \ldots, \tau_{\lambda_n}) - E\big) \log \big[C_{\pm,\omega}^{(n)} G\big(H_n(\tau_{\lambda_1}, \ldots, \tau_{\lambda_n}) - E\big)\big] =$$

$$= -\frac{k}{n!} C_{\pm,\omega}^{(n)} \log C_{\pm,\omega}^{(n)} \sum_{\lambda_1, \ldots, \lambda_n} g_\pm(\lambda_1, \ldots, \lambda_n) G\big(H_n(\tau_{\lambda_1}, \ldots, \tau_{\lambda_n}) - E\big) = - k \log C_{\pm,\omega}^{(n)}.$$

In the derivation of (101) we used the normalization condition:

$$(102) \qquad \frac{1}{n!} C_{\pm,\omega}^{(n)} \sum_{\lambda_1, \ldots, \lambda_n} g_\pm(\lambda_1, \ldots, \lambda_n) G\big(H_n(\tau_{\lambda_1}, \ldots, \tau_{\lambda_n}) - E\big) = 1.$$

The use of the ensembles $\overset{\pm}{R}_{\omega,\mathrm{mic}}$ is obviously related to the ordinary elementary method of the energy states, in which a macroscopical state of energy E is defined by the numbers of particles in the different one particle quantal states. This method of the energy states appears rather unsatisfactory and has been criticized (see P. JORDAN: *Statistische Mechanik*, Vorwort, Braunschweig, 1944). Our treatment shows clearly that the so-called energy state is simply a mixture described by a suitable density operator. From this point of view the special enumeration procedures for bosons and fermions appear entirely justified, since they follow immediately from the structure of the density operators.

6. – Inadequacy of the classical wave functions for the definition of the entropy.

The results of the two preceding sections allow us to understand why the wave functions are inadequate for the definition of the entropy. Let us consider a normalized wave function $\Theta_n(\tau_1, ..., \tau_n)$

$$(103) \qquad \int_\Omega |\Theta_n(\tau_1, ..., \tau_n)|^2 d\tau_1 ... d\tau_n = 1 \,,$$

describing a condition of a n-particle system in which the amount of information is less than the maximal possible. In the case of distinguishable particles we may use Θ_n to describe an ensemble whose entropy is given by the Gibbs formula:

$$(104) \qquad S_n = -k \int_\Omega |\Theta_n(\tau_1, ..., \tau_n)|^2 \log |\Theta_n(\tau_1, ..., \tau_n)|^2 d\tau_1 ... d\tau_n \,.$$

For instance, a canonical ensemble can be obtained by taking:

$$(105) \qquad |\Theta_n(\tau_1, ..., \tau_n)|^2 = \exp\left[\frac{\Psi_n - H_n(\tau_1, ..., \tau_n)}{\theta}\right].$$

The situation is no more the same when the particles are indistinguishable. Thus, in the case of fermions, it is not possible to find any wave function such that

$$(106) \qquad |\Theta_n^{(-)}(\tau_1, ..., \tau_n)|^2 = \exp\left[\frac{\Psi_-^{(n)} - H_n(\tau_1, ..., \tau_n)}{\theta}\right],$$

because the left hand side vanishes when two of the points τ_i do coincide in Ω. In the same way it is seen that it is not possible to describe a microcanonical ensemble for fermions by a wave function $\Theta_n^{(-)}$.

In the case of bosons, it is possible to take

$$(107) \qquad \Theta_n^{(+)}(\tau_1, ..., \tau_n) = \exp\left[\frac{\Psi_+^{(n)} - H_n(\tau_1, ..., \tau_n)}{2\theta}\right],$$

but the normalization (103) does not lead to the correct value of $\Psi_+^{(n)}$. If we try to avoid this difficulty, by taking quite arbitrarily

$$(108) \qquad \frac{1}{n!} \int_\Omega |\Theta_n^{(+)}(\tau_1, ..., \tau_n)|^2 d\tau_1 ... d\tau_n = 1 \,,$$

instead of the normalization (103), we will get trouble from (104), since

$$(109) \quad -k \int_{\Omega} |\Theta_n^{(+)}(\tau_1, \dots \tau_n)|^2 \log |\Theta_n^{(+)}(\tau_1, \dots, \tau_n)|^2 \, d\tau_1 \dots d\tau_n =$$

$$= -k \int_{\Omega} \exp \left[\frac{\Psi_+^{(n)} - H_n(\tau_1, \dots, \tau_n)}{\theta} \right] \frac{\Psi_+^{(n)} - H_n(\tau_1, \dots, \tau_n)}{\theta} \, d\tau_1 \dots d\tau_n ,$$

is not the correct value of the entropy. It would be necessary to divide the right hand side of (104) by $n!$ to get the correct expression for the entropy and this is also not satisfactory.

The possibility of introducing ensembles in two essentially different ways is an advantage of the present formalism, because it allows to distinguish the two totally different applications of the ensembles denoted by (a) and (b) in the discussion at the beginning of section 4. Whereas (a) may be considered as a rather subjective matter, (b) is obviously an entirely objective problem which can not depend on the limitations of our information.

The above considerations lead to an important question: *What is the nature of a condition of a mechanical system described by a density operator? It seems satisfactory to assume that a density operator, which is not equivalent to a wave function, describes the condition of a mechanical system submitted to the action of very small and irregular external influences not included in its hamiltonian.* The importance of such small irregular external actions was already shown by BOREL [14], a long time ago, and has again been emphasized more recently in the *Statistical Thermodynamics* of FOWLER and GUGGENHEIM (§ 102 of the Introduction, Cambridge, 1952). BOREL pointed out that the effect of the small irregular perturbations, which do always exists, will very rapidly put a closed system into a condition corresponding to a microcanonical ensemble.

As a matter of fact, it is possible to combine the two kinds on ensembles and to consider density operators built with wave functions describing incompletely specified states, such as the $R_\omega^{(n)+}$ and $R_{\omega,\mathrm{mic}}^{(n)\pm}$, discussed in sections 4 and 5. It is not altogether clear whether the consideration of these more complicated ensembles, which combine the methods of Boltzmann and Gibbs, is strictly necessary in a purely classical theory. These more complicated ensembles may be of practical convenience to get approximations to the quantal theory, because of the finite cells introduced by quantization.

[14] E. BOREL: *Introduction géométrique à quelques théories physiques* (Paris, 1914); *Enc. Sci. Math.*, tome IV-2, suppl. 2 (Paris, 1915).

7. – Statistical treatment of the fields in phase space along Boltzmann lines.

The « quantized » fields in phase space give the most satisfactory and complete theory of the systems of indistinguishable particles from the purely mechanical point of view. It will be seen that the same is true also from a thermodynamical point of view. The von Neumann density operators allow us to describe the microcanonical and canonical ensembles in the wave mechanics of the phase space, we shall see that the field formalism allows us to get the grand ensembles, i.e. the most general and powerful tool of the statistical mechanics.

It is remarkable that the theory of the classical « quantized » fields in phase space leads very naturally to the consideration of finite cells in the phase space Ω. Let us introduce the operators $N(\omega)$, already discussed in I:

$$(110) \qquad N(\omega) = \int_\omega \psi^*(\tau)\psi(\tau)\,\mathrm{d}\tau \,.$$

It was shown in I that the $N(\omega)$ have the eigenvalues $0, 1, 2, \dots (\infty)$ and that

$$(111) \qquad [N(\omega), N(\omega')] = 0 \,,$$

for any pair of volumes ω and ω'. The group of all the $N(\omega)$ is a complete set of commutable operators for the field. Indeed, the wave functional of the field χ may be expanded in a series of the following type (Fock expansion)

$$(112) \qquad \chi = \Theta_0\chi_0 + \sum_{n=1}^{\infty} \frac{1}{\sqrt{n!}} \int_\Omega \Theta_n(\tau_1, \dots, \tau_n)\, \chi(\tau_1, \dots \tau_n)\,\mathrm{d}\tau_1 \dots, \mathrm{d}\tau_n \,,$$

χ_0 being the wave functional of the vacuum and

$$(113) \qquad \chi(\tau_1, \dots, \tau_n) = \psi^*(\tau_1) \dots \psi^*(\tau_n)\chi_0 \,,$$

as shown in section 5 of I. When χ_0 is normalized, $|\Theta_n(\tau_1, \dots, \tau_n)|^2\,\mathrm{d}\tau_1 \dots \mathrm{d}\tau_n$ gives the probability of finding n particles in the field and located in the elements of volume $\mathrm{d}\tau_i$ containing the corresponding τ_i. The wave functionals are therefore determined by the probability amplitudes for the phase space distributions of any number of particles and this shows that the group of all the $N(\omega)$ is a complete set of commutable operators.

In the representation in which all the $N(\omega)$ are diagonal, the wave functional of the field is a functional of a domain function $N'(\omega)$ taking the values $0, 1, 2, \dots (\infty)$ for any volume ω: $\chi[N'(\omega)]$, $|\chi[N'(\omega)]|^2$ being proportional

to the probability of finding $N'(\omega)$ particles in the volume ω. Therefore the « quantized » field formalism leads naturally to the consideration of finite volumes of ω and their occupation numbers. The occupation numbers N' take however all the positive integer values both for fermions and bosons. The operator for the energy of the field is $\mathcal{H}$:

$$(114) \qquad \mathcal{H} = \int_{\Omega} \psi^*(\tau) \frac{\boldsymbol{p}^2}{2m} \psi(\tau) \, d\tau + \frac{1}{2} \int_{\Omega} \psi^*(\tau)\psi^*(\tau')\Phi(\boldsymbol{x} - \boldsymbol{x}')\psi(\tau')\psi(\tau) \, d\tau \, d\tau' \, .$$

The first term in the right hand side of (114) corresponds to the kinetic energy and the second one to the potential energy. We shall denote them by $\mathcal{H}_{\text{kin}}$ and $\mathcal{H}_{\text{pot}}$. When $\Phi(0)$ is finite, we may write:

$$(115) \qquad \mathcal{H} = \int_{\Omega} \psi^*(\tau)\psi(\tau) \frac{\boldsymbol{p}^2}{2m} \, d\tau + \frac{1}{2} \int_{\Omega} \psi^*(\tau)\psi(\tau)\Phi(\boldsymbol{x} - \boldsymbol{x}')\psi^*(\tau')\psi(\tau') \, d\tau \, d\tau'$$
$$- \frac{1}{2} \Phi(0) \int_{\Omega} \psi^*(\tau)\psi(\tau) \, d\tau \, .$$

When the $\psi(\tau)$ and $\psi^*(\tau)$ are expanded in series of orthogonal and normalized functions

$$(116) \qquad \psi(\tau) = \sum_{\lambda} a_{\lambda} u_{\lambda}(\tau) \, , \qquad \psi^*(\tau) = \sum_{\lambda} a_{\lambda}^* u_{\lambda}^*(\tau) \, ,$$

the $u_{\lambda}(\tau)$ being the functions of a complete set, we have

$$(117) \qquad [a_{\lambda}, a_{\lambda'}^*]_{\pm} = \delta_{\lambda,\lambda'} \, , \qquad [a_{\lambda}, a_{\lambda'}]_{\pm} = [a_{\lambda}^*, a_{\lambda'}^*]_{\pm} = 0 \, ,$$

the signs $-$ and $+$ corresponding to bosons and fermions respectively. We have also:

$$(118) \qquad N_{\text{op}} = \sum_{\lambda} N_{\lambda} \, , \qquad N_{\lambda} = a_{\lambda}^* a_{\lambda} \, .$$

The N_{λ} have the eigenvalues $0, 1, 2 \ldots (\infty)$ in the case of bosons, but in the case of fermions the only eigenvalues are 0 and 1. By introducing the expansions (116) into (114) we get

$$(119) \qquad \mathcal{H} = \frac{1}{2m} \sum_{\lambda', \lambda''} a_{\lambda'}^* a_{\lambda''} \langle \lambda' | \boldsymbol{p}^2 | \lambda'' \rangle +$$
$$+ \frac{1}{2} \sum_{\lambda', \lambda'', \lambda''', \lambda^{\text{IV}}} a_{\lambda'}^* a_{\lambda''}^* a_{\lambda^{\text{IV}}} a_{\lambda'''} \langle \lambda', \lambda'' | \Phi(\boldsymbol{x}_1 - \boldsymbol{x}_2) | \lambda''' \lambda^{\text{IV}} \rangle,$$

with

$$(120) \qquad \langle \lambda' \mid \boldsymbol{p}^2 \mid \dot{\lambda}'' \rangle = \int_{\Omega} u_{\lambda'}(\tau) u_{\lambda''}(\tau) \boldsymbol{p}^2 \, \mathrm{d}\tau \,,$$

$$(121) \quad \lambda', \lambda'' \mid \Phi(\boldsymbol{x}_1 \quad \boldsymbol{x}_2) \mid \lambda''', \lambda^{\mathrm{IV}} = \int_{\Omega} u_{\lambda'}(\tau_1) u_{\lambda''}^*(\tau_2) u_{\lambda'''}(\tau_1) u_{\lambda^{\mathrm{IV}}}(\tau_2) \Phi(\boldsymbol{x}_1 \quad \boldsymbol{x}_2) \, \mathrm{d}\tau_1 \, \mathrm{d}\tau_2 \,.$$

In the representation in which the N_λ are diagonal, the wave functional of the field is a function of the eigenvalues N_λ' of the N_λ. The functions $f(\tau; \omega_\lambda)$ introduced in section **4** are orthogonal and normalized but do *not constitute a complete set*. Nevertheless, if the cells ω_λ are small in all the dimensions, the set of the $u_\lambda(\tau) = f(\tau; \omega_\lambda)$ will be approximately complete and we may use the formalism corresponding to the expansions into the functions of a complete orthonormal set to get a description of *incompletely* specified states of the field. In this treatment we have:

$$(122) \qquad \langle \lambda' \mid \boldsymbol{p}^2 \mid \lambda'' \rangle = \boldsymbol{p}_{\lambda'}^2 \, \delta_{\lambda', \lambda''} \qquad \boldsymbol{p}_{\lambda'}^2 = \frac{1}{\omega_\lambda} \int_{\omega_\lambda} \boldsymbol{p}^2 \, \mathrm{d}\tau \,,$$

$$(123) \quad \begin{cases} \langle \lambda', \lambda'' \mid \Phi(\boldsymbol{x}_1 - \boldsymbol{x}_2) \mid \lambda''', \lambda^{\mathrm{IV}} \rangle = \Phi_{\lambda', \lambda''} \delta_{\lambda', \lambda'''} \delta_{\lambda'', \lambda^{\mathrm{IV}}} \\[2mm] \Phi_{\lambda' \lambda''} = \dfrac{1}{\omega_{\lambda'} \omega_{\lambda''}} \int_{\omega_{\lambda'}} \mathrm{d}\tau_1 \int_{\omega_{\lambda''}} \Phi(\boldsymbol{x}_1 - \boldsymbol{x}_2) \, \mathrm{d}\tau_2 \,, \end{cases}$$

$$(124) \qquad \mathcal{H}_\omega = \frac{1}{2m} \sum_{\lambda'}^{(\omega)} \overset{(\omega)}{N}_{\lambda'} \, \boldsymbol{p}_{\lambda'}^2 + \frac{1}{2} \sum_{\lambda', \lambda''}^{(\omega)} \overset{(\omega)}{N}_{\lambda'} \overset{(\omega)}{N}_{\lambda''} \Phi_{\lambda' \lambda''} \quad \frac{1}{2} \sum_{\lambda'}^{(\omega)} \overset{(\omega)}{N}_{\lambda'} \Phi_{\lambda' \lambda'} \,.$$

In the above formulas we did not assume that the volumes of all the cells are equal.

We shall now assume that each incompletely specified state $\chi_\omega(\overset{(\omega)}{N_1}, \overset{(\omega)}{N_2}, \ldots)$ has an entropy $S[\chi_\omega]$

$$(125) \qquad S[\chi_\omega] = - k \sum_\lambda \sum_{N_\lambda'} | \overset{(\omega)}{\chi_\omega(N')} |^2 \log | \overset{(\omega)}{\chi_\omega(N')} |^2 \,, \qquad \left(\sum_\lambda \sum_{N_\lambda'} | \overset{(\omega)}{\chi_\omega(N')} |^2 = 1 \right).$$

Let us consider the χ determined by the conditions of extremal entropy with given average number of particles N and given average value of the energy E:

$$(126) \qquad N = (\chi_\omega, N_{\mathrm{op}} \chi_\omega) = \sum_\lambda \sum_{\overset{(\omega)}{N_\lambda'}} | \overset{(\omega)}{\chi_\omega(N')} |^2 \overset{(\omega)}{N_\lambda'} \,.$$

$$(127) \quad E = (\chi_\omega, \mathcal{H}_\omega \chi_\omega) = \sum_\lambda \sum_{\overset{(\omega)}{N'}} \chi_\omega(\overset{(\omega)}{N'})^{.2} \left\{ \overset{(\omega)}{N_{\lambda'}} \left(\frac{\boldsymbol{p}_{\lambda'}^2}{2m} \quad \frac{1}{2} \Phi_{\lambda', \lambda'} \right) + \frac{1}{2} \overset{(\omega)}{N_{\lambda'}} \overset{(\omega)}{N_{\lambda''}} \Phi_{\lambda', \lambda''} \right\}.$$

By introducing the Lagrange multipliers $k\alpha$, $k\beta$ and $k\gamma$ we get the equation

$$(128) \qquad \delta\left\{ S[\chi_\omega] - k\alpha(\chi_\omega, N_{\mathrm{op}}\chi_\omega) - k\beta(\chi_\omega, \mathcal{H}_\omega\chi_\omega) - k\gamma(\chi_\omega, \chi_\omega)\right\} = 0,$$

hence

$$(129) \qquad |\chi_\omega(\overset{(\omega)}{N'})|^2 =$$

$$= \exp\left[-(\gamma+1) - \alpha \sum_{\lambda'} \overset{(\omega)}{N'_{\lambda'}} - \beta\left\{ \sum_{\lambda'} \overset{(\omega)}{N'_{\lambda'}}\left(\frac{\boldsymbol{p}_{\lambda'}^2}{2m} - \frac{1}{2}\,\Phi_{\lambda',\lambda'}\right) + \frac{1}{2}\sum_{\lambda',\lambda''} \overset{(\omega)}{N'_{\lambda'}}\,\overset{(\omega)}{N'_{\lambda''}}\Phi_{\lambda',\lambda''}\right\}\right].$$

The formula (129) is obtained directly by giving a variation to $|\chi_\omega|^2$ in (128), without splitting it into the factors χ_ω^* and χ_ω. By variating separately χ_ω^* and χ_ω we get:

$$(130a) \qquad \chi_\omega[\log|\chi_\omega|^2 + \gamma + 1] = -(\alpha N_{\mathrm{op}} + \beta\,\mathcal{H}_\omega)\chi_\omega,$$

$$(130b) \qquad \chi_\omega^*[\log|\chi_\omega|^2 + \gamma + 1] = -\{(\alpha N_{\mathrm{op}} + \beta\,\mathcal{H}_\omega)\chi_\omega\}^*.$$

These equations are satisfied as a consequence of (129) by taking χ, α, β and γ real. We shall denote the χ thus obtained by $\chi_{\mathrm{can}}^{(\omega)}$:

$$(131) \qquad \chi_{\mathrm{can}}^{(\omega)} = \exp\left[-\frac{\gamma+1}{2} - \frac{\alpha}{2}\sum_\lambda \overset{(\omega)}{N'_\lambda} - \right.$$

$$\left. - \frac{\beta}{2}\left\{ \sum_{\lambda'} \overset{(\omega)}{N'_{\lambda'}}\left(\frac{\boldsymbol{p}_{\lambda'}^2}{2m} - \frac{1}{2}\,\Phi_{\lambda',\lambda'}\right) + \frac{1}{2}\sum_{\lambda',\lambda''} \overset{(\omega)}{N'_{\lambda'}}\,\overset{(\omega)}{N'_{\lambda''}}\Phi_{\lambda',\lambda''}\right\}\right].$$

It follows from the first equation (125) that:

$$(132) \qquad S[\chi_{\mathrm{can}}^{(\omega)}] = k\sum_{N'} |\chi_{\mathrm{can}}^{(\omega)}|^2\left[\gamma + 1 + \alpha\sum_\lambda \overset{(\omega)}{N'_\lambda} + \right.$$

$$\left. + \beta\left\{ \sum_{\lambda'} \overset{(\omega)}{N'_\lambda}\left(\frac{\boldsymbol{p}_{\lambda'}^2}{2m} - \frac{\Phi_{\lambda'\lambda'}}{2}\right) + \frac{1}{2}\sum_{\lambda'\lambda''} \overset{(\omega)}{N'_{\lambda'}}\,\overset{(\omega)}{N'_{\lambda''}}\Phi_{\lambda',\lambda''}\right\}\right].$$

By taking into account the second equation (125), (126) and (127) we get:

$$(133) \qquad S[\chi_{\mathrm{can}}^{(\omega)}] = k(\gamma' + \alpha N + \beta E) \qquad\qquad \gamma' = \gamma + 1.$$

Therefore we have

$$(134) \qquad \alpha = -\frac{\mu}{kT}, \qquad \beta = \frac{1}{kT}, \qquad \gamma' = \frac{PV}{kT},$$

T, μ and P being the temperature, chemical potential and pressure, respectively. The incompletely specified state described by $\chi_{\text{can}}^{(\omega)}$ corresponds thereby to a canonical grand ensemble.

In the particular case of non interacting particles

$$(135) \qquad |\chi_{\text{can}}^{(\omega)}(\overset{(\omega)}{N'})|^2 = e^{-\gamma'} \prod_{\lambda'} \exp\left[-\overset{(\omega)}{N'_{\lambda'}}(\alpha + \beta\varepsilon_{\lambda'})\right], \qquad \left(\varepsilon_{\lambda'} = \frac{p_{\lambda'}^2}{2m}\right),$$

so that the average number of particles in the cell ω_λ is:

$$(136) \qquad \langle N_\lambda \rangle_{\text{can}}^{(\omega)} = \sum_{N'}^{(\omega)} \overset{(\omega)}{N'_\lambda} |\chi_{\text{can}}^{(\omega)}(\overset{(\omega)}{N'})|^2 =$$

$$= e^{-\gamma'} \sum_{N'_\lambda} \overset{(\omega)}{N'_\lambda} \exp\left[-\overset{(\omega)}{N'_\lambda}(\alpha + \beta\varepsilon_\lambda)\right] \prod_{\lambda' \neq \lambda} \sum_{N'_{\lambda'}} \exp\left[-\overset{(\omega)}{N'_{\lambda'}}(\alpha + \beta\varepsilon_{\lambda'})\right].$$

In the case of fermions the N' take only the values 0 and 1, hence:

$$(137) \qquad \langle N_\lambda \rangle_{\text{can}}^{(\omega)(F)} = e^{-\gamma'} \exp\left[-\alpha - \beta\varepsilon_\lambda\right] \prod_{\lambda' \neq \lambda} \left[1 + \exp\left[-\alpha - \beta\varepsilon_{\lambda'}\right]\right] =$$

$$= \frac{\exp\left[-\alpha - \beta\varepsilon_\lambda\right]}{1 + \exp\left[-\alpha - \beta\varepsilon_\lambda\right]} \sum_{N'} |\chi_{\text{can}}^{(\omega)}(\overset{(\omega)}{N'})|^2 = \frac{1}{\exp\left[\alpha + \beta\varepsilon_\lambda\right] + 1},$$

$$(138) \qquad \langle N_\lambda \rangle_{\text{can}}^{(\omega)(B)} = \frac{\sum_{N'_\lambda = 0}^{\infty} \overset{(\omega)}{N'_\lambda} \exp\left[-\overset{(\omega)}{N'_\lambda}(\alpha + \beta\varepsilon_\lambda)\right]}{\sum_{N'_\lambda = 0}^{\infty} \exp\left[-\overset{(\omega)}{N'_\lambda}(\alpha + \beta\varepsilon_\lambda)\right]} \sum_{N'} |\chi_{\text{can}}^{(\omega)}(\overset{(\omega)}{N'})|^2 =$$

$$= -\frac{\partial}{\partial\alpha} \log\left\{ \sum_{N'_\lambda = 0}^{\infty} \exp\left[-\overset{(\omega)}{N'_\lambda}(\alpha + \beta\varepsilon_\lambda)\right] \right\} =$$

$$= \frac{\partial}{\partial\alpha} \log\left\{1 - \exp\left[-\alpha - \beta\varepsilon_\lambda\right]\right\} = \frac{1}{\exp\left[\alpha + \beta\varepsilon_\lambda\right] - 1}.$$

8. – The Boltzmann method in the classical wave mechanics.

In sections **4** and **5** the Boltzmann division of the phase space into finite cells was combined with the von Neumann method of the density operators. We shall now apply to the wave mechanics in phase space the method of

expansion into series of orthogonal functions which do not constitute a complete set. The wave function $\Theta_n^{(\pm)}$ will be replaced by an approximate one $\Theta_{n,\omega}^{(\pm)}$ represented by a series

$$(139) \qquad \Theta_{n,\omega}^{(\pm)}(\tau_1, ..., \tau_n) = \frac{1}{n!} \sum_{\lambda_1,...,\lambda_n} g_\pm(\lambda_1,...,\lambda_n) A_{\lambda_1,...,\lambda_n}^{(\pm)} D_\pm(\tau_1, ..., \tau_n;\ \omega_{\lambda_1}, ..., \omega_{\lambda_n}),$$

the $D_\pm$ being defined by (78) and (79). The normalization condition for $\Theta_{n,\omega}^{(\pm)}$ is:

$$(140) \qquad \int_\Omega |\Theta_{n,\omega}^{(\pm)}|^2 d\tau_1 ... d\tau_n = \frac{1}{n!} \sum_{\lambda_1,...,\lambda_n} g_\pm(\lambda_1, ..., \lambda_n) |A_{\lambda_1,...,\lambda_n}^{(\pm)}|^2 = 1,$$

$A_{\lambda_1,...,\lambda_n}^{(+)}$ and $A_{\lambda_1,...,\lambda_n}^{(-)}$ are respectively symmetrical and anti-symmetrical with respect to the indices $\lambda_1,\ \lambda_2, ..., \lambda_n$. We shall now consider the following definition of the entropy:

$$(141) \qquad S_{n,\omega}^{(\pm)} = -\frac{k}{n!} \sum_{\lambda_1,...,\lambda_n} g_\pm(\lambda_1, ..., \lambda_n) |A_{\lambda_1,...,\lambda_n}^{(\pm)}|^2 \log |A_{\lambda_1,...,\lambda_n}^{(\pm)}|^2.$$

The average value of the energy in the state $\Theta_{n,\omega}^{(\pm)}$ is:

$$(142) \qquad H[\Theta_{n,\omega}^{(\pm)}] = \int_\Omega |\Theta_{n,\omega}^{(\pm)}(\tau_1, ..., \tau_n)|^2 H_n(\tau_1, ..., \tau_n) d\tau_1 ... d\tau_n =$$

$$= \frac{1}{n!} \sum_{\lambda_1,...,\lambda_n} g_\pm(\lambda_1, ..., \lambda_n) |A_{\lambda_1,...,\lambda_n}^{(\pm)}|^2 H_{\lambda_1,...,\lambda_n}^{(\pm)},$$

$$(143) \qquad H_{\lambda_1,...,\lambda_n}^{(\pm)} = \int_\Omega \{D_\pm(\tau_1, ..., \tau_n;\ \omega_{\lambda_1}, ..., \omega_{\lambda_n})\}^2 H_n(\tau_1, ..., \tau_n) d\tau_1 ... d\tau_n.$$

The condition of a system in thermal equilibrium can be defined by the $\Theta_{n,\omega}^{(\pm)\mathrm{can}}$ whose coefficients are:

$$(144) \qquad A_{\lambda_1,...,\lambda_n}^{(\pm)\mathrm{can}} = \exp\left[\frac{\Psi_{n,\omega}^{(\pm)} - H_{\lambda_1,...,\lambda_n}^{(\pm)}}{2\theta}\right] \qquad (\lambda_1 < \lambda_2 < ... < \lambda_n \text{ for fermions}).$$

It is easily seen that the entropy $S_{n,\omega}^{(\pm)\mathrm{can}}$ of the state $\Theta_{n,\omega}^{(\pm)\mathrm{can}}$ is:

$$(145) \qquad S_{n,\omega}^{(\pm)\mathrm{can}} = \frac{k}{\theta}\{H[\Theta_{n,\omega}^{(\pm)\mathrm{can}}] - \Psi_{n,\omega}^{(\pm)}\}.$$

Hence, by taking as usual $\theta = kT$, $\Psi_{n,\omega}^{(\pm)}$ will be the Helmholtz free energy. The $\Psi_{n,\omega}^{(\pm)}$ are determined by the normalization condition (140):

$$(146) \qquad \Psi_{n,\omega}^{(\pm)} = - \theta \log \left\{ \frac{1}{n!} \sum_{\lambda_1, \ldots, \lambda_n} g_{\pm}(\lambda_1, \ldots, \lambda_n) \exp \left| -\frac{H_{\lambda_1, \ldots, \lambda_n}^{(\pm)}}{\theta} \right| \right\} .$$

These expressions of the free energies are equivalent to those obtained in section **4** for the density operators $\overset{\pm}{R_{\omega}^{(n)}}$.

The above method can also be applied to systems of distinguishable particles by using the following expansion for $\Theta_{n,\omega}$:

$$(147) \qquad \Theta_{n,\omega}(\tau_1, \ldots, \tau_n) = \sum_{\lambda_1, \ldots, \lambda_n} A_{\lambda_1, \ldots, \lambda_n} D(\tau_1, \ldots, \tau_n; \omega_{\lambda_1}, \ldots \omega_{\lambda_n}) ,$$

$$(147a) \qquad \sum_{\lambda_1, \ldots, \lambda_n} g_{+}(\lambda_1, \ldots, \lambda_n) |A_{\lambda_1, \ldots, \lambda_n}|^2 = 1 ,$$

$$(148) \qquad D(\tau_1, \ldots, \tau_n; \omega_{\lambda_1}, \ldots, \omega_{\lambda_n}) = \frac{1}{\sqrt{\omega^n}} f(\tau_1; \omega_{\lambda_1}) \ldots f(\tau_n; \omega_{\lambda_n}) .$$

The average value of the energy in the state $\Theta_{n,\omega}$ is:

$$(149) \qquad H[\Theta_{n,\omega}] = k \sum_{\lambda_1, \ldots, \lambda_n} g_{+}(\lambda_1, \ldots, \lambda_n) |A_{\lambda_1, \ldots, \lambda_n}|^2 H_{\lambda_1, \ldots, \lambda_n} .$$

$$(149a) \qquad H_{\lambda_1, \ldots, \lambda_n} = \int_{\Omega} \{D(\tau_1, \ldots, \tau_n; \omega_{\lambda_1}, \ldots, \omega_{\lambda_n})\}^2 H_n(\tau_1, \ldots, \tau_n) \, d\tau_1 \ldots d\tau_n .$$

We shall take as entropy:

$$(150) \qquad S_{n,\omega} = - k \sum_{\lambda_1, \ldots, \lambda_n} g_{+}(\lambda_1, \ldots, \lambda_n) |A_{\lambda_1, \ldots, \lambda_n}|^2 \log |A_{\lambda_1, \ldots, \lambda_n}|^2 .$$

The coefficients of the canonical wave function $\Theta_{n,\omega}^{\mathrm{can}}$ are

$$(151) \qquad A_{\lambda_1, \ldots, \lambda_n}^{\mathrm{can}} = \exp \left[\frac{\Psi_{n,\omega} - H_{\lambda_1, \ldots, \lambda_n}}{2\theta} \right] .$$

The free energy $\Psi_{n,\omega}$ is:

$$(152) \qquad \Psi_{n,\omega} = - \theta \log \left\{ \sum_{\lambda_1, \lambda_2, \ldots, \lambda_n} g_{+}(\lambda_1, \ldots \lambda_n) \exp \left[-\frac{H_{\lambda_1, \ldots, \lambda_n}}{\theta} \right] \right\} .$$

9. – Statistical treatment of the phase space fields by density operators.

The definition (51) of the canonical density operator must be modified in the application to the fields, because of the existence of the integral of motion N_{op}. The canonical density operator is now characterized by rendering the entropy extremal with the conditions of given average values of the energy and the number of particles, whereas the expression (51) is obtained by rendering the entropy extremal with the only condition of given average energy, as well known ([15]). By applying the method of the Lagrange multipliers and taking into account the von Neumann definition of the entropy (48), the expression (49) of $\langle H \rangle$ and the following equation

$$\langle N_{\text{op}} \rangle = \sum_a q_a N_a' , \tag{153}$$

we get the variational equation

$$\delta(S - k\beta_1 \langle N_{\text{op}} \rangle - k\beta_2 \langle H \rangle) = - k \sum_a \delta q_a [1 + \log q_a + \beta_1 N_a' + \beta_2 E_a] = 0, \tag{154}$$

$k\beta_1$ and $k\beta_2$ being the Lagrange multipliers. Thus we get

$$q_a = \exp\left[- \beta_1 N_a' - \beta_2 E_a - 1\right], \tag{155}$$

and by taking into account the normalization $\sum_a q_a = 1$ we may write

$$q_a = \frac{\exp\left[- \beta_1 N_a' - \beta_2 E_a\right]}{\sum_{a'} \exp\left[- \beta_1 N_{a'}' - \beta_2 E_{a'}\right]} = \exp[\eta - \beta_1 N_a' - \beta_1 E_a] , \tag{156}$$

with

$$e^{-\eta} = \sum_{a'} \exp\left[- \beta_1 N_{a'}' - \beta_2 E_{a'}\right] . \tag{157}$$

Finally we get, instead of (51)

$$R_{\text{can}} = \exp\left[\eta - \beta_1 N_{\text{op}} - \beta_2 \mathscr{H}\right] , \tag{158}$$

([15]) KÔDI HUSIMI: *Proc. Phys. Math. Soc. Japan*, **22**, 264 (1940).

since the energy operator of the field is denoted by $\mathcal{H}$. The entropy of R_{can} is

$$(159) \qquad S_{\text{can}} = - k \sum_a (\eta - \beta_1 N'_a - \beta_2 E_a) \exp\left[\eta - \beta_1 N'_a - \beta_2 E_a\right] =$$
$$= - k(\eta - \beta_1 \langle N_{\text{op}} \rangle_{\text{can}} - \beta_2 \langle \mathcal{H} \rangle_{\text{can}}),$$

hence:

$$(160) \qquad \beta_1 = - \frac{\mu}{kT}, \qquad \beta_2 = \frac{1}{kT}, \qquad \eta = - \frac{PV}{kT}.$$

The canonical ensemble for the field corresponds to a canonical grand ensemble for the particles, as shown by (156). Thus the statistics of the field leads automatically to the introduction of the grand ensemble. This fact shows that the grand ensembles are of a more fundamental nature than the petits ensembles in the theory of indistinguishable particles. The quantal formula (158) can be taken over without modification into the theory of the « quantized » fields.

It follows from the formulas (60) and (138) of I that

$$(161) \qquad \exp\left[-\beta_1 N_{\text{op}}\right] = \sum_{n=0}^{\infty} \exp\left[-\beta_1 n\right] P_n =$$
$$= P_0 + \sum_{n=1}^{\infty} \exp\left[-\beta_1 n\right] \int_{\Omega} P(\tau_1, \tau_2, ..., \tau_n) \, d\tau_1 ... d\tau_n,$$

P_n being the projection operator on the linear manifold of the eigenfunctionals of N_{op} corresponding to the eigenvalue n and $P(\tau_1, ..., \tau_n)$ the projection operator on the direction of the vector $\chi(\tau_1, ..., \tau_n)$ in χ-space:

$$(162) \qquad P(\tau_1, ..., \tau_n)\chi = \frac{1}{n!}\left(\chi(\tau_1, ..., \tau_n), \chi\right)\chi(\tau_1, ..., \tau_n),$$

$$(163) \qquad P(\tau_1, ..., \tau_n) = \frac{1}{n!}\psi^*(\tau_1) ... \psi^*(\tau_n)P_0\psi(\tau_n) ... \psi(\tau_1).$$

The operators $\mathcal{H}_{\text{kin}}$ and $\mathcal{L}_{\text{pot}}$ being commutable, we have:

$$(164) \qquad \exp\left[-\beta_2\mathcal{H}\right] = \exp\left[-\beta_2\mathcal{H}_{\text{kin}}\right] \exp\left[-\beta_2\mathcal{H}_{\text{pot}}\right].$$

Let us consider now a numerical function $F(\tau_1, ..., \tau_r)$ and the corresponding operator F_{op}:

$$(165) \qquad F_{\text{op}} = \frac{1}{r!} \int_{\Omega} F(\tau_1, ..., \tau_r)\psi^*(\tau_1) ... \psi^*(\tau_r)\psi(\tau_r) ... \psi(\tau_1) \, d\tau_1 ... d\tau_r.$$

Is was shown in I that

$$(166) \quad \begin{cases} P(\tau_1, ..., \tau_n)P(\tau_1', ..., \tau_n') = \delta_{\pm}^{(n)}(\tau, \tau')P(\tau_1, ..., \tau_n) \\ P(\tau_1, ..., \tau_n)P(\tau_n', ..., \tau_{n'}') = 0 \quad \text{for} \quad n \neq n', \end{cases}$$

and

$$(167) \quad F_{\text{op}} = \sum_{n=r}^{\infty} \binom{n}{r} \int_{\Omega} F(\tau_1, ..., \tau_r)P(\tau_1, ..., \tau_n)\, d\tau_1 ... d\tau_n.$$

By taking into account (166) and (167) we get

$$(168) \quad (F_{\text{op}})^s = \sum_{n=r}^{\infty} \binom{n}{r}^s \int_{\Omega} [F(\tau_1, ..., \tau_r)]^s P(\tau_1, ..., \tau_n)\, d\tau_1 ... d\tau_n,$$

so that

$$(169) \exp[-v\, F_{\text{op}}] = \sum_{l=r}^{r-1} P_l + \sum_{n=r}^{\infty} \int_{\Omega} \exp\left[v \binom{n}{r} F(\tau_1, ..., \tau_r)\right] P(\tau_1,...,\tau_n)d\tau_1 ... d\tau_n$$

v being a number.   We get from (169)

$$(170) \quad \exp[-\beta_2\, \mathcal{H}_{\text{kin}}] = P_0 + \sum_{n=1}^{\infty} \int_{\Omega} \exp\left[-\frac{\beta_2}{2m} \sum_{l=1}^{n} \boldsymbol{p}_l^2\right] P(\tau_1, ..., \tau_n)\, d\tau_1 ... d\tau_n,$$

$$(171) \quad \exp[-\beta_2\, \mathcal{H}_{\text{pot}}] = P_0 + P_1 +$$
$$+ \sum_{n=2}^{\infty} \int_{\Omega} \exp\left[-\frac{\beta_2}{2} \sum_{l=1}^{n} \sum_{l' \neq l} \Phi(\boldsymbol{x}_l - \boldsymbol{x}_{l'})\right] P(\tau_1, ..., \tau_n)\, d\tau_1 ... d\tau_n,$$

so that:

$$(172) \quad \exp[-\beta_2\mathcal{H}] = P_0 + \int_{\Omega} \exp\left[-\frac{\beta_2}{2m} \boldsymbol{p}_1^2\right] P(\tau_1)\, d\tau_1 +$$
$$+ \sum_{n=2}^{\infty} \int_{\Omega} \exp[-\beta_2 H_n(\tau_1, ..., \tau_n)]P(\tau_1, ..., \tau_n)\, d\tau_1 ... d\tau_n.$$

By combining (161) and (172) we get finally the spectral decomposition of R_{can}:

$$(173) \quad R_{\text{can}} = P_0 e^{\eta} + \sum_{n=1}^{\infty} \int_{\Omega} \exp[\eta - \beta_1 n - \beta_2 H_n(\tau_1, ..., \tau_n)]P(\tau_1, ..., \tau_n)\, d\tau_1 ... d\tau_n.$$

Equation (173) shows that we must take:

$$(174) \qquad e^{-\eta} = 1 + \sum_{n=1}^{\infty} \exp\left[-\beta_1 n\right] \int_{\Omega} \exp\left[-\beta_2 H_n(\tau_1, \ldots, \tau_n)\right] d\tau_1 \ldots d\tau_n .$$

Thus we get the same η for both fermions and bosons, as should be expected from the results obtained in section **4**. A difference in the thermodynamical behaviour can be obtained by the introduction of finite cells. This can be done by a suitable modification of the density operator R_{can}.

10. – The super-classical field.

We shall now prove that the theory of the « quantized » fields in the phase space Ω can be obtained by a kind of « quantization » of c-number fields in Ω. Let us consider the variational principle

$$(175) \qquad \delta \mathcal{L} = \delta \int_{t_0}^{t_1} \Lambda \, dt ,$$

$$(176) \qquad \Lambda = i \int_{\Omega} \psi_c^*(t; \tau) \, \frac{\partial}{\partial t} \, \psi_c(t; \tau) \, d\tau - \int_{\Omega} \psi_c^*(t; \tau) L_{\mathrm{kin}}(\tau) \psi_c(t; \tau) \, d\tau$$

$$- \frac{1}{2} \int_{\Omega} \psi_c^*(t; \tau) \psi_c^*(t; \tau') L_{\mathrm{pot}}(\tau, \tau') \psi_c(t; \tau') \psi_c(t; \tau) \, d\tau \, d\tau' ,$$

$$(177) \qquad L_{\mathrm{kin}}(\tau) = -\frac{i\boldsymbol{p}}{m} \cdot \frac{\partial}{\partial \boldsymbol{x}} , \quad L_{\mathrm{pot}}(\tau, \tau') = i \frac{\partial \Phi(\boldsymbol{x} - \boldsymbol{x}')}{\partial \boldsymbol{x}} \cdot \frac{\partial}{\partial \boldsymbol{p}} + i \frac{\partial \Phi(\boldsymbol{x} - \boldsymbol{x}')}{\partial \boldsymbol{x}'} \cdot \frac{\partial}{\partial \boldsymbol{p}'} ,$$

for the c-numbers $\psi_c(t, \tau)$ and $\psi_c^*(t, \tau)$. The Euler equations are:

$$(178a) \qquad \frac{\partial}{\partial t} \psi_c(t; \tau) = -\frac{\boldsymbol{p}}{m} \cdot \frac{\partial}{\partial \boldsymbol{x}} \psi(t; \tau) +$$

$$+ \int_{\Omega} \psi_c^*(t; \tau') \left\{ \frac{\partial \Phi(\boldsymbol{x} - \boldsymbol{x}')}{\partial \boldsymbol{x}} \cdot \frac{\partial}{\partial \boldsymbol{p}} + \frac{\partial \Phi(\boldsymbol{x} - \boldsymbol{x}')}{\partial \boldsymbol{x}'} \cdot \frac{\partial}{\partial \boldsymbol{p}'} \right\} \psi_c(t; \tau') \psi_c(t; \tau) \, d\tau' .$$

$$(178b) \qquad \frac{\partial}{\partial t} \psi_c^*(t; \tau) = -\frac{\boldsymbol{p}}{m} \cdot \frac{\partial}{\partial \boldsymbol{x}} \psi_c^*(t; \tau) +$$

$$+ \int_{\Omega} \left\{ \left(\frac{\partial \Phi(\boldsymbol{x} - \boldsymbol{x}')}{\partial \boldsymbol{x}} \cdot \frac{\partial}{\partial \boldsymbol{p}} + \frac{\partial \Phi(\boldsymbol{x} - \boldsymbol{x}')}{\partial \boldsymbol{x}'} \cdot \frac{\partial}{\partial \boldsymbol{p}'} \right) \psi_c^*(t; \tau) \psi_c^*(t; \tau') \right\} \psi_c(t; \tau') \, d\tau' .$$

We can develop a hamiltonian formalism in the ordinary way. The conjugated momentum of $\psi_c(t; \tau)$ is $\Pi_{\psi_c}(t; \tau)$ and the hamiltonian $\mathcal{K}_c$:

$$(179) \qquad \Pi_{\psi_c}(t, \tau) = \frac{\partial \Lambda(t)}{\partial \left(\dfrac{\partial \psi_c(t; \tau)}{\partial t} \right)} = i\psi_c^*(t; \tau) \, ,$$

$$(180) \qquad \mathcal{K}_c(t) = \int_{\Omega} \Pi_{\psi_c}(t; \tau) \frac{\partial}{\partial t} \psi_c(t; \tau) \, \mathrm{d}\tau - \Lambda(t) =$$

$$= \int_{\Omega} \psi_c^*(t; \tau) L_{\mathrm{kin}}(\tau) \psi_c(t; \tau) \, \mathrm{d}\tau +$$

$$+ \frac{1}{2} \int_{\Omega} \psi_c^*(t; \tau)\psi_c^*(t; \tau') L_{\mathrm{pot}}(\tau, \tau') \psi_c(t; \tau')\psi_c(t; \tau) \, \mathrm{d}\tau \, \mathrm{d}\tau' \, .$$

The equations (178) can be obtained as Hamilton equations:

$$(181) \qquad \frac{\partial \psi_c}{\partial t} = \frac{\delta \mathcal{K}_c}{\delta \Pi_{\psi_c}} \, , \qquad\qquad \frac{\partial}{\partial t} \Pi_{\psi_c} = - \frac{\delta \mathcal{K}_c}{\delta \psi_c} \, .$$

The field described by ψ_c will be called the super-classical field. Our « quantized » field in phase space can be obtained from the super-classical field by replacing the ψ_c and Π_{ψ_c} by operators ψ and Π_ψ satisfying the commutation rules:

$$(182) \qquad \begin{cases} [\psi(t; \tau), \ \Pi_\psi(t; \tau')]_{\pm} = i\delta(\tau - \tau') \\[2mm] [\psi(t; \tau), \ \psi(t; \tau')]_{\pm} = [\Pi_\psi(t; \tau), \ \Pi_\psi(t; \tau')]_{\pm} = 0. \end{cases}$$

Thus we get the commutation rules of the « quantized » field in the phase space Ω (Heisenberg representation). The Hamilton equations

$$(183) \qquad i\frac{\partial \psi}{\partial t} = [\psi, \mathcal{K}] = i\frac{\delta \mathcal{K}}{\delta \Pi_\psi} \, , \qquad\qquad i\frac{\partial \Pi_\psi}{\partial t} = [\Pi_\psi, \mathcal{K}] = - i\frac{\delta \mathcal{K}}{\delta \psi} \, ,$$

give for ψ and ψ^* equations of the same form as (178). From now on we shall use the same notation for the corresponding quantities of the super-classical and quantized fields, except when it will be necessary to distinguish both cases.

From the fact that our fields are in a six dimensional space or a seven dimensional phase-space-time follow some interesting results. Thus, instead of a four vector of density and current, we have a seven vector. Indeed we,

get from equations (178) or their analogue for the « quantized » field

$$(184) \qquad \frac{\partial}{\partial t}(\psi^*\psi) + \mathrm{div}_x\left(\psi^* \frac{\boldsymbol{p}}{m}\psi\right)$$
$$- \mathrm{div}_p\left(\psi^*\left\{\int_\Omega \psi^*(t; \tau') \frac{\partial \Phi}{\partial x} \psi(t; \tau') \, d\tau'\right\}\psi\right) = 0 \,,$$

so that the time component of the current seven-vector is $\psi^*\psi$, the space components are $\psi^*(\boldsymbol{p}/m)\psi$ and the momentum components $\psi^*\left\{\int_\Omega \psi^*(t; \tau') \cdot (\partial\Phi/\partial x)\psi(t; \tau')\, d\tau\right\}\psi$. By integrating both sides of (184) over the momentum space, we get the ordinary continuity equation

$$(185) \qquad \frac{\partial}{\partial t}\left(\int_{\infty}^{+\infty} \psi^*\psi \, d\boldsymbol{p}\right) + \mathrm{div}_x\left(\int_{-\infty}^{+\infty} \psi^* \frac{\boldsymbol{p}}{m} \psi \, d\boldsymbol{p}\right) = 0 \,,$$

whereas the integration over the configuration space gives the continuity equation in momentum space:

$$(186) \qquad \frac{\partial}{\partial t}\left(\int_V \psi^*\psi \, d\boldsymbol{x}\right) + \mathrm{div}_p\left(\int_V d\boldsymbol{x}\, \psi^*\left\{\int_\Omega \psi^*(t; \tau') \frac{\partial\phi}{\partial x} \psi(t; \tau')\, d\tau'\right\}\psi\right) = 0 \,.$$

By integrating over the entire phase space we get:

$$(187) \qquad \frac{\partial}{\partial t}\int_\Omega \psi^*\psi \, d\tau = 0 \,.$$

This equation in the case of the « quantized » field shows that $N_{0})$, is an integral of motion, and in the case of the super-classical field that the total mass is constant.

The « quantized » field in phase space gives a classically exact description of the motion of systems of indistinguishable particles. The description corresponding to the super-classical field is less accurate than the classical one, but it may be useful in the discussion of the behaviour of matter in bulk when the fluctuation effects arising from the molecular structure become negligible. In the super-classical approximation there are no particles but only a continuous distribution of matter with density $m\varrho_c(t, \boldsymbol{x})$:

$$(188) \qquad \varrho_c(t, \boldsymbol{x}) = \int_{-\infty}^{+\infty} |\psi_c(t; \tau)|^2 \, d\boldsymbol{p} \,.$$

The microscopic kinetic and potential energies of the super-classical field are:

$$(189) \qquad \mathcal{H}^{(c)}_{\mathrm{kin}} = \frac{1}{2m} \int_{\Omega} |\psi_c(t;\tau)|^2 \boldsymbol{p}^2 \, \mathrm{d}\boldsymbol{p} \,,$$

$$(190) \qquad \mathcal{H}^{(c)}_{\mathrm{pot}} = \frac{1}{2} \int_{V} \varrho_c(t,\boldsymbol{x})\varrho_c(t,\boldsymbol{x}')\Phi(\boldsymbol{x}-\boldsymbol{x}') \, \mathrm{d}\boldsymbol{x}\,\mathrm{d}\boldsymbol{x}' =$$

$$= \frac{1}{2} \int_{\Omega} |\psi_c(t;\tau)|^2 |\psi_c(t;\tau')|^2 \Phi(\boldsymbol{x}-\boldsymbol{x}') \, \mathrm{d}\tau\,\mathrm{d}\tau'$$

It is easily seen that, as a consequence of (184), we have:

$$(191) \qquad \frac{\mathrm{d}}{\mathrm{d}t} (\mathcal{H}^{(c)}_{\mathrm{kin}} + \mathcal{H}^{(c)}_{\mathrm{pot}}) = 0 \,.$$

The potential energy $\mathcal{H}^{(c)}_{\mathrm{pot}}$ can not be rigorously expressed as the space integral of a density of potential energy, because of the existence of actions at a distance. It is nevertheless possible to get a coarse-grained potential energy, which is the space integral of a coarse-grained density of potential energy, when the forces have short range, by dividing the space into cells V_σ large enough to take:

$$(192) \qquad \mathcal{H}^{(c)}_{\mathrm{pot}} \cong \sum_\sigma \mathcal{H}^{(c)}_{\mathrm{pot}} (V_\sigma) \,.$$

$$(193) \qquad \mathcal{H}^{(c)}_{\mathrm{pot}} (V_\sigma) = \frac{1}{2} \int_{V_\sigma} \varrho_c(t,\boldsymbol{x})\varrho_c(t,\boldsymbol{x}')\Phi(\boldsymbol{x}-\boldsymbol{x}') \, \mathrm{d}\boldsymbol{x}\,\mathrm{d}\boldsymbol{x}' \,.$$

It results from (184) that

$$(194) \qquad \frac{\partial}{\partial t} \{\varrho(t;\tau)p_\alpha\} + \mathrm{div}_x \left\{ \frac{\boldsymbol{p}}{m}\, \varrho(t;\tau)p_\alpha \right\} +$$

$$+ \; \psi^*(t,\tau) \left\{ \frac{\partial}{\partial x_\alpha} \int_{\Omega} \varrho(t;\tau')\Phi(\boldsymbol{x}-\boldsymbol{x}') \, \mathrm{d}\tau' \right\} \psi(t;\tau) =$$

$$= \mathrm{div}_p \left\{ p_\alpha \psi^*(t;\tau) \int_{\Omega} \varrho(t,\tau') \frac{\partial}{\partial \boldsymbol{x}}\, \Phi(\boldsymbol{x}-\boldsymbol{x}') \, \mathrm{d}\tau'\, \psi(t;\tau) \right\} \,,$$

with

$$(195) \qquad \varrho(t;\tau) = \psi^*(t;\tau)\psi(t;\tau) \,,$$

for both the super-classical and « quantized » fields. Hence we get:

$$(196) \qquad \frac{\partial}{\partial t} \int\limits_{-\infty}^{+\infty} \varrho(t;\tau) p_\varkappa \,\mathrm{d}\boldsymbol{p} + \mathrm{div}_x \int\limits_{-\infty}^{+\infty} \frac{\boldsymbol{p}}{m} \,\varrho(t;\tau) p_\alpha \,\mathrm{d}\boldsymbol{p} +$$

$$- \int\limits_{-\infty}^{-\infty} \psi^*(t;\tau) \left\{ \frac{\partial}{\partial r_\varkappa} \int\limits_{\Omega} \varrho(t;\tau') \Phi(\boldsymbol{x} - \boldsymbol{x}') \,\mathrm{d}\tau' \right\} \psi(t;\tau) \,\mathrm{d}\boldsymbol{p} = 0 \;.$$

In the case of the super-classical field there is no difficulty in introducing a macroscopic velocity, of the matter $\boldsymbol{W}_c(t,\boldsymbol{x})$:

$$(197) \qquad \frac{1}{m} \int\limits_{-\infty}^{+\infty} \varrho_c(t;\tau) \boldsymbol{p} \,\mathrm{d}\boldsymbol{p} = \varrho_c(t;\boldsymbol{x}) \boldsymbol{W}_c(t;\boldsymbol{x}) \;.$$

This   is   not   possible   for   the   « quantized »   field,   because   the   operator $\int\limits_{-\infty}^{+\infty} \psi^*(t;\tau) \psi(t;\tau) \,\mathrm{d}\boldsymbol{p}$ does not admit an inverse. With $\boldsymbol{W}$ we get in the usual way the total derivative $\mathrm{d}/\mathrm{d}t$:

$$(198) \qquad \frac{\mathrm{d}}{\mathrm{d}t} = \frac{\partial}{\partial t} + \boldsymbol{W}_c \cdot \frac{\partial}{\partial \boldsymbol{x}} \;.$$

It is easily seen by, taking into account (185) and (197), that

$$(199) \qquad \frac{\partial}{\partial t} \int\limits_{-\infty}^{+\infty} \varrho_c(t;\tau) \frac{\boldsymbol{p}}{m} \,\mathrm{d}\boldsymbol{p} = \varrho_c(t;\boldsymbol{x}) \frac{\partial \boldsymbol{W}_c}{\partial t} - \boldsymbol{W}_c \,\mathrm{div}\, \{\varrho_c(t;\boldsymbol{x}) \boldsymbol{W}_c\} \;,$$

and since

$$(200) \qquad \int\limits_{-\infty}^{-\infty} \frac{\boldsymbol{p}}{m} \,\varrho_c(t;\tau) \frac{p_\varkappa}{m} \,\mathrm{d}\boldsymbol{p} = \int\limits_{-\infty}^{-\infty} \left(\frac{\boldsymbol{p}}{m} - \boldsymbol{W}_c\right)\left(\frac{p_\varkappa}{m} - W_{c,\varkappa}\right) \varrho_c(t;\tau) \,\mathrm{d}\boldsymbol{p} - \boldsymbol{W}_c W_{c,\varkappa} \varrho_c(t;\boldsymbol{x}) \;.$$

we get from (196) the equation of motion

$$(201) \qquad m\varrho_c(t,\boldsymbol{x}) \cdot \frac{\mathrm{d}W_{c,\alpha}}{\mathrm{d}t} = - \frac{\partial T_{\alpha\beta}^{(\mathrm{kin})}}{\partial x_\beta} - \varrho_c(t,\boldsymbol{x}) \frac{\partial}{\partial r_\varkappa} \int\limits_{\Gamma} \varrho_c(t;\boldsymbol{x}') \Phi(\boldsymbol{x} - \boldsymbol{x}') \,\mathrm{d}\boldsymbol{x}' \;.$$

the kinetic stress tensor being:

$$(202) \qquad T_{\alpha\beta}^{(\mathrm{kin})} = m \int\limits_{-\infty}^{+\infty} \left(\frac{p_\alpha}{m} - W_{c,\alpha}\right)\left(\frac{p_\beta}{m} - W_{c\,\beta}\right) \varrho_c(t;\tau)\,\mathrm{d}\boldsymbol{p}\,.$$

The equation of motion (201) corresponds to the absence of external forces. There is of course no difficulty in introducing such forces.

The consideration of the macroscopic equations af motion leads to a macroscopic definition of the kinetic energy different from the microscopic kinetic energy given by (189):

$$(203) \qquad \mathcal{H}_{\mathrm{kin}}^{(\mathrm{mac})} = \frac{1}{2}\int\limits_{V} \varrho_c(t;\,\boldsymbol{x})\boldsymbol{W}_c^2\,\mathrm{d}\boldsymbol{x}\,.$$

The explanation of this difference is immediate by taking into account that a part of the total microscopic kinetic energy corresponds to heat. We shall define the local temperature $T_c(t,\boldsymbol{x})$ by the condition that the total microscopic kinetic energy of a macroscopic element of matter in its rest-system of reference be equal to $^3/_2 k$ of the number of its particles multiplied by the local temperature:

$$(204) \qquad \frac{m}{2} \int\limits_{-\infty}^{+\infty} \varrho_c(t;\tau)\left(\frac{\boldsymbol{p}}{m} - \boldsymbol{W}_c\right)^2 \mathrm{d}\boldsymbol{p} = \frac{3}{2}\,k\varrho_c(t;\,\boldsymbol{x})T_c(t,\boldsymbol{x})\,.$$

It is easily seen that:

$$(205) \qquad \frac{m}{2} \int\limits_{-\infty}^{+\infty} \varrho_c(t;\tau)\left(\frac{\boldsymbol{p}}{m} - \boldsymbol{W}_c\right)^2 \mathrm{d}\boldsymbol{p} = \int\limits_{-\infty}^{+\infty} \varrho_c(t;\tau)\,\frac{\boldsymbol{p}^2}{2m}\,\mathrm{d}\boldsymbol{p} - \frac{m}{2}\,\varrho_c(t,\boldsymbol{x})\boldsymbol{W}_c^2\,.$$

Hence the density of microscopic kinetic energy is the sum of the density of macroscopic kinetic energy plus $^3/_2\,k\varrho_c(t;\,x)T_c(t,\boldsymbol{x})$.

We shall now take as density of entropy $s_c(t,\boldsymbol{x})$:

$$(206) \qquad s_c(t,\boldsymbol{x}) = -\,k\int\limits_{-\infty}^{+\infty} \varrho_c(t;\tau)\log\varrho_c(t;\tau)\,\mathrm{d}\boldsymbol{p}\,.$$

This entropy has the usual unsatisfactory behaviour of the Gibbs entropy: the total entropy of the super-classical field is time independent. Indeed, let

us compute the time derivative of $s_c(t, \boldsymbol{x})$ by means of (184):

$$(207) \quad \frac{\partial}{\partial t} s_c(t, \boldsymbol{x}) = - k \int\limits_{\infty}^{+\infty} \{\log \varrho_c(t; \tau) + 1\} \frac{\partial}{\partial t} \varrho_c(t; \tau)\, \mathrm{d}\boldsymbol{p} =$$

$$= k \operatorname{div}_x \{\varrho_c(t; \boldsymbol{x}) \boldsymbol{W}_c\} + k \int\limits_{\infty}^{+\infty} \log \varrho_c(t; \tau) \operatorname{div}_x \left\{ \varrho_c(t; \tau) \frac{\boldsymbol{p}}{m} \right\} \mathrm{d}\boldsymbol{p} -$$

$$- k \int\limits_{-\infty}^{-\infty} \log \varrho_c(t; \tau) \operatorname{div}_p \left\{ \varrho_c(t; \tau) \int\limits_{\Omega} \varrho_c(t; \tau') \frac{\partial \Phi}{\partial \boldsymbol{x}}\, \mathrm{d}\tau' \right\} \mathrm{d}\boldsymbol{p} =$$

$$= k \operatorname{div}_x \int\limits_{\infty}^{+\infty} \frac{\boldsymbol{p}}{m} \varrho_c(t; \tau) \log \varrho_c(t; \tau)\, \mathrm{d}\boldsymbol{p}\ .$$

It follows from (207) that for a volume V' of boundary Σ' we have

$$(208) \quad \frac{\partial}{\partial t} \int\limits_{V'} s_c(t, \boldsymbol{x})\, \mathrm{d}\boldsymbol{x} = k \int\limits_{\Sigma'} \mathrm{d}\Sigma \int\limits_{\infty}^{+\infty} \left(\boldsymbol{n} \cdot \frac{\boldsymbol{p}}{m} \right) \varrho_c(t; \tau) \log \varrho_c(t, \tau)\, \mathrm{d}\boldsymbol{p}\ .$$

$\boldsymbol{n}$ denoting the outer normal at the points of the boundary Σ'. In the particular case of $V' = V$ the integral in the right hand side vanishes and the total entropy remains constant. It is easily seen that equation (208) can be written as follows

$$(209) \quad \frac{\partial}{\partial t} \int\limits_{V'} s_c(t, \boldsymbol{x})\, \mathrm{d}\boldsymbol{x} = k \int\limits_{\Sigma'} \mathrm{d}\Sigma \int\limits_{\infty}^{+\infty} \left(\boldsymbol{n} \cdot \left\{ \frac{\boldsymbol{p}}{m} - \boldsymbol{W}_c \right\} \right) \varrho_c(t; \tau) \log \varrho_c(t; \tau)\, \mathrm{d}\boldsymbol{p} -$$

$$- \int\limits_{\Sigma'} (\boldsymbol{n} \cdot \boldsymbol{W}_c) s_c(t, \boldsymbol{x})\, \mathrm{d}\Sigma\ .$$

Both terms in the right hand side of (209) are fluxes through the boundary and this shows again that there is no creation of entropy, with the definition (206). Since the second term corresponds to the flow of matter, the first must correspond to the flow of heat. It is important to notice that the first term in the right hand side of (209) behaves satisfactorily under a change of units, because the contribution of the additive constant due to $\log \varrho_c$ is nil.

Equation (184) for the super-classical field can be written as:

$$(210) \quad \left(\frac{\partial}{\partial t} + \frac{\boldsymbol{p}}{m} \cdot \frac{\partial}{\partial \boldsymbol{x}} + \boldsymbol{\mathscr{F}} \cdot \frac{\partial}{\partial \boldsymbol{p}} \right) \varrho_c(t; \tau) = 0\ ,$$

$$(211) \quad \boldsymbol{\mathscr{F}}(t, \boldsymbol{x}) = - \frac{\partial}{\partial \boldsymbol{x}} \int\limits_{\Omega} \varrho_c(t; \tau') \Phi(\boldsymbol{x} - \boldsymbol{x}')\, \mathrm{d}\tau' = - \frac{\partial}{\partial \boldsymbol{x}} \varphi(\boldsymbol{x})\ .$$

Equation (210) is the same derived from the Vlassov formalism ([7]) for a system with a large number of similar particles. In the case of a stationary motion of the super-classical field we may apply Vlassov's method of solution by taking:

$$\text{(212)} \qquad \varrho_c(\tau) = \varrho_s(\boldsymbol{x})\sigma_c(\varepsilon)\,, \qquad \left(\varepsilon = \frac{\boldsymbol{p}^2}{2m}\right).$$

It is easily seen that

$$\text{(213)} \qquad \sigma_c(\varepsilon) = \alpha e^{-\beta\varepsilon}\,,$$

α and β being constants related by the normalization condition:

$$\text{(214)} \qquad \int_{\infty}^{\infty} \sigma(\varepsilon)\,\mathrm{d}\boldsymbol{p} = 1\,.$$

$\varrho_c(\boldsymbol{x})$ is of the form

$$\text{(215)} \qquad \varrho_c(\boldsymbol{x}) = \varrho_c(\boldsymbol{x}_0) \exp\left[-\beta\{\varphi(\boldsymbol{x}) - \varphi(\boldsymbol{x}_0)\}\right],$$

the potential $\varphi(\boldsymbol{x})$ satisfying a non linear integral equation:

$$\text{(216)} \qquad \varphi(\boldsymbol{x}) = \varrho(\boldsymbol{x}_0)\int_V \boldsymbol{\Phi}(\boldsymbol{x} - \boldsymbol{x}') \exp\left[-\beta\{\varphi(\boldsymbol{x}) - \varphi(\boldsymbol{x}_0)\}\right]\mathrm{d}\boldsymbol{x}'.$$

We shall not discuss here the solutions of the Vlassov integral equation (216). The parameter β is related to the temperature, according to Vlassov, by the equation:

$$\text{(217)} \qquad \beta = \frac{1}{kT}\,.$$

We shall now prove that this follows from the general definition (204). In the case of a stationary solution (212) the macroscopic velocity vanishes

$$\text{(218)} \qquad \boldsymbol{W}_c(t, \boldsymbol{x}) = 0\,,$$

and (204) becomes simply:

$$\text{(219)} \qquad \frac{3}{2}\,kT_c(\boldsymbol{x}) = \int_{-\infty}^{+\infty} \sigma(\varepsilon)\varepsilon\,\mathrm{d}\boldsymbol{p} = -\alpha\frac{\mathrm{d}}{\mathrm{d}\beta}\int_{-\infty}^{+\infty} \exp\left[-\beta\varepsilon\right]\mathrm{d}\boldsymbol{p} = \frac{3}{2\beta}\,.$$

It is easily seen that the stationary solutions of the type (212) are characterized by the condition of rendering the entropy extremal with a given energy and a given mass. The entropy corresponding to the definition (206)

is therefore convenient for the discussion of the equilibrium, notwithstanding its unsatisfactory behaviour for non stationary motions.

In the case of short range forces it is convenient to express the second term in the right hand side of (201) in terms of a potential stress tensor defined by the equation:

$$(220) \qquad \frac{\partial T^{(\mathrm{pot})}_{\alpha\beta}}{\partial x_\beta} = \varrho_c(t; \boldsymbol{x}) \int_r \varrho_c(t; \boldsymbol{x}') \frac{\partial \Phi(\boldsymbol{x} - \boldsymbol{x}')}{\partial x_\alpha} \, \mathrm{d}\boldsymbol{x}' \; .$$

Equation (201) becomes:

$$(221) \qquad m\varrho_c(t, \boldsymbol{x}) \frac{\mathrm{d} W_{c,\alpha}}{\mathrm{d}t} = - \frac{\partial}{\partial x_\beta} (T^{(\mathrm{kin})}_{\alpha\beta} + T^{(\mathrm{pot})}_{\alpha\beta}) \; .$$

13. – The Boltzmann equation.

Equation (184) can be written as follows:

$$(222) \qquad \left\{ \frac{\partial}{\partial t} + \frac{\boldsymbol{p}}{m} \cdot \frac{\partial}{\partial \boldsymbol{x}} \right\} \varrho_c(t; \tau) = \left\{ \frac{\partial}{\partial \boldsymbol{p}} \varrho_c(t; \tau) \right\} \cdot \frac{\partial}{\partial \boldsymbol{x}} \int_\Omega \varrho_c(t; \tau') \Phi(\boldsymbol{x} - \boldsymbol{x}') \, \mathrm{d}\tau' \; .$$

Equation (222) has a remarkable resemblance with the fundamental equation of the kinetic gas theory, the Boltzmann integro-differential equation. The difference consists in the replacement of the right hand side of (222) by the Boltzmann collision integral. This change is of course of capital importance, as shown by the fact that (222) leads to the time independence of the entropy, whereas the Boltzmann equation leads to the H-theorem.

We shall now obtain the Boltzmann equation in a way which allows to see clearly the different assumptions on which it depends. It is often assumed that the entropy increase allowed by the Boltzmann equation results from the incomplete specification of the motion or else that it is due to the hypothesis of molecular chaos. Neither the incomplete specification nor the molecular chaos lead to an increase of the entropy, as we shall see. Let $f_N(t; \tau_1, ..., \tau_N)$ be the distribution function in the phase space of a system of N identical particles. f_N satisfies the Liouville equation and is normalized to $N!$:

$$(223) \qquad \frac{\partial f_N}{\partial t} + (f_N, H_N)_N = 0 \; , \qquad \int_\Omega f_N(t; \tau_1, ..., \tau_N) \, \mathrm{d}\tau_1 ... \, \mathrm{d}\tau_N = N! \; .$$

The r-particle distribution functions

$$(224) \qquad f^{(r)}_N(t; \tau_1, ..., \tau_r) = \frac{1}{(N-r)!} \int_\Omega f_N(t; \tau_1, ..., \tau_N) \, \mathrm{d}\tau_{r+1} ... \, \mathrm{d}\tau_N \; ,$$

satisfy the equation of YVON [8], BORN and GREEN [9] and KIRKWOOD [10]:

$$(225) \quad \frac{\partial}{\partial t} f_N^{(r)}(t; \tau_1, ..., \tau_r) + (f_N^{(r)}(t; \tau_1, ..., \tau_r), H_r(\tau_1, ..., \tau_r))_r =$$

$$= \int_{\Omega} d\tau_{r+1} \left(\sum_{l=1}^{r} \Phi(\boldsymbol{x}_{r+1} - \boldsymbol{x}_l), f_N^{(r+1)}(t; \tau_1, ..., \tau_{r+1}) \right)_{r+1}$$

The hypothesis of molecular chaos consists in assuming that:

$$(226) \quad f_N^{(2)}(t; \tau_1, \tau_2) = \frac{N-1}{N} f_N^{(1)}(t; \tau_1) f_N^{(1)}(t; \tau_2) = \frac{N-1}{N} f(t; \tau_1) f(t; \tau_2) .$$

In this case we get from (225) (*):

$$(227) \quad \left(\frac{\partial}{\partial t} + \frac{\boldsymbol{p}_1}{m} \cdot \frac{\partial}{\partial \boldsymbol{x}_1} \right) f(t; \tau_1) - \frac{N-1}{N} \left\{ \frac{\partial}{\partial \boldsymbol{p}_1} f(t; \tau_1) \right\} \cdot \frac{\partial}{\partial \boldsymbol{x}_1} \int_{\Omega} f(t_1; \tau_2) \Phi(\boldsymbol{x}_1 - \boldsymbol{x}_2) d\tau_2 = 0 .$$

For large N this equation is equivalent to (222). The factor $(N-1)/N$ arises from the exclusion of the self-forces, as is clearly seen for $N = 1$.

The Boltzmann definition of the entropy of the N particles system

$$(228) \quad S_N = -k \int_{\Omega} f(t; \tau) \log f(t; \tau) d\tau ,$$

associated to the molecular chaos hypothesis leads to a time independent entropy, when the variation of the one particle distribution function f is computed with (227). This results from the reasoning of section **12**, since (227) goes over into (222) by replacing the potential Φ by $\Phi N/(N-1)$. Therefore the time variation of the entropy is not a consequence of the incomplete specification of the motion associated with the description by a probability distribution, and the situation is not changed in this connection by the introduction of the molecular chaos hypothesis. The essential step is the replacement of the third term in the left hand side of (227) by a suitable time average which transforms (227) into the Boltzmann equation. We shall now define more precisely this time averaging.

(*) It is necessary to assume that the spatial distribution is not homogeneous, otherwise the third term in the left hand side of (227) will be nil. This indicates that (226) is not quite satisfactory an assumption. In section **14** a better method will be given.

It follows from the definitions (177) that equation (227) can be transformed into the following

$$(229) \qquad \frac{\partial}{\partial t} f(t; \tau_1) = -\frac{N-1}{N} \int_{\Omega} D_t \{f(t; \tau_1) f(t; \tau_2)\} \, d\tau_2 + i(N-2) L_{\mathrm{kin}}(\tau_1) f(t; \tau_1),$$

the operator D_t being:

$$(230) \qquad D_t F(\tau_1, \tau_2) = i\{L_{\mathrm{kin}}(\tau_1) + L_{\mathrm{kin}}(\tau_2) + L_{\mathrm{pot}}(\tau_1, \tau_2)\} F(\tau_1, \tau_2) \, .$$

Let us consider a function $F(\tau_1(t), \tau_2(t))$ of the two points $\tau_1(t)$ and $\tau_2(t)$ in Ω, which correspond to a two-particle system with the interaction $\Phi(x_1 - x_2)$, the two particles having the same mass m. It is clear that $D_t F(\tau_1(t), \tau_2(t))$ is simply the time derivative of $F(\tau_1(t), \tau_2(t))$ taken along the motion of the particles. We shall assume that the forces have a range small enough to be treated as a first order infinitesimal quantity in connection with the space variation of $F(\tau_1, \tau_2)$. The time of collision corresponding to a collision finishing when the two particles are at the points τ_1 and τ_2 of Ω will be denoted by $\theta(\tau_1, \tau_2)$ and treated as a first order infinitesimal quantity in connection with the space variation of $F(\tau_1, \tau_2)$. In other words we shall take:

$$(231) \quad F\big(\tau_1(t-\theta), \tau_2(t-\theta)\big) = F(x_1(t), p_1(t-\theta); x_2(t), p_2(t-\theta)) -$$

$$\frac{\theta}{m} \left\{ p_1(t) \cdot \frac{\partial}{\partial x_1(t)} + p_2(t) \cdot \frac{\partial}{\partial x_2(t)} \right\} F(x_1(t), p_1(t-\theta); x_2(t), p_2(t-\theta)) \, ,$$

$$(232) \qquad \qquad \theta = \theta\big(\tau_1(t), \tau_2(t)\big) \, .$$

It follows from (231) that, for a slow spatial variation of F, we can take:

$$(233) \quad \int_{\Omega} d\tau_2(t) \left\{ \frac{1}{\theta} \int_{t-\theta}^{t} D_t F(\tau_1(t'), \tau_2(t')) \, dt' \right\} \simeq i L_{\mathrm{kin}}(\tau_1(t)) \int_{\Omega} F\big(\tau_1(t), \tau_2(t)\big) \, d\tau_2(t) -$$

$$- \int_{\Omega} \frac{1}{\theta} \{ F(x_1(t), p_1(t-\theta); x_2(t), p_2(t-\theta)) - F(\tau_1(t), \tau_2(t))\} \, d\tau_2(t) =$$

$$= \frac{1}{m} p_1(t) \cdot \frac{\partial}{\partial x_1(t)} \int_{\Omega} F\big(\tau_1(t), \tau_2(t)\big) \, d\tau_2(t) -$$

$$- \frac{1}{m} \int_{-\infty}^{+\infty} dp_2(t) \int_{V} \{F(x_1(t), p_1(t-\theta); x_2(t), p_2(t-\theta)) - F\big(\tau_1(t), \tau_2(t)\big)\} \, |p_1(t) - p_2(t)| \, dq_2(t) \, ,$$

$$(234) \qquad \qquad dq_2(t) = dx_2^{(1)}(t) \, dx_2^{(2)}(t) \, , \qquad x_2^{(3)} \text{ axis } // \, p_1(t) - p_2(t) \, .$$

We shall now replace in the right hand side of (229) $D_t\{f(t; \tau_1)f(t; \tau_2)\}$ by its time average $(1/\theta) \int_{t-\theta}^{t} D_t \{f(t: \tau_1(t')) f(t; \tau_2(t'))\} \, dt'$, making use of the equation (233). Thus we get the Boltzmann equation for the modified distribution function $\bar{f}(t; \tau_1)$:

$$(235) \quad \left(\frac{\partial}{\partial t} + \frac{\boldsymbol{p}_1}{m} \cdot \frac{\partial}{\partial \boldsymbol{x}_1}\right) \bar{f}(t; \tau_1) =$$

$$= \frac{N-1}{Nm} \int_{-\infty}^{+\infty} d\boldsymbol{p}_2 \int_V \{\bar{f}(t; \boldsymbol{x}_1, \boldsymbol{p}_1^\dagger)\bar{f}(t; \boldsymbol{x}_2, \boldsymbol{p}_2^\dagger) - \bar{f}(t; \tau_1)\bar{f}(t; \tau_2)\} \, |\, \boldsymbol{p}_1 - \boldsymbol{p}_2|\, d\boldsymbol{q}_2 \, ,$$

$$(236) \qquad \boldsymbol{p}_1^\dagger = \boldsymbol{p}_1(t - \theta') \, , \qquad \boldsymbol{p}_2^\dagger = \boldsymbol{p}_2(t - \theta') \, , \qquad \theta' = \theta(\tau_1, \tau_2) \, .$$

The above derivation of the Boltzmann equation is less elementary but simpler than the ordinary one, since it does not require the discussion of the direct and inverse collisions. This advantage becomes clearer when collisions between particles with internal degrees of freedom are considered. Another important feature consists in the fact that triple and higher order collisions do not come in in our method of time averaging. This corresponds to the usual approximation in the derivation of the Boltzmann equation, in which only binary collisions are taken into account.

The Boltzmann equation leads to the H theorem, which shows that the entropy may increase but never decrease. Thereby it is clear that the increase of the entropy defined by (228) results from the time averaging. It has already been shown by KIRKWOOD ([11]) that the derivation of the Boltzmann equation requires a time averaging, so that the Boltzmann equation is satisfied by a time-coarse-grained distribution function. The method of Kirkwood differs essentially from ours, because we did not average the distribution function over a time interval along the real motion, but averaged instead the effect of the interaction along a virtual motion of a two particle system. Our method of time averaging is simpler and in a certain sense quite naturally suggested by the form of the equation of evolution of the distribution function. It must nevertheless be recognized that the need of a time averaging does still require a deeper justification. The current point of view is based on the consideration of the time necessary to make an observation (see KIRKWOOD ([10])), but it is hardly conceivable that the increase of entropy should depend essentially on the fact that our observations require a time large with respect to the duration of the molecular collisions. It does not seems unreasonable to think that the definition of the entropy is not altogether satisfactory for non equilibrium states and requires some modification. This is suggested by the « quantized »

field formalism. Indeed, from the point of view of the « quantized » field formalism the analogue of the Boltzmann definition would be the introduction of some kind of entropy operator with a structure corresponding to that of the entropy of the super-classical field:

$$(237) \qquad S_c = - k \int_{\Omega} \varrho_c(t; \tau) \log \varrho_c(t; \tau) \mathrm{d}\tau \,.$$

It does not seem possible to define an operator $\log \varrho$, but it is possible to divide Ω into cells and to take as entropy operator $S_{\mathrm{op}}^{(\omega)}$:

$$(238) \qquad S_{\mathrm{op}}^{(\omega)} = - k \sum_{\lambda} N_{\lambda} \log N_{\lambda} \,.$$

The entropy of a state of the field would then be the average value of the entropy operator (coarse-grained entropy):

$$(239) \qquad \langle S_{\mathrm{op}}^{(\omega)} \rangle_{\chi} = \int_{\mu\text{-space}} \chi^* S_{\mathrm{op}}^{(\omega)} \chi \, \mathrm{d}\mu \,, \qquad \left(\int_{\mu\text{-space}} |\chi|^2 \, \mathrm{d}\mu = 1 \right) .$$

It is easily seen that

$$(240) \quad \langle S_{\mathrm{op}}^{(\omega)} \rangle_{\chi} =$$

$$= - k \sum_{n=1}^{\infty} \sum_{\lambda} \int_{\Omega} |\Theta_n(t; \tau_1, ..., \tau_n)|^2 N(\omega_{\lambda}; \tau_1, ..., \tau_n) \log N(\omega_{\lambda}; \tau_1, ..., \tau_n) \mathrm{d}\tau_1 ... \mathrm{d}\tau_n \,,$$

the Θ_n being the coefficients of the Fock expansion (112) and $N(\omega_{\lambda}; \tau_1, ..., \tau_n)$ the number of points $\tau_1, ..., \tau_n$ inside the cell ω_{λ}: The definition (239) is obviously not equivalent to those discussed previously. Formula (125) suggests that, if an entropy is to be attached to a pure state χ, it should be taken as $S[\chi]$:

$$(241) \qquad S[\chi] = - k \int_{\mu\text{-space}} |\chi|^2 \log |\chi|^2 \mathrm{d}\mu \,.$$

We shall discuss this point further in a forthcoming paper.

14. – It is interesting to notice that the method of time averaging of section **13** can be applied directly to the exact equation

$$(242) \qquad \left(\frac{\partial}{\partial t} + \frac{\boldsymbol{p}_1}{m} \cdot \frac{\partial}{\partial \boldsymbol{x}_1} \right) f(t; \tau_1) = \int_{\Omega} \frac{\partial}{\partial \boldsymbol{p}_1} f_N^{(2)}(t; \tau_1, \tau_2) \cdot \frac{\partial}{\partial \boldsymbol{x}_1} \Phi(\boldsymbol{x}_1 - \boldsymbol{x}_2) \mathrm{d}\tau_2 \,,$$

without introducing the molecular chaos hypothesis. Thus we get a generalized Boltzmann equation involving modified distribution functions $\bar{f}$ and $\bar{f}_N^{(2)}$:

$$(243) \quad \left(\frac{\partial}{\partial t} + \frac{\boldsymbol{p}_1}{m} \cdot \frac{\partial}{\partial \boldsymbol{x}_1}\right) \bar{f}(t; \tau_1) =$$

$$= \frac{1}{m} \int\limits_{-\infty}^{+\infty} \mathrm{d}\boldsymbol{p}_2 \int\limits_V \{ \bar{f}_N^{(2)}(t; \boldsymbol{x}_1, \boldsymbol{p}_1^\dagger; \boldsymbol{x}_2, \boldsymbol{p}_2^\dagger) - \bar{f}_N^{(2)}(t; \tau_1, \tau_2) \} \, |\boldsymbol{p}_1 - \boldsymbol{p}_2| \, \mathrm{d}\boldsymbol{q}_2 \, .$$

It is preferable to perform first the time averaging and then to intrudoce in (243) the molecular chaos hypothesis in terms of the modified distribution functions $\bar{f}$.

Let us consider now the equation (225) for $r = 2$. It is easily seen that this equation can be written as follows:

$$(244) \quad \frac{\partial}{\partial t} f_N^{(2)}(t; \tau_1, \tau_2) = \int\limits_\Omega (H_3(\tau_1, \tau_2, \tau_3), f_N^{(3)}(t; \tau_1, \tau_2, \tau_3))_3 \, \mathrm{d}\tau_3 -$$

$$- (N - 3)(H_2(\tau_1, \tau_2), f_N^{(2)}(t; \tau_1, \tau_2))_2 = - \int\limits_\Omega D_t^{(3)} f_N^{(3)}(t; \tau_1, \tau_2, \tau_3) \, \mathrm{d}\tau_3 -$$

$$- (N - 3)(H_2(\tau_1, \tau_2), f_N^{(2)}(t; \tau_1, \tau_2))_2 \, .$$

The operator $D_t^{(3)}$ is the three particle analogue of D_t:

$$(245) \qquad \qquad D_t^{(3)} F(\tau_1, \tau_2, \tau_3) = (F(\tau_1, \tau_2, \tau_3), H_3(\tau_1, \tau_2, \tau_3))_3 \, .$$

It seems plausible that the same kind of time averaging which led to the Boltzmann equation will also give satisfactory results when applied to (244). We shall replace in (244) $D_t^{(3)} f_N^{(3)}(\tau_1, \tau_2, \tau_3)$ by its time average during the collision of one of the particles with the couple of the other two $(1/\theta) \int\limits_{t-\theta}^{t} D_t^{(3)} f_N^{(3)} \cdot$ $\cdot (\tau_1(t'), \tau_2(t'), \tau_3(t')) \, \mathrm{d}t'$, assuming that the collision finishes at the time t with the particles at the phase space points τ_1, τ_2, τ_3 and denoting by $\theta = \theta(\tau_1, \tau_2, \tau_3)$ the time of collision. Since $f_N^{(3)}(\tau_1, \tau_2, \tau_3)$ is symmetrical with respect to the variables of the three particles, we may assume that particle 3 collides with the couple $(1, 2)$, the distance between 3 and the other two being larger than $|\boldsymbol{x}_1 - \boldsymbol{x}_2|$. In order to simplify the results we shall neglect the difference between the forces exerted by particle 3 on the other two, so that the variation of $\boldsymbol{p}_r = \boldsymbol{p}_1 - \boldsymbol{p}_2$ will be taken as due only to the forces between particles 1

and 2. We shall also assume that the variation of $\boldsymbol{p}_r$ is small. With the above assumptions the positions of all the three particles and $\boldsymbol{p}_r$ may be taken as varying little during the collision and it is easily seen that:

$$(246) \qquad F\big(\tau_1(t-\theta),\, \tau_2(t-\theta),\, \tau_3(t-\theta)\big) =$$

$$= \widetilde{F}\big(\boldsymbol{x}_1(t-\theta),\, \boldsymbol{x}_2(t-\theta),\, \boldsymbol{x}_3(t-\theta);\; \boldsymbol{p}_r(t-\theta),\, \boldsymbol{p}_b(t-\theta),\, \boldsymbol{p}_3(t-\theta)\big) \cong$$

$$\cong \left[1 - \frac{\theta}{m}\,\boldsymbol{p}_3(t)\cdot\frac{\partial}{\partial\boldsymbol{x}_3(t)} - \theta\left\{ \sum_{l=1}^{2}\frac{1}{m}\,\boldsymbol{p}_l(t)\cdot\frac{\partial}{\partial\boldsymbol{x}_l(t)} - 2\,\frac{\partial}{\partial\boldsymbol{x}_1(t)}\,\varPhi\big(\boldsymbol{x}_1(t)\quad\boldsymbol{x}_2(t)\big)\cdot\frac{\partial}{\partial\boldsymbol{p}_r(t)} \right\} \right]\cdot$$

$$\cdot\, \widetilde{F}\big(\boldsymbol{x}_1(t),\, \boldsymbol{x}_2(t),\, \boldsymbol{x}_3(t);\; \boldsymbol{p}_r(t),\, \boldsymbol{p}_b(t-\theta),\, \boldsymbol{p}_3(t-\theta)\big)\,,$$

$$(\boldsymbol{p}_b = \boldsymbol{p}_1 + \boldsymbol{p}_2)\,.$$

This equation replaces now (231), F is assumed to be a slowly varying function. The analogue of (233) is:

$$(247) \qquad \int_{\Omega}\mathrm{d}\tau_3(t)\left\{ \frac{1}{\theta}\int_{t-\theta}^{t} D_i^{(3)}F\big(\tau_1(t'),\, \tau_2(t'),\, \tau_3(\tau')\big)\,\mathrm{d}t' \cong \right.$$

$$\cong -\left(H_2\big(\tau_1(t),\, \tau_2(t)\big),\, \int_{\Omega} F\big(\tau_1(t),\, \tau_2(t),\, \tau_3(t)\big)\,\mathrm{d}\tau_3(t) \right)_2 -$$

$$- \frac{1}{m}\int_{-\infty}^{+\infty}\mathrm{d}\boldsymbol{p}_3(t)\int_{V}\left\{ \widetilde{F}\big(\boldsymbol{x}_1(t),\, \boldsymbol{x}_2(t),\, \boldsymbol{x}_3(t);\; \boldsymbol{p}_r(t),\, \boldsymbol{p}_b(t-\theta),\, \boldsymbol{p}_3(t-\theta)\big) - \right.$$

$$- F\big(\tau_1(t),\, \tau_2(t),\, \tau_3(t)\big)\Big\}\,\big|\,\boldsymbol{p}_3(t) - \boldsymbol{p}_b(t)\,\big|\,\mathrm{d}\boldsymbol{q}_3(t)\,,$$

$$(248) \qquad \mathrm{d}\boldsymbol{q}_3(t) = \mathrm{d}x_3^{(1)}(t)\,\mathrm{d}x_3^{(2)}(t)\,,\qquad x_3^{(3)}\text{ axis }//\,\boldsymbol{p}_3(t) - \boldsymbol{p}_b(t)\,.$$

It follows from (247) that the analogue of (234) for the two particle distribution function is:

$$(249) \qquad \frac{\partial}{\partial t}\bar{f}_N^{(2)}(t;\,\tau_1,\,\tau_2) + \big(\bar{f}_N^{(2)}((t;\,\tau_1,\,\tau_2),\, H_2(\tau_1,\,\tau_2)\big)_2 =$$

$$= \frac{1}{m}\int_{-\infty}^{+\infty}\mathrm{d}\boldsymbol{p}_3\int_{V}\left\{ \bar{f}_N^{(3)}(t;\,\boldsymbol{x}_1,\,\boldsymbol{p}_1^{\dagger};\,\boldsymbol{x}_2,\,\boldsymbol{p}_2^{\dagger},\,\boldsymbol{x}_3,\,\boldsymbol{p}_3^{\dagger}) - \bar{f}_N^{(3)}(t;\,\tau_1,\,\tau_2,\,\tau_3)\right\}\,\big|\,\boldsymbol{p}_3 - \boldsymbol{p}_1 - \boldsymbol{p}_2\,\big|\,\mathrm{d}\boldsymbol{q}_3\,,$$

$$(250)\quad \boldsymbol{p}_1^{\dagger} = \frac{1}{2}\{\boldsymbol{p}_b(t-\theta') + \boldsymbol{p}_r(t)\}\,,\quad \boldsymbol{p}_2^{\dagger} = \frac{1}{2}\{\boldsymbol{p}_b(t-\theta') - \boldsymbol{p}_r(t)\}\,,\quad \boldsymbol{p}_3^{\dagger} = \boldsymbol{p}_3(t-\theta')\,,$$

$$\theta' = \theta(\tau_1,\,\tau_2,\,\tau_3)\,.$$

We can also get the analogue of the Boltzmann equation by using the three particle analogue of the hypothesis of molecular chaos, the superposition principle of KIRKWOOD and BOGGS ([16]):

$$(252) \qquad f_N^{(3)}(t; \tau_1, \tau_2, \tau_3) = \frac{f_N^{(2)}(t; \tau_2, \tau_3) f_N^{(2)}(t; \tau_3, \tau_1) f_N^{(2)}(t; \tau_1, \tau_2)}{f(t; \tau_1) f(t; \tau_2) f(t; \tau_3)} .$$

I thank Prof. PRIGOGINE for many useful discussions which helped me to clarify several points of the present paper.

([16]) J. G. KIRKWOOD and E. M. BOGGS: *Journ. Chem. Phys.*, **10**, 394 (1942).

RIASSUNTO (*)

Il lavoro sviluppa ulteriormente la meccanica classica delle particelle indistinguibili trattate in I. Si discutono i fondamenti meccanici della termodinamica in termini della teoria ondulatoria classica e dei campi « quantizzati » nello spazio delle fasi. Si dimostra che questo formalismo elimina automaticamente il paradosso di Gibbs. Si tratta la statistica classica col metodo di Gibbs e von Neumann nonchè con una forma generalizzata del metodo di Boltzmann che consente di tener conto delle interazioni. L'introduzione di celle finite nello spazio delle fasi conduce a formule simili a quelle della statistica quantistica per particelle libere ma non così per particelle interagenti. Il trattamento statistico del campo « quantizzato » nello spazio delle fasi conduce immediatamente al *grand ensemble* canonico. Si dimostra che la teoria dei campi « quantizzati » nello spazio delle fasi si può derivare dalla teoria di un campo « non quantizzato » nello spazio delle fasi, in cui si hanno solo distribuzioni di materia continue, per mezzo di un processo di « quantizzazione » del tutto simile a quello della teoria quantistica dei campi, ma tuttavia escludente la costante di Planck, o qualsiasi altra costante universale. Il campo « non quantizzato » nello spazio delle fasi corrisponde a una teoria meno esatta di quella della meccanica classica e da una approssimazione dello stesso tipo di quella data dall'ipotesi del caos molecolare della teoria cinetica dei gas e comprende sia la dinamica sia la teoria del calore di un mezzo continuo. Si dà una nuova derivazione dell'equazione di Boltzmann che richiede un tipo speciale di media temporale e si stabilisce una funzione simile per la funzione di distribuzione di due particelle.

Sull'energia di legame dell'He^5 e del Li^6.

G. Morpurgo

Istituto di Fisica dell'Università - Roma
Istituto Nazionale di Fisica Nucleare - Sezione di Roma (*)

Riassunto. — Facendo uso di funzioni d'onda descriventi un deutone ed una particella α ((3) e (4)) l'energia di legame del Li^6 viene calcolata al variare della distanza tra il baricentro del deutone e quello della particella α. La massima energia di legame, quando si impongano le usuali condizioni di saturazione, si ottiene per una distanza infinita (figg. 1 e 3) ciò essendo dovuto al fatto che l'energia potenziale cresce — in valore assoluto — troppo poco al diminuire della distanza tra il deutone e la particella α. Di questa lenta crescita sono presumibilmente responsabili le condizioni di saturazione. Analoghi calcoli vengono svolti per l'He^5. In accordo col momento magnetico nel Li^6 lo stato S (3) dà luogo per ogni distanza ad una maggiore energia di legame che lo stato P (4); nell'He^5 capita l'opposto.

ntroduzione.

Il presente lavoro contiene una discussione del problema dell'energia di legame dell'He^5 e del Li^6. Esso si riallaccia ai lavori di Inglis [1], Margenau [2], Tyrrell [3], Humblet [4].

È noto che se in un'espressione della forza tra due nucleoni della

---

(*) Ora all'Institute for Nuclear Studies, Chicago, con una borsa di studio del C.N.R.

[1] D. Inglis: *Phys. Rev.*, **51**, 531 (1937).

[2] H. Margenau and K. Carroll: *Phys. Rev.*, **54**, 705 (1938).

[3] W. Tyrrell Jr.: *Phys. Rev.*, **56**, 250 (1939).

[4] J. Humblet: *Physica*, **14**, 285 (1948).

forma:

(1)
$$J(r_{ik}) = - Af\left(\frac{r_{ik}}{a}\right)\{w + bP_\sigma + hP_x P_\sigma + mP_x\},$$

(2)
$$w + b + h + m = 1$$

si aggiustano i parametri in modo da essere in accordo [5]:

a) con l'energia di tripletto e di singoletto del deutone (ciò implica due relazioni indipendenti tra A, a e $w + m$);

b) con l'energia di legame dell'H^3 (terza relazione tra A, a e $w + m$) allora l'energia di legame della particella α risulta essere alquanto troppo grande [6].

Ma non appena dalla particella α si passa alla considerazione dei nuclei ad essa immediatamente superiori le energie di legame calcolate con la sopradetta espressione della forza risultano estremamente inferiori al vero. Ciò è in particolare per il Li^6, il primo nucleo stabile superiore alla particella α. La ragione di ciò è dovuta in parte al fatto che i calcoli diventando più complicati, essi devono essere svolti in maniera meno perfezionata; ma in parte è dovuta anche al fatto che il Li^6 è il primo nucleo nel quale a causa del principio di Pauli, le restrizioni imposte sulla forza dalle condizioni di saturazione dei nuclei pesanti si fanno sentire (nel caso dei nuclei fino alla particella α compare nell'espressione dell'energia soltanto la combinazione: $w + m$).

Lo studio del Li^6 si presta perciò allo studio delle proprietà di saturazione della forza.

1. – Discussione dei lavori precedenti ed impostazione del problema.

Per l'He^5 sono stati fatti due tipi di calcoli dell'energia di legame [3] [4]:

a) calcoli nei quali si parte da un'approssimazione zero nella quale i cinque nucleoni vengono, tutti e cinque, riguardati come muoventisi nello stesso campo di forze elastiche ed in cui la differenza tra la forza fittizia elastica e la somma delle interazioni tra i nucleoni viene trattata poi perturbativamente;

---

[5] I parametri così determinati risultano essere per una $f(r_{ik}/a)$ gaussiana, come assumeremo nel seguito:

$$A = 35{,}6 \text{ MeV}; \quad a = 2{,}25 \cdot 10^{-13} \text{ cm}; \quad w + m = 0{,}8 \,.$$

[6] Vedi, ad esempio, L. ROSENFELD: *Nuclear Forces* (Amsterdam, 1948), p. 305, per la discussione di questo fatto rilevato la prima volta da RARITA e PRESENT (*Phys. Rev.*, **51**, 788 (1937)).

b) calcoli variazionali nei quali la funzione variazionale è caratterizzata da due parametri l'uno associato, per così dire, alle dimensioni della particella α, l'altro, che indicheremo con $1/\beta$, caratterizzante la distanza del neutrone esterno dalla particella α.

Questo secondo tipo di calcolo è il più interessante e conduce alla conclusione che la massima energia di legame si ha per $\beta = 0$, ossia per una distanza infinita tra il neutrone e la particella α [7].

Nel caso del Li⁶ sono stati fatti soltanto i calcoli del tipo a); ossia i sei nucleoni vengono riguardati in approssimazione zero come muoventisi indipendentemente in uno stesso campo di forze elastiche, e la differenza tra la forza fittizia elastica e la somma delle interazioni viene trattata poi perturbativamente. Il risultato di questi calcoli è che l'energia di legame ottenuta è sempre assai inferiore a quella effettiva (31,94 MeV). Nel caso del Li⁶ tuttavia non sono stati fatti calcoli in cui si possa esaminare l'andamento dell'energia di legame al variare della distanza tra i nucleoni esterni e la particella α.

Scopo di questo lavoro è di colmare questa lacuna e presentare questi calcoli. Più precisamente, come risulterà dalla forma delle funzioni variazionali usate. che scriveremo nel num. seguente. il Li⁶ verrà riguardato come composto di un deutone e di una particella α. E l'energia di legame sarà espressa in funzione di un parametro rappresentante le dimensioni della particella α, un parametro rappresentante le dimensioni del deutone ed un parametro rappresentante la distanza del baricentro del deutone da quello della particella α.

Si noti che una descrizione del Li⁶ del tipo ora detto è consistente con il fatto che il Li⁶ possiede un livello eccitato a 2,12 MeV [8] e con il fatto che il momento magnetico del Li⁶, è, grosso modo, eguale a quello del deutone [9].

2. – Funzioni variazionali usate e cenni sui calcoli.

Le funzioni variazionali con le quali per il Li⁶ e per l'He⁵ si è fatto il calcolo sono le seguenti:

— Li⁶:

$$(3) \qquad \Phi_\iota = \sum_P (-1)^P P u(1)\alpha(1)u(2)\beta(2)r(3)\alpha(3)r(4)\beta(4)u(5)\chi(5)r(6)\chi(6)\,|56)_\iota$$

$$(4) \qquad \Phi_\mu = \sum_P (-1)^P P u(1)\alpha(1)u(2)\beta(2)v(3)\alpha(3)r(4)\beta(4)u(5)\alpha(5)r(6)\alpha(6)\,|56)_\mu$$

[7] Nei calcoli in questione TYRRELL ha fatto uso di un'interazione gaussiana ed HUMBLET di un'interazione yukawiana: i risultati sono qualitativamente gli stessi.

[8] W. M. HARRIS: *Phys. Rev.*, **84**, 1249 (1951); F. AJZENBERG e T. LAURITSEN: *Rev. Mod. Phys.*, **24**, 321 (1952).

[9] Il momento magnetico del deutone è 0,86 magnetoni nucleari, quello del Li⁶ 0,82 (vedi, ad esempio, J. BLATT e V. WEISSKOPF: *Theoretical Nuclear Physics* (New-York, 1952)).

dove u, v ed α, β sono rispettivamente le funzioni di spin isotopico e di spin, $\sum_P$ indica la solita somma sulle permutazioni, e si è posto:

$$(5) \qquad |56)_s = \exp\left[-\sigma(r_{12}^2 + r_{13}^2 + r_{14}^2 + r_{23}^2 + r_{24}^2 + r_{34}^2) - \right.$$
$$\left. - \delta r_{56}^2 - \beta\left(\frac{\boldsymbol{r}_5 + \boldsymbol{r}_6}{2} - \frac{\boldsymbol{r}_1 + \boldsymbol{r}_2 + \boldsymbol{r}_3 + \boldsymbol{r}_4}{4}\right)^2\right],$$

e:

$$(6) \qquad |56)_p = [2(\boldsymbol{r}_5 + \boldsymbol{r}_6) - (\boldsymbol{r}_1 + \boldsymbol{r}_2 + \boldsymbol{r}_3 + \boldsymbol{r}_4)]_z |56)_s.$$

Tanto (3) quanto (4) sono invarianti rispetto a traslazioni [10] e corrispondono ad uno spin pari ad 1; (3) è uno stato N, (4) uno stato P. Il significato dei parametri σ, β e δ nelle (5) (6) è, dopo la discussione precedente, ovvio.

— He^5:

$$(8) \qquad F_s = \sum_P (-1)^P P u(1)\alpha(1)u(2)\beta(2)v(3)\alpha(3)v(4)\beta(4)u(5)\alpha(5)|5)_s,$$

$$(8) \qquad F_p = \sum_P (-1)^P P u(1)\alpha(1)u(2)\beta(2)v(3)\alpha(3)v(4)\beta(4)u(5)\alpha(5)|5)_p$$

dove:

$$(9) \qquad |5)_s = \exp\left[-\sigma(r_{12}^2 + r_{13}^2 + r_{14}^2 + r_{23}^2 + r_{24}^2 + r_{34}^2) + \right.$$
$$\left. + \beta\left(\boldsymbol{r}_5 - \frac{\boldsymbol{r}_1 + \boldsymbol{r}_2 + \boldsymbol{r}_3 + \boldsymbol{r}_4}{4}\right)^2\right],$$

$$(10) \qquad |5)_p = [4\boldsymbol{r}_5 - (\boldsymbol{r}_1 + \boldsymbol{r}_2 + \boldsymbol{r}_3 + \boldsymbol{r}_4)]_z |5)_s.$$

Senza entrare nei dettagli dei calcoli diamo i risultati di essi che possono essere utili in future ricerche su questo problema.

Con la ovvia notazione: $(ik|G|hl)_s$ indicheremo l'elemento di matrice di un generico operatore G tra funzioni di tipo (3); analogo significato avranno i simboli $(ik|G|hl)_p$, $(i|G|h)_s$, $(i|G|h)_p$, in riferimento rispettivamente alle funzioni (4), (7), (8). Nel seguito affiggeremo di un indice s quantità riferen-

---

[10] Il calcolo perturbativo dianzi accennato degli Autori [1] [2] [3] è stato fatto in coordinate individuali sottraendo a conti fatti l'energia cinetica del baricentro; sebbene questo procedimento sia abbastanza ragionevole non è tuttavia chiaro che genere di errori si compiano in esso.

tisi a calcoli eseguiti con la funzione S (tanto per il Li⁶ quanto per l'He⁵), di un indice p quantità calcolate con la funzione P. L'operatore G può essere in particolare l'unità, nel qual caso interverranno simboli come: $(ik|hl)_s$, $(ik|hl)_p$, $(i|h)_s$, $(i|h)_p$; o può essere l'energia potenziale $J(r_{mn})$ tra due nucleoni n, m; nel qual caso interverranno simboli come $(ik|J(r_{mn})|hl)_s$ che abbrevieremo in $(ik|mn|hl)_s$, ecc. L'energia coulombiana non sarà nel seguito considerata.

2·1. – Calcoli relativi al Li⁶.

Il valor medio dell'energia potenziale, $\bar{V}_s$, è una combinazione lineare degli elementi di matrice che compaiono nella prima colonna della seguente tab. I, il coefficiente che moltiplica ciascun elemento di matrice essendo la opportuna combinazione di w, m, b, h, determinata dalle altre colonne della tabella. (Esempio: $(16|12|26)_s$ va moltiplicato per: $2w + 8m + 4h + 4b$). Una volta costruita la ora detta combinazione lineare, $\bar{V}_s$ si ottiene moltiplicandola per A e dividendola per il fattore di normalizzazione della funzione (3) N_s; questo è pari a: $N_s = (56|56)_s - 2(16|56)_s + (13|56)_s$.

La tabella II contiene le espressioni esplicite degli elementi di matrice che compaiono nella prima colonna della tabella I.

Il valor medio della energia cinetica $\bar{T}_s$ è dato da:

$$(11) \qquad \bar{T}_s = \frac{1}{N_s} \sum_1^6{}_i \int \Phi_s^* T_i \Phi_s \, d\tau =$$

$$= \frac{1}{N_s} \sum_1^6{}_i \{ (56|T_i|56)_s - 2(16|T_i|56)_s + (13|T_i|56)_s \}$$

e, poichè è:

$$(12) \qquad \sum_1^6{}_i T_i|56)_s \equiv - \sum_1^6{}_i \frac{\hbar^2}{2M} \Delta_i|56)_s =$$

$$= \frac{\hbar^2}{2M} \left[\frac{q}{2}\beta + 12\delta + 72\sigma + 3\beta^2 \frac{\partial}{\partial\beta} + 16\sigma^2 \frac{\partial}{\partial\sigma} + 8\delta^2 \frac{\partial}{\partial\delta} \right]|56)_s ,$$

il calcolo di $\bar{T}_s$ è ricondotto alla valutazione dei nove elementi di matrice che si trovano nella tabella III.

Nel caso della funzione P il fattore di normalizzazione è: $N_p = (56|56)_p - 2(16|56)_p + (13|56)_p$ ed il valor medio dell'energia potenziale si ottiene in modo completamente analogo al caso della funzione S sostituendo N_s con N_p

e la tabella II con la tabella IV. L'energia cinetica media $\bar{T}_p$ è data da:

$$(13) \qquad \bar{T}_p = \frac{1}{N_p} \left[\sum_1^6 {}_i(56 \,|\, T_i \,|\, 56)_p - 2(16 \,|\, T_i \,|\, 56)_p + (13 \,|\, T_i \,|\, 56)_p \right]$$

e la sua valutazione è facilitata dall'osservazione che è:

$$(14) \qquad \sum T_i \,|\, 56)_p = \frac{\hbar^2}{2M} \left[\frac{15}{2}\,\beta + 12\delta + 72\sigma + 3\beta^2\frac{\partial}{\partial\beta} + 16\sigma^2\frac{\partial}{\partial\sigma} + 8\delta^2\frac{\partial}{\partial\delta} \right] |\, 56)_p\,,$$

ed è perciò ricondotta agli elementi di matrice che si trovano nella tabella V.

Dalle formule precedentemente date si può verificare, ad esempio, che al tendere di β a zero tanto $E_s = \bar{T}_s + V_s$ quanto $E_p = \bar{T}_p + V_p$ tendono a $E_\alpha + E_d$ con:

$$(15) \qquad E_\alpha = \frac{\hbar^2}{M}\,8\sigma - 6A(w + m)\left[\frac{\sigma}{\sigma + \alpha/4} \right]^{3/2},$$

$$(16) \qquad E_d = \frac{\hbar^2}{M}\,3\delta - A(w + m + b + h)\left[\frac{\delta}{\delta + \alpha/2} \right]^{3/2}.$$

Queste espressioni coincidono con quelle date da altri Autori per l'energia di legame della particella α e del deutone.

2·2. – Calcoli relativi all'He⁵.

Il valor medio dell'energia potenziale $\bar{U}_s$ è una combinazione lineare degli elementi di matrice che si trovano nella prima colonna della tabella VI, il coefficiente di ciascun elemento essendo la opportuna combinazione di w, m, b, h determinata dalle altre colonne della tabella. (Esempio: il coefficiente di $(1\,|\,14\,|\,4)_s$ è: $-w + 4m + 2h - 2b$). Una volta costruita la ora detta combinazione lineare, $\bar{U}_s$ si ottiene moltiplicandola per $-A$ e dividendola per il fattore di normalizzazione n_s; questo è pari a: $(5\,|\,5)_s - (2\,|\,5)_s$.

La tabella VII contiene le espressioni degli elementi di matrice in questione.

Il valor medio della energia cinetica:

$$\mathcal{T}_s = \frac{1}{n_s}\sum_1^5 {}_i \int F_s^* T_i F_s\,\mathrm{d}\tau = \frac{1}{n_s}\sum_1^5 {}_i \left\{ (5\,|\,T_i\,|\,5)_s - (2\,|\,T_i\,|\,5)_s \right\},$$

si ottiene facilmente tenendo presente che è:

$$(17) \qquad \sum_1^5 T_i\,|\,5)_s = \frac{\hbar^2}{2M}\left[\frac{15}{2}\,\beta + 72\sigma + 16\sigma^2\frac{\partial}{\partial\sigma} + 5\beta^2\frac{\partial}{\partial\beta} \right]|\,5)_s\,,$$

onde è ricondotto agli elementi di matrice che compaiono nella tabella VIII.

Nel caso della funzione P (8) tutto procede in modo analogo; il fattore di normalizzazione è: $n_p = (5|5)_p - (2|5)_p$; la tabella VII va sostituita con la tabella IX; e la valutazione del valor medio della energia cinetica:

$$\mathcal{T}_p = \frac{1}{n_p} \sum_1^5 {}_i \{(5|T_i|5)_p - (2|T_i|5)_p\}$$

è facilitata dall'osservazione che è:

$$(18) \qquad \sum_1^5 {}_i \, T_i|5)_p = \frac{\hbar^2}{2M} \left[\frac{25}{2} \beta + 72\sigma + 16\sigma^2 \frac{\partial}{\partial\sigma} + 5\beta^2 \frac{\partial}{\partial\beta} \Big| 15)_p \right. ,$$

ed è perciò ricondotto agli elementi di matrice che si trovano nella tabella X. Si può controllare che tanto $\mathcal{E}_s = \overline{U}_s + \overline{\mathcal{T}}_s$ quanto $\mathcal{E}_p = \overline{U}_p + \mathcal{T}_p$ tendono, al tendere di β a zero ad E_α (15) come deve essere.

3. − Valutazioni numeriche e discussione.

Le valutazioni numeriche sono state fatte nel caso dell'He⁵ e del Li⁶ per un valore di σ tale da rendere massima separatamente la energia di legame della particella α. In unità in cui il range delle forze è assunto eguale ad 1 esso è: $\sigma = 0,33$; ed il corrispondente valore calcolato dell'energia della particella α è 25,21 MeV. Per δ si è scelto pure il valore che massimizza l'energia di legame (16) del deutone; δ risulta (casualmente) [12] pure eguale a 0,33 e la corrispondente energia di legame del deutone è: 0,9 MeV. Questo basso valore dell'energia di legame del deutone dipende dal notorio [13] fatto che una gaussiana è una cattiva funzione d'onda variazionale per il deutone. Per β si sono considerati, tanto nel caso dell'He⁵ quanto in quello del Li⁶ i valori: 0, 1/24, 1/16, 1/8, 1/5.

Per i parametri di saturazione si sono scelti i valori:

$$(19) \qquad w = -\frac{2}{15}, \qquad m = \frac{14}{15}, \qquad h = \frac{4}{15}, \qquad b = \frac{7}{15}.$$

---

[11] Sebbene tale stato P sia in contraddizione con il momento magnetico (vedi nota [9]) abbiamo svolto il calcolo anche per tale stato in modo da poter esaminare in dettaglio il meccanismo che dà luogo a maggior legame nello stato S che nello stato P, al contrario di quel che avviene nell'He⁵.

[12] In effetti i valori di σ e δ che veramente massimizzano le rispettive energie di legame differiscono di qualche percento; per semplificare i calcoli numerici abbiamo attribuito a σ e δ lo stesso valore.

[13] H. MARGENAU and K. CARROL: *Phys. Rev.*, **54**, 705 (1938).

in accordo con:

(20) $$b + h = 0,2 \; ,$$

e con la condizione:

(21) $$4w + 2b - h - m = 0 \; .$$

Questa condizione è la più favorevole, cioè quella che dà più energia di legame, compatibile con le condizioni di saturazione dei nuclei pesanti. È facile constatare, con l'aiuto delle tabelle I e VI, ed avendo alla mano i valori numerici degli integrali, che una volta imposte le condizioni (2), (20), (21), le variazioni dei parametri compatibili con esse non influiscono praticamente sulla energia di legame del Li^6 e dell'He^5.

I valori dei parametri (19) coincidono con quelli degli altri Autori.

I risultati sono riportati nelle figg. 1, 2, 3 seguenti, tanto per la funzione S, quanto per la funzione P. La fig. 1 dà, al variare di β i valori dell'energia cinetica e dell'energia potenziale per il Li^6, la fig. 2 gli stessi valori per l'He^6. E la fig. 3 dà, tanto per il Li^6 quanto per l'He^5 la variazione con β dell'energia di legame.
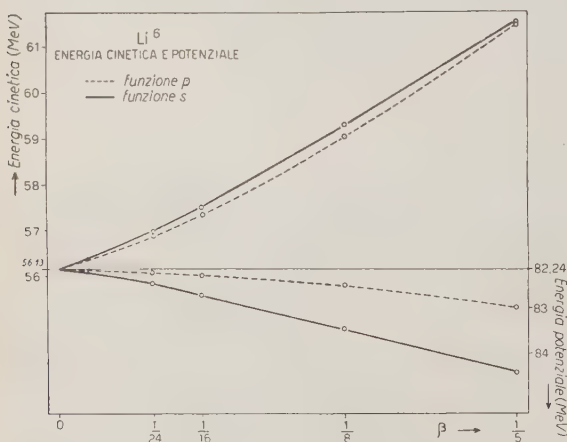
Fig. 1.

Si vede dalla fig. 3 anzitutto che la massima energia di legame si ottiene per ogni β con la funzione P nel caso dell'He^5 e con la funzione S nel caso del Li^6. Ciò è in accordo con il modello a shell.

Ma ciò che più si nota è che l'energia di legame del Li^6 decresce monotonicamente al decrescere della distanza. La massima energia di legame si ottiene quando il deutone è a distanza infinita dalla particella α.

Che nell'He^5 la massima energia di legame si ottenga quando il neutrone è a distanza infinita dalla particella α è ragionevole in quanto l'He^5 è instabile. Ma è spiacevole che nel Li^6 capiti la stessa cosa. La ragione sta, come si vede, nel fatto che la energia potenziale cresce (in valore assoluto) molto meno della

energia cinetica. Ciò è dovuto essenzialmente alle condizioni di saturazione le quali danno luogo a troppo forti interazioni repulsive.

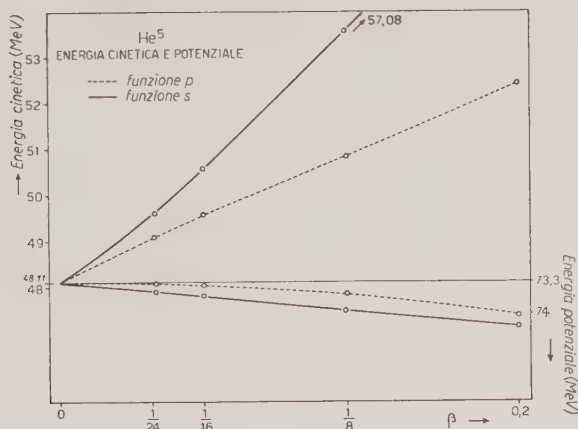Ci si può chiedere come si modificherebbero le curve delle figg. 1, 2, 3, nel

Fig. 2.

caso che modificassimo i parametri w, m, b, h, rinunciando alla condizione di saturazione (21). È possibile, rinunciando a tale condizione, in particolare assumendo egual dose di forze di scambio e non di scambio (tipo Serber) spiegare simultaneamente la stabilità del Li^6 e l'instabilità dell'He^5? La risposta sembra possa essere affermativa in virtù del diverso momento angolare orbitale nei due casi, che fa sì che l'energia potenziale cresca nell'He^5 assai più lentamente che nel Li^6.

Speriamo comunque di poter presentare in futuro più estesi calcoli numerici a partire dalle formule qui stabilite, sì da poter rispondere alla domanda sopra posta.
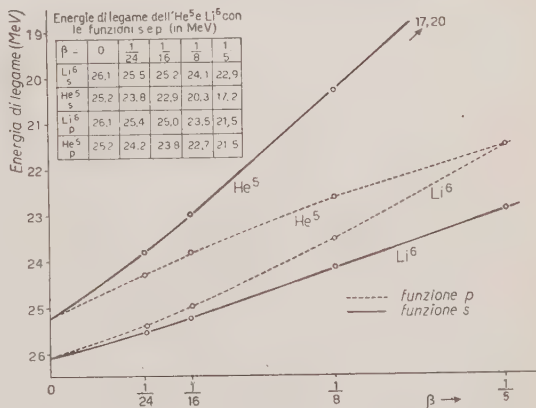

Fig. 3.

Per il momento la conclusione, valida sotto l'ipotesi naturalmente che le funzioni d'onda variazionali qui usate siano sufficientemente aderenti alla realtà, è, che le condizioni di saturazione quali si scrivono di solito, sono incompatibili con l'energia di legame del Li[6]; questo fatto, unito alla loro incompatibilità con le esperienze di scattering n-p a 90 MeV è un altro argomento a favore della idea che la saturazione dei nuclei pesanti debba essere spiegata con qualche altro meccanismo.

Desidero ringraziare il prof. B. FERRETTI per varie utili discussioni avute. Inoltre sono grato all'Istituto Nazionale per le Applicazioni del Calcolo, nelle persone del Direttore, prof. M. PICONE, e del dott. W. GROSS, per l'esecuzione dei calcoli numerici a partire dalle espressioni algebriche contenute nelle tabelle.

TABELLE RELATIVE AL Li[6]

TABELLA I.

Coefficienti di w, m, b, h, che moltiplicano i vari integrali tanto nel caso della funzione P quanto in quello della funzione S.

	w	m	b	h
(12|12|12)	+ 1	+ 1	+ 1	+ 1
(12|12|26)	− 4	− 4	− 4	− 4
(16|12|16)	+ 8	− 2	+ 4	− 4
(16|12|15)	− 6	+ 4	− 2	+ 6
(16|12|26)	− 2	+ 8	− 4	+ 4
(15|12|26)	+ 4	− 6	+ 6	− 2
(12|12|56)	+ 2	+ 2	+ 2	+ 2
(16|12|56)	− 12	− 12	0	0
(13|12|56)	+ 8	+ 8	− 4	− 4
(34|12|56)	+ 1	+ 1	+ 1	+ 1
(36|12|56)	− 6	− 6	0	0
(56|12|56)	+ 6	+ 6	0	0

TABELLA II.

Integrali che compaiono in V_s e, per $\alpha = 0$ in N_s. Tutte le espressioni qui date sono da moltiplicarsi per un inessenziale fattore numerico. Il simbolo El (-3/2)[ ] indica che tutta l'espressione entro parentesi va elevata alla potenza — 3/2.

$$(12|12|56)_s = \text{El}\left(-\frac{3}{2}\right)\left[8\sigma(4\sigma + 2\delta + 2\alpha)(4\sigma + 2\delta)\left\{\left(4\sigma + \frac{5}{4}\beta\right)^2 - \beta^2\right\}\right]$$

$$(34|12|56)_s = \text{El}\left(-\frac{3}{2}\right)\left[(4\sigma + 2\delta)^2(8\sigma + 2\alpha)\left\{\left(4\sigma + \frac{5}{4}\beta\right)^2 - \beta^2\right\}\right]$$

$$(12|12|12)_s = \text{El}\left(-\frac{3}{2}\right)\left[64\sigma^2(4\delta - 2\alpha)\left\{\left(8\sigma + \frac{1}{2}\beta\right)2\beta \quad \beta^2\right\}\right]$$

$$(56|12|56)_s = \text{El}\left(-\frac{3}{2}\right)\left[32\cdot16\sigma^2\beta\delta(8\sigma + 2\alpha)\right]$$

$$(15|12|26)_s = \text{El}\left(-\frac{3}{2}\right)\left[\left(4\sigma + \frac{1}{4}\beta\right)(4\sigma + 2\delta)8\sigma\left\{(\alpha + 4\sigma + 2\delta)\left(4\sigma + \frac{9}{4}\beta + 2\alpha\right) - 2\alpha^2\right\}\right]$$

$$(16|12|15)_s = \text{El}\left(-\frac{3}{2}\right)\left[\left(4\sigma + \frac{3}{4}\beta + \frac{4}{3}\delta\right)8\sigma\left\{24\sigma^2\beta + 96\sigma^2\delta + 18\sigma\beta\delta + 24\sigma\alpha\delta + \right.\right.$$
$$\left.\left. - \frac{3}{2}\alpha\beta\delta - 48\sigma^2\alpha - 3\sigma\alpha\beta\right\}\right]$$

$$(12|12|26)_s = \text{El}\left(-\frac{3}{2}\right)\left[64\sigma^2\left\{\left(4\sigma + \frac{3}{4}\beta + \frac{4}{3}\delta + \frac{2}{3}\alpha\right)\cdot\right.\right.$$
$$\left.\left. \cdot\left[\left(4\sigma + \frac{3}{4}\beta\right)\left(\frac{3}{4}\beta + 3\delta + \frac{3}{2}\alpha\right) - \frac{9}{16}\beta^2\right] - \alpha^2\left(4\sigma + \frac{3}{4}\beta\right)\right\}\right]$$

$$(16|12|16)_s = \text{El}\left(-\frac{3}{2}\right)\left[64\sigma^2\left\{64\sigma\beta\delta + 8\sigma\beta\alpha + 32\sigma\alpha\delta + 6\alpha\beta\delta\right\}\right]$$

$$(13|12|56)_s = \text{El}\left(-\frac{3}{2}\right)\left[(4\sigma + 2\delta)\left\{[32\sigma^2 + 6\sigma\alpha + 16\sigma\delta + \alpha\delta]\left[\left(4\sigma + \frac{5}{4}\beta\right)^2 - \beta^2\right] + \right.\right.$$
$$\left.\left. 8\alpha\sigma\left(4\sigma - \frac{5}{4}\beta\right)(4\sigma + 2\delta)\right\}\right]$$

$$(36|12|56)_s = \text{El}\left(-\frac{3}{2}\right)\left[8\sigma(8\sigma + 2\alpha)\left(4\sigma + \frac{3}{4}\beta + \frac{4}{3}\delta\right)\left(3\beta\sigma + 12\sigma\delta + \frac{9}{4}\beta\delta\right)\right]$$

$$(16|12|26)_s = \text{El}\left(-\frac{3}{2}\right)\left[64\sigma^2\left(4\sigma + \frac{3}{4}\beta + \frac{4}{3}\delta + \frac{8}{3}\alpha\right)\left\{\left(\frac{3}{4}\beta + 3\delta\right)\left(4\sigma + \frac{3}{4}\beta\right) - \frac{9}{16}\beta^2\right\}\right]$$

$$(16|12|56)_s = \text{El}\left(-\frac{3}{2}\right)\left[8\sigma\left\{\left(4\sigma + \frac{3}{4}\beta + \frac{4}{3}\delta\right)\left(8\sigma + \frac{2}{3}\alpha\right)\left[\left(4\sigma - \frac{3}{4}\beta\right)\left(\frac{3}{4}\beta - 3\delta\right) - \frac{9}{16}\beta^2\right] + \right.\right.$$
$$\left.\left. + 8\sigma\cdot\frac{4}{3}\alpha\left[\left(4\sigma + \frac{3}{4}\beta - \frac{2}{3}\delta\right)\left(\frac{3}{4}\beta + 3\delta\right) - \frac{9}{32}\beta^2\right]\right\}\right]$$

Tabella III.

Integrali che compaiono in T_s; stessa avvertenza che per la tabella II.

$$(56\,|\,\sigma^2(\partial/\partial\sigma)\,|\,56)_s = -\,128\cdot 72\,r^{-5/2}\sigma^4\delta\beta$$

$$(56\,|\,\beta^2(\partial/\partial\beta)\,|\,56)_s = -\,128\cdot 24\,r^{-5/2}\beta^2\delta\sigma^3$$

$$(56\,|\,\delta^2(\partial/\partial\delta)\,|\,56)_s = -\,128\cdot 24\,r^{-5/2}\beta\delta^2\sigma^3$$

$$(13\,|\,\sigma^2(\partial/\partial\sigma)\,|\,56)_s = -\,24\,t^{-5/2}\sigma^2(2\sigma + \delta)\left\{\left[16\sigma^2 + 10\beta\sigma + \frac{9}{16}\,\beta^2\right][6\sigma + \delta] + 2\sigma(2\sigma + \delta)\cdot\right.$$
$$\left.\cdot\,(16\sigma + 5\beta)\right\}$$

$$(13\,|\,\beta^2(\partial/\partial\beta)\,|\,56)_s = -\,48\,t^{-5/2}\beta^2\sigma(2\sigma + \delta)^2\left(5\sigma + \frac{9}{16}\,\beta\right)$$

$$(13\,|\,\delta^2(\partial/\partial\delta)\,|\,56)_s = -\,48\,t^{-5/2}\sigma\delta^2(2\sigma + \delta)\left[16\sigma^2 + 10\beta\sigma + \frac{9}{16}\,\beta^2\right]$$

$$(16\,|\,\sigma^2(\partial/\partial\sigma)\,|\,56)_s = -\frac{3}{2}\,z^{-5/2}\sigma^2\left[\frac{z}{\sigma} + 32\sigma^2\left\{96\sigma\delta + 16\delta^2 + 22\delta\beta + 24\beta\sigma + \frac{9}{4}\,\beta^2\right\}\right]$$

$$(16\,|\,\beta^2(\partial/\partial\beta)\,|\,56)_s = -\frac{3}{2}\,z^{-5/2}\beta^2\cdot 32\sigma^2\left\{22\delta\sigma + \frac{27}{8}\,\beta\delta + 3\delta^2 + 12\sigma^2 + \frac{9}{2}\,\beta\sigma\right\}$$

$$(16\,|\,\delta^2(\partial/\partial\delta)\,|\,56)_s = -\frac{3}{2}\,z^{-5/2}\delta^2\cdot 32\sigma^2\left\{22\beta\sigma + 32\sigma\delta + 48\sigma^2 + 6\beta\delta + \frac{27}{16}\,\beta^2\right\}$$

$$r = (64)^2\sigma^3\delta\beta \qquad t = 8\sigma(4\sigma + 2\delta)^2\left[\left(4\sigma + \frac{5}{4}\,\beta\right)^2 - \beta^2\right]$$

$$z = 64\sigma^2\left(4\sigma + \frac{3}{4}\,\beta + \frac{4}{3}\,\delta\right)\left[\left(\frac{3}{4}\,\beta + 3\delta\right)\left(4\sigma + \frac{3}{4}\,\beta\right) - \frac{9}{16}\,\beta^2\right]$$

<center>TABELLA IV.</center>

Integrali che compaiono in $\bar{V}_p$ e, per $\alpha = 0$, in N_p. Stessa avvertenza che per la tabella II.

$$(56|12|56)_p = \frac{3}{2} \cdot 32 \cdot 256 \cdot \sigma^2 \delta (8\sigma + 2\alpha)(56|12|56)_s^{5/3}$$

$$(12|12|12)_p \quad \frac{3}{2} \cdot 64 \cdot 256 \cdot \sigma^3(4\delta + 2\alpha)\,(12|12|12)_s^{5/3}$$

$$(16|12|16)_p = \frac{3}{2} \cdot 16 \cdot 64\sigma^2(64\sigma\delta + 8\sigma\alpha + 6\alpha\delta)\,(16|12|16)_s^{5/3}$$

$$(34|12|56)_p \quad -\frac{3}{2} \cdot \frac{8}{9} \cdot 144\sigma(4\sigma + 2\delta)^2(8\sigma + 2\alpha)(34|12|56)_s^{5/3}$$

$$(12|12|56)_p \quad -\frac{3}{2} \cdot \frac{8}{9} \cdot 144 \cdot 8\sigma^2(4\sigma + 2\delta + 2\alpha)(4\sigma + 2\delta)\,(12|12|56)_s^{5/3}$$

$$(13|12|56)_p \quad -\frac{3}{2} \cdot 144 \cdot (4\sigma + 2\delta)\left[\frac{8}{9}\sigma\{6\alpha\sigma + 32\sigma^2 + \delta\alpha + 16\sigma\delta\} + \frac{32}{9}\alpha\sigma^2 + \frac{32}{18}\alpha\sigma\delta\right] \cdot$$
$$\cdot (13|12|56)_s^{5/3}$$

$$(36|12|56)_p = \frac{3}{2} \cdot 144 \cdot 8\sigma(8\sigma + 2\delta)\left[\frac{\delta}{9}(4\sigma + 3\delta) + \frac{4}{3}\sigma^2\right](36|12|56)_s^{5/3}$$

$$(15|12|26)_p \quad \frac{3}{2} \cdot 144 \cdot 8\sigma(4\sigma + 2\delta)\left[2(4\sigma + 2\delta)\left(\frac{\alpha}{36} - \frac{4}{9}\sigma\right) - \frac{8}{9}\alpha\sigma\right](15|12|26)_s^{5/3}$$

$$(12|12|26)_p = \frac{3}{2} \cdot 64 \cdot 144\sigma^2\left[(4\sigma + 3\delta)\left(\frac{\delta}{9} + \frac{\alpha}{18}\right) + \frac{\alpha\delta}{6} + \frac{4}{3}\sigma^2\right](12|12|26)_s^{5/3}$$

$$(16|12|56)_p \quad -\frac{3}{2} \cdot 144 \cdot 8\sigma\left[\left(8\sigma - \frac{2}{3}\alpha\right)\left\{(4\sigma - 3\delta)\left(\frac{\sigma}{3} - \frac{\delta}{9}\right) - \sigma\delta\right\} - \frac{32}{9}\sigma^2\alpha - \frac{16}{27}\sigma\alpha\delta\right] \cdot$$
$$\cdot (16|12|56)_s^{5/3}$$

$$(16|12|15)_p = \frac{3}{2} \cdot 144 \cdot 8\sigma\left[-(32\sigma^2 + 24\sigma\delta + 4\alpha\sigma + 2\delta\alpha)\left(\frac{8}{3}\sigma + \frac{8}{9}\delta\right) + \right.$$
$$\left. + 3(2\sigma + \delta)^2\left(8\sigma + \frac{2}{3}\alpha\right)\right](16|12|15)_s^{5/3}$$

$$(16|12|26)_p = \frac{3}{2} \cdot 144 \cdot 64\sigma^2\left[\left(\frac{\delta}{9} + \frac{2\alpha}{9}\right)(4\sigma + 3\delta) + \frac{4}{3}\sigma^2\right](16|12|26)_s^{5/3}$$

TABELLA V.

Integrali che ocmpaiono in $\overline{T}_p$. *Stessa avvertenza che per la tabella* II.

$$(56\,|\,\sigma^2(\partial/\partial\sigma)\,|\,56)_p = 2\cdot\frac{16}{3}\cdot 144\cdot 32\left\{2\cdot\frac{5}{3}\,(56\,|\,\sigma^2(\partial/\partial\sigma)\,|\,56)_s\,r^{-1}\cdot\delta\sigma^3 + 3r^{-5/2}\sigma^4\delta\right\}$$

$$(56\,|\,\delta^2(\partial/\partial\delta)\,|\,56)_p = 2\cdot\frac{16}{3}\cdot 144\cdot 32\left\{2\cdot\frac{5}{3}\,(56\,|\,\delta^2(\partial/\partial\delta)\,|\,56)_s\,r^{-1}\delta\sigma^3 + \sigma^3\delta^2 r^{-5/2}\right\}$$

$$(56\,|\,\beta^2(\partial/\partial\beta)\,|\,56)_p \quad 2\cdot\frac{16}{3}\cdot 144\cdot 32\left\{2\cdot\frac{5}{3}\,(56\,|\,\beta^2(\partial/\partial\beta)\,|\,56)_s\,r^{-1}\right\}$$

$$(13\,|\,\sigma^2(\partial/\partial\sigma)\,|\,56)_p = 4\cdot\frac{3}{2}\cdot 1024\left\{-\frac{5}{3}\,(13\,|\,\sigma^2(\partial/\partial\sigma)\,|\,56)_s\,t^{-1}(2\sigma + \delta)^2\sigma^2 - \sigma^2 t^{-5/2}\cdot\right.$$
$$\left.\cdot[2\sigma^2(2\sigma + \delta) + \sigma(2\sigma + \delta)^2]\right\}$$

$$(13\,|\,\delta^2(\partial/\partial\delta)\,|\,56)_p \quad 4\cdot\frac{3}{2}\cdot 1024\left\{-\frac{5}{3}\,(13\,|\,\delta^2(\partial/\partial\delta)\,|\,56)_s\,t^{-1}(2\sigma + \delta)^2\sigma^2 - \delta^2 t^{-5/2}\sigma^2(2\sigma + \delta)\right\}$$

$$(13\,|\,\beta^2(\partial/\partial\beta)\,|\,56)_p \quad 4\cdot\frac{3}{2}\cdot 1024\left\{-\frac{5}{3}\,(13\,|\,\beta^2(\partial/\partial\beta)\,|\,56)_s\,t^{-1}(2\sigma + \delta)^2\sigma^2\right\}$$

$$(16\,|\,\sigma^2(\partial/\partial\sigma)\,|\,56)_p = 4\cdot\frac{3}{2}\cdot 256\left\{\frac{5}{3}\,(16\,|\,\sigma^2(\partial/\partial\sigma)\,|\,56)_s\,z^{-1}\sigma^2(4\delta\sigma + 3\delta^2 + 12\sigma^2) +\right.$$
$$\left.+ \sigma^2 z^{-5/2}(6\delta\sigma^2 + 3\delta^2\sigma + 24\sigma^3)\right\}$$

$$(16\,|\,\delta^2(\partial/\partial\delta)\,|\,56)_p \quad \frac{3}{2}\cdot 64\cdot 16\cdot\left\{\frac{5}{3}\,(16\,|\,\delta^2(\partial/\partial\delta)\,|\,56)_s\,z^{-1}\sigma^2(4\delta\sigma + 3\delta^2 + 12\sigma^2) +\right.$$
$$\left.+ \sigma^2\delta^2 z^{-5/2}(3\delta + 2\sigma)\cdot\right\}$$

$$(16\,|\,\beta^2(\partial/\partial\beta)\,|\,56)_p = \frac{3}{2}\cdot 64\cdot 16\left\{\frac{5}{3}\,(16\,|\,\beta^2(\partial/\partial\beta)\,|\,56)_s\,z^{-1}\sigma^2(4\delta\sigma + 3\delta^2 + 12\sigma^2)\right\}$$

Le espressioni di z, r, t sono date nella tabella III.

TABELLE RELATIVE ALL' He⁵

TABELLA VI.

Coefficienti di w, m, b, h, che moltiplicano i vari integrali tanto nel caso della funzione S, quanto in quello della funzione P.

	w	m	b	h
$(5\,|\,14\,|\,5)$	6	6	0	0
$(4\,|\,14\,|\,4)$	4	-1	$+2$	-2
$(2\,|\,14\,|\,5)$	-3	-3	0	0
$(4\,|\,14\,|\,5)$	-6	-6	0	0
$(1\,|\,14\,|\,4)$	-1	$+4$	-2	$+2$

TABELLA VII.

Integrali che compaiono in V_s e (per $\alpha = 0$) in n_s. Stessa avvertenza che per la tabella II.

$$(5\,|\,14\,|\,5)_s = \text{El}\left(-\frac{3}{2}\right)\left[(8\sigma)^2\,\frac{8}{3}\,\beta(8\sigma + 2\alpha)\right]$$

$$(2\,|\,14\,|\,5)_s = \text{El}\left(-\frac{3}{2}\right)\left[8\sigma(8\sigma + 2\alpha)\left\{\left(4\sigma + \frac{17}{12}\,\beta\right)^2 - \frac{4}{9}\,\beta^2\right\}\right]$$

$$(4\,|\,14\,|\,5)_s = \text{El}\left(-\frac{3}{2}\right)\left[\frac{32}{3}\,\sigma\left\{\left(6\sigma + \frac{\alpha}{2}\right)\left[\left(4\sigma + \frac{17}{12}\,\beta\right)^2 - \frac{4}{9}\,\beta^2\right] + 8\sigma\alpha\left(4\sigma + \frac{17}{12}\,\beta\right)\right\}\right]$$

$$(1\,|\,14\,|\,4)_s = \text{El}\left(-\frac{3}{2}\right)\left[64\sigma^2\left\{\left(4\sigma + \frac{4}{3}\,\alpha + \frac{17}{12}\,\beta\right)^2 - \left(\frac{4}{3}\,\alpha + \frac{2}{3}\,\beta\right)^2\right\}\right]$$

N.B. Non abbiamo riportato l'espressione di $(4\,|\,14\,|\,4)_s$ perchè in base alla tabella VI e alla condizione di saturazione (21) va moltiplicata per zero.

<div align="center">

TABELLA VIII.

Integrali che compaiono in $\mathcal{C}_s$; stessa avvertenza che per la tabella II.

</div>

$$(5\,|\,\sigma^2(\partial/\partial\sigma)\,|\,5)_s = -\,48\sigma^2\beta\Gamma^{-5/2}(8\sigma)^2$$

$$(5\,|\,\beta^2(\partial/\partial\beta)\,|\,5)_s = -\,2\beta^2\Gamma^{-5/2}(8\sigma)^3$$

$$(4\,|\,\sigma^2(\partial/\partial\sigma)\,|\,5)_s = -\,\frac{3}{2}\cdot 64\sigma^3\cdot S^{-5/2}\left[\left(4\sigma + \frac{17}{12}\,\beta\right)\left(8\sigma + \frac{17}{12}\,\beta\right) - \frac{4}{9}\,\beta^2\right]$$

$$(4\,|\,\beta^2(\partial/\partial\beta)\,|\,5)_s = -\,\frac{3}{2}\,\beta^2 S^{-5/2}(8\sigma)^2\left(\frac{17}{3}\,\sigma + \frac{225}{144}\,\beta\right)$$

$$\Gamma = \frac{8}{3}\,\beta(8\sigma)^3 \qquad S = 64\sigma^2\left[\left(4\sigma + \frac{17}{12}\,\beta\right) - \frac{4}{9}\,\beta^2\right]$$

<div align="center">

TABELLA IX.

Integrali che compaiono in V_p; stessa avvertenza che in tabella II.

</div>

$$(5\,|\,14\,|\,5)_p = 64(8\sigma)^2(8\sigma + 2\alpha)\,(5\,|\,14\,|\,5)_s^{5/3}$$

$$(2\,|\,14\,|\,5)_p = -\,16(8\sigma^2)(8\sigma + 2\alpha)\,(2\,|\,14\,|\,5)_s^{5/3}$$

$$(4\,|\,14\,|\,5)_p = -\,128\cdot 8\sigma^2(8\sigma + 2\alpha)\,(4\,|\,14\,|\,5)_s^{5/2}$$

$$(1\,|\,14\,|\,4)_p = -\,16\cdot 64\sigma^2(8\sigma - 3\alpha)\,(1\,|\,14\,|\,4)_s^{5/3}$$

Vedi N.B. alla tabella VII.

<div align="center">

TABELLA X.

Integrali che compaiono in $\overline{\mathcal{C}}_p$; stessa avvertenza che per la tabella II.

</div>

$$(5\,|\,\sigma^2(\partial/\partial\sigma)\,|\,5)_p = (64)^2\sigma^2\left\{\frac{5}{3}\,(5\,|\,\sigma^2(\partial/\partial\sigma)\,|\,5)_s\cdot 8\sigma\Gamma^{-1} + 12\sigma^2\Gamma^{-5/2}\right\}$$

$$(5\,|\,\beta^2(\partial/\partial\beta)\,|\,5)_p = 64(8\sigma)^3\frac{5}{3}\,\Gamma^{-1}(5\,|\,\beta^2(\partial/\partial\beta)\,|\,5)_s$$

$$(4\,|\,\sigma^2(\partial/\partial\sigma)\,|\,5)_p = -\,16\cdot 64\sigma^2\left\{\frac{5}{3}\,(4\,|\,\sigma^2(\partial/\partial\sigma)\,|\,5)_s 8\sigma S^{-1} + 12\sigma^2 S^{-5/2}\right\}$$

$$(4\,|\,\beta^2(\partial/\partial\beta)\,|\,5)_p = -\,16(8\sigma)^3\frac{5}{3}\,S^{-1}(4\,|\,\beta^2(\partial/\partial\beta)\,|\,5)_s$$

Γ e S sono dati in fondo alla tabella VIII.

SUMMARY

By making use of wave functions describing a deuteron and an α particle ((3) and (4)) we have calculated the dependence of the binding energy of Li^6 on the distance between the center of mass of the α particle and the center of mass of the deuteron. The largest binding energy is obtained (if the nuclear parameters are subjected to the saturation conditions) when the deuteron and the α particle are an infinite distance apart (see fig. 1 and 3); this is due to the fact that the absolute value of the potential energy increases much slower than the kinetic energy when the distance decreases; probably the saturation conditions are responsible for this slow increase. For purpose of comparison analogous calculations have been done for He^5 (fig. 2 and 3). In agreement with the magnetic moment, in Li^6 the S wave function (3) gives rise, for each distance, to an higher binding energy than the P state (4); the opposite is true for He^5.

Electrons Associated with Negative μ Mesons (*).

W. F. FRY

Department of Physics, University of Wisconsin, Madison, Wis.

Summary. — A study has been made in photographic emulsions of low energy electrons associated with stopped negative μ-mesons from the University of Chicago cyclotron. A total of 1000 meson endings has been studied. Of these mesons, 358 decayed into a high energy electron and 32 caused a star. The remaining 610 mesons stopped in the emulsion with no associated tracks other than tracks of low energy electrons ($10 < E_e < 100$ keV). A low energy electron track is observed from 17 of the $^-\mu$-e decays (5 percent). The energy distribution of the low energy electrons from the μ-e decays is consistent with the assumption that the low energy electrons are monoenergetic. The average energy of these electrons is about 17 keV. The low energy electrons are thought to be due to « Auger » transitions of the negative μ-meson from the atomic capture in the light elements of the emulsion. One or more low energy electron tracks are observed from 255 stopped μ-mesons which did not decay or cause a star. These electrons are thought to be due to mesonic « Auger » transitions from the heavy elements in the emulsion. The large difference in the probabilities of electron ejection from the mesonic capture in the light and heavy elements (5 percent as compared to 44 percent) is confirmed by a study of low energy electrons associated with negative μ-meson stars.

1. – Introduction.

It is generally accepted, that a negative μ meson which stops in a solid is captured in various mesonic « Bohr » orbits of an atom and goes by various transitions to the lowest possible mesonic level. The meson may then be

---

either captured by the nucleus or it may decay into an electron. The negative meson many undergo « Auger » transitions as well as radiative transitions in the process of going to the lowest state. A number of investigators have studied, in photographic emulsions ([1,2,3]) and in cloud chambers ([4,5]), the low energy electrons which accompany stopped mesons. These low energy electrons are interpreted as due to non-radiative « Auger » transitions of the meson.

In the previous studies the mesons were obtained from cosmic rays. Both positive and negative π mesons as well as μ mesons are found in the cosmic rays. In the case of the emulsions studies, the number of negative μ mesons was estimated from the stopping power of the various constituents of the emulsions for very low energy mesons, the probability of nuclear capture and the number of μ-e decays, if an assumption is made regarding the ratio of negative to positive μ mesons. From the number of μ meson endings which have only an associated low energy electron track and the estimated number of negative μ mesons, the probability of low energy electron ejection from the capture in the heavy elements in the emulsion could be estimated.

From previous studies ([6,7]) it has been found possible to obtain, from the University of Chicago cyclotron, a relatively high flux of negative μ mesons with a low negative π meson contamination. By determining the percentage of the negative μ mesons which decay in the emulsion ([6]), the percentage of the mesons which stop in the light and heavy elements can be computed. Because of the possible uncertainty in the number of negative μ mesons in the cosmic ray studies, it seemed worthwhile to redetermine the percentage of stopped negative μ mesons which give rise to one or more low energy electrons. Also it seemed of interest to determine if the atomic capture of a ⁻μ meson in the light elements in the emulsion leads to the ejection of electrons in the energy range which can be detected by photographic emulsions.

Aside from the study of the fundamental processes that are involved in the electron ejection, the low energy electrons which occasionally accompany meson capture have been used as a criterion for distinguishing negative meson capture in the light elements from the capture in the heavy elements ([8]). The validity of this criterion can be readily verified by a study of the association of low energy electrons with other phenomena caused by stopped μ mesons.

([1]) M. G. E. COSYNS, C. C. DILWORTH, G. OCCHIALINI and M. SCHÖNBERG: *Proc. Phil. Soc.*, A **62**, 801 (1949).

([2]) W. F. FRY: *Phys. Rev.*, **79**, 893 (1950); **83**, 594 (1951).

([3]) A. BONETTI and G. TOMASINI: *Nuovo Cimento*, **8**, 693 (1951).

([4]) W. Y. CHANG: *Rev. Mod. Phys.*, **21**, 166 (1949).

([5]) G. GROETZINGER, L. LEDER and F. RIBE: *Phys. Rev.*, **81**, 626 (1951).

([6]) W. F. FRY: *Phys. Rev.*, **85**, 676 (1952).

([7]) H. MORINAGA and W. F. FRY: *Nuovo Cimento*, **10**, 324 (1953).

([8]) M. MENON, H. MUIRHEAD and O. ROCHAT: *Phil. Mag.*, **41**, 583 (1950).

2. – Procedure:

Ilford G-5 emulsions 400 microns in thickness were exposed behind ab-
sorbers to the 122 MeV negative π meson beam of the University of Chicago
cyclotron. The π meson beam contains also a small percentage of μ meson
from the decay of π mesons while still in the vicinity of the target. The
μ mesons were separated from the π mesons of the same momentum by utilizing
the greater range of the μ mesons in a Cu absorber [6]. About 10^4 meson
endings per cm^3 of emulsion were obtained in the plates with an exposure
of two hours. The background of tracks in the plates is quite low. It is
estimated that more than 50 percent of the tracks in the plates are due to
negative μ mesons.

The emulsion was searched with an over all magnification of $250 \times$. Only
those meson tracks which stopped well inside the emulsion and were longer
than 200 microns were accepted for this study. Each meson ending was
studied carefully with a magnification of $980 \times$.

3. – Results.

A total of 1 007 meson endings has been studied. In 7 cases it was not
possible to determine whether the μ meson caused the emission of one or
more low energy nuclear particles or low energy electrons. The results of the
study of the remaining 1 000 meson endings are summarized in Table I.

TABLE I. – *Phenomena Associated with Stopped $^-\mu$ Mesons.*

Phenomena	Number of Events			
$^-\mu$-e decay	341	} 358		atomic capture
$^-\mu$-e decay with an additional one or				in the light ele-
more low energy electrons	17			ments
$^-\mu$ ending with no associated tracks .	355		} 610	
$^-\mu$ ending with one low energy electron				
track	180			atomic capture
$^-\mu$ ending with two low energy electron				mainly in the
tracks	57	} 255		heavy elements
$^-\mu$ ending with three low energy electron				
tracks	18			
$^-\mu$ meson stars	32			

A minimum ionizing track associated with the $^-\mu$ meson ending has been
considered to be due to a decay electron, if the energy of the particle is greater

Fig. 1. – A photograph of a negative μ-e decay with a low energy electron is shown in the above figure. The low energy electron track is indicated by the arrow. The energy of this electron is about 15 keV.

than 5 MeV, as determined from the multiple scattering of the track. The expression « low energy electron » refers to an electron in the energy range from 10 keV to 100 keV. Only in 5 cases, an electron from a μ meson was found to have an energy in the interval from 100 keV to 5 MeV. These 5 cases have been included among the μ meson endings with low energy electrons.

The percentage of negative μ mesons which decay in the emulsion is found to be $(341 + 17)$ $(100)/(1000) = 36 \pm 2$ percent which is in good agreement with the previous results [6] $(39 \pm 3$ percent). The emulsion consists principally of two groups of elements; namely a heavy group, Ag and Br, and a light group O, N, C and H. Mesons which stop in the emulsion, stop either in silver bromide crystals or in the gelatine so there is essentially no competition in the atomic capture of the mesons by the light and heavy groups of elements. The probability of nuclear capture has been calculated to be proportional [9] to Z^4 for the light elements, with equal probability of capture and decay in elements [10] with $Z = 11$, therefore essentially all of the negative μ mesons which stop in the silver bromide crystals are expected to be captured while 92 percent of the negative μ mesons that stop in the gelatine are expected to decay, if it is assumed that the atomic « catching » probability is proportional [11] to Z for the light elements of the gelatine. Thus it was found that 39 percent of the mesons which stop in a photographic emulsion, stop in the gelatine and 61 percent stop in the silver bromide crystals.

Fig. 2. – The energy distribution of low energy electrons, which accompany negative μ-e decays, is shown in the above histogram.

In 16 cases the ⁻μ-e decay is accompanied by one low energy electron and in one case the ⁻μ-e decay is accompanied by two low energy electrons. An example of a ⁻μ-e decay accompanied by a low energy electron is shown in Fig. 1. The energy of the electrons was estimated from the measurement of the range and using the range-energy relationship [12,2]. For electrons of energy between 10 and 20 keV, the estimation of the energy from the range of the track, is necessarily quite poor but it is thought to be superior to the estimation of the energy from the number of grains. The energy distribution
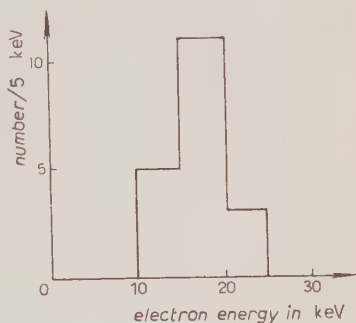
[9] J. W. WHEELER: *Phys. Rev.*, **71**, 462A (1947).

[10] H. K. TICHO: *Phys. Rev.*, **74**, 1337 (1948).

[11] E. FERMI and E. TELLER: *Phys. Rev.*, **72**, 399 (1947).

[12] B. ZAJAC and M. ROSS: *Nature*, **164**, 311 (1949).

of the low energy electrons associated with $^-\mu$-e decays is shown in Fig. 2. The distribution is consistent with the assumption that the electrons are mono-energetic, however the results do not prove by any means that this assumption is correct. In each of the 17 cases the energy of the high energy electron was estimated from the multiple scattering of the track and was found to be greater than 10 MeV. Therefore it is extremely improbable that the high energy electrons were ejected during the atomic capture of the $^-\mu$ meson in the heavy elements. The high energy electrons in these 17 cases are un-doubtedly decay electrons from the negative μ mesons. The probability that the low energy electrons associated with the $^-\mu$-e decays are due to the acci-dental association of δ rays produced by the decay electron at the μ-e junctions has been experimentally determined and found to be negligeably small. The low energy electrons are most probably due to non-radiative meson « Auger » transitions from the atomic capture of the negative μ mesons in the light elements of the gelatine. The probability that the capture of a negative μ meson in the light elements will lead to the ejection of one or more low energy electrons of energy greater than about 10 keV is then found to be $(17/358) (100) = 4.7$ percent.

In 610 cases the meson stopped in the emulsion without associated tracks other than low energy electron tracks. One or more low energy electron tracks are associated with 255 of these meson endings. The energy distribution of these electrons was not obtained since the energy distribution has been pre-viously studied by several investigators ([1,2,3]). These electrons are considered to be due to non-radiative transitions from various mesonic « Bohr » orbits in the heavy elements of the emulsion. The probability that the capture in the heavy elements will lead to the ejection of an electron of energy greater than about 10 keV is then $\big(255/[610 - (0.08)(358)]\big)(100) = 44$ percent. This percentage may be low because it is not always possible to distinguish a very low energy electron track from the end of the μ meson track. Nevertheless the probability of electron ejection is much higher from the capture in the heavy elements than from the capture in the light elements.

The large difference in the probabilities of electron ejection from the capture in light and heavy elements is confirmed by a study of negative μ meson stars. It has been found ([7]) that the bulk of the one prong μ meson stars are due to the nuclear capture in Ag and Br while a portion of the multiply pronged μ meson stars can be attributed to the capture in C, N, and O. A total of 75 one prong stars has been studied of which 39 (52 percent) have one or more low energy electrons associated with the star. Likewise 30 nega-tive μ meson stars have been studied where the characteristics of the stars establish with reasonable assurance that the mesons were captured by the light elements. Only in one of these 30 stars is a low energy electron track observed to originate from the star. Although the atomic capture of a negative meson

in the light elements can lead to the ejection of a low energy electron, as evidenced by the electron from ⁻μ-e decays, the probability of electron ejection is much smaller from the light elements than from the heavy elements; therefore the absence of electrons from stars caused by stopped negative mesons can be used to distinguish capture in the light elements from capture in the heavy elements.

The author is greatly indebted to Professor H. L. ANDERSON for his permission to use the facilities of the University of Chicago cyclotron. The author is also indebted to Mr. ARTHUR ROSENFELD for many interesting discussions and for his help in making the exposures.

RIASSUNTO (*)

Si sono studiati in emulsioni fotografiche gli elettroni di bassa energia associati con mesoni μ negativi in fine corsa prodotti dal ciclotrone dell'Università di Chicago. È stato studiato un totale di 1000 mesoni in fine corsa. Di questi mesoni, 358 disintegrarono in un elettrone d'alta energia e 32 produssero una stella. I restanti 610 mesoni si arrestarono nell'emulsione mostrando solo tracce associate di elettroni di bassa energia ($10 < E_e < 100$ keV). In 17 dei decadimenti ⁻μ-e (5%) è visibile la traccia di un elettrone di bassa energia. La distribuzione energetica degli elettroni di bassa energia originati nelle disintegrazioni μ-e è compatibile con l'ipotesi che gli elettroni di bassa energia siano monoenergetici. L'energia media di questi elettroni è circa 17 keV. Si suppone che gli elettroni di bassa energia derivino da transizioni «Auger» del mesone μ negativo originate dalla cattura atomica negli elementi leggeri dell'emulsione. 255 dei mesoni μ arrestati che non disintegrarono o non produssero stelle mostrano una o più tracce dovute a elettroni di bassa energia. Si suppone che questi elettroni siano dovuti a transizioni Auger derivanti dalle catture atomiche negli elementi pesanti dell'emulsione. L'elevata differenza fra le probabilità di emissione di elettroni derivanti dalla cattura di mesoni negli elementi leggeri e pesanti (5% in confronto del 44%) è confermata dallo studio degli elettroni di bassa energia associati con le stelle dovute ai mesoni μ negativi.

_____

(*) _Traduzione a cura della Redazione._

LETTERE ALLA REDAZIONE

(La responsabilità scientifica degli scritti inseriti in questa rubrica è completamente lasciata dalla Direzione del periodico ai singoli autori)

On a Recent Interpretation of Star Data.

H. MESSEL

School of Physics, University of Sydney - Sydney, Australia

R. B. POTTS

University of Adelaide - Adelaide, Australia

In a recent paper [1], CORTINI *et al.* have analyzed data from nuclear explosions observed in emulsions e posed at high altitudes. One of their conclusions, arrived at after a comparison of their results with theories of meson production, was that «the plural theory is not sufficient to explain the experimental data». This conclusion would be of great importance in the present controversy concerning the actual mode of meson production, but we shall show that it does not follow from their experimental results.

CORTINI *et al.* have based their arguments on rather a rough comparison (the best available at the time) of their results with the plural theory as formulated by HEITLER and JÁNOSSY. Subsequently, detailed numerical results derived from various models of plural production have been presented in a form which makes possible a better comparison of theory with experiment [2,3].

It will be sufficient for present purposes to consider the integral multiplicity spectra of shower particles as con-
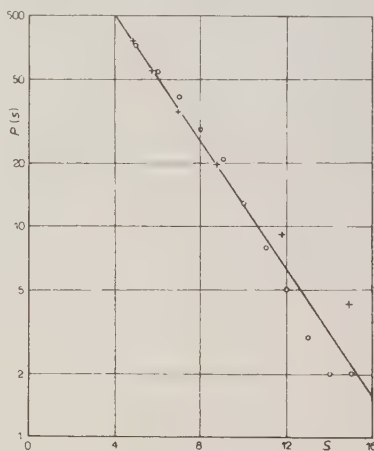

Fig. 1. – Integral multiplicity spectra of shower particles. s = number of shower particles, $P(s)$ = = number of stars having $> s$ shower particles. ◯ and straight line are taken from CORTINI et al.; + values predicted by plural theory,

sidered by CORTINI *et al.* Their experimental results are reproduced in Fig. 1, the straight line being the one drawn by

[1] G. CORTINI, A. MANFREDINI, and G. SE-GRE: *Nuovo Cimento*, **9**, 659 (1952).

[2] H. MESSEL, R. B. POTTS, and C. B. A. McCUSKER: *Phil. Mag.*, **43**, 889 (1952).

[3] H. MESSEL, R. B. POTTS: *Phys. Rev.*, **88**, 488 (1952).

them as a best fit to the experimental points. On the same figure are plotted the results predicted by us assuming plural theory on the HJ(1) model (in which it is assumed that the primary proton initiates a cascade within the nucleus and in each individual nucleon-nucleon collision one meson is produced which escapes from the nucleus without further interactions). The agreement of the two sets of results is quite good.

We have obtained our results as follows. For energies E_0 greater than the primary cut-off energy E_c (≈ 3 GeV for latitude 47º N), the average number of protons with energ $\geqslant E_0$ is

$$(1) \qquad N(E_0) = kE_0^{-\gamma},$$

where k is a constant and γ is the primary power law exponent (we shall take $\gamma = 1.1$, the value used by CORTINI et al.). From Table IV, reference 3, we can determine from the first and eighth columns the average number of shower particles s (or n_s in our notation) produced in a collision of a proton of energy E_0 with a silver or bromine nucleus in the emulsion. Hence we can plot the absolute number $P(s)$ of stars having $\geqslant s$ shower particles against the number of shower particles s, normalising our results to agree with those of CORTINI et al. at $s = 4.9$.

This gives

$$(2) \qquad P(s) \approx 75(15/E_0)^{1.1}$$

and the points plotted in Fig. 1 correspond to

$$E_0 = 20, \ 30, \ 50, \ 100, \ 200.$$

In interpreting this comparison of our results with the experimental ones it has to be borne in mind that (a) the experimental results do not definitely distinguish collisions with light nuclei from those with heavy nuclei, whereas the theoretical results are for heavy nuclei (b) the statistics of the experimental data for large s are very poor. Because of these and other uncertainties we do not claim that the agreement of the results is proof that the plural theory is correct; what we do claim is that the plural theory is sufficient to explain the experimental data, contrary to the conclusion of CORTINI et al. It should be noted that other models of plural production ([2,3]) could explain the results equally well.

Un esempio elettrodinamico di teorema di ortogonalità alla **Van Hove**.

A. LOINGER

Istituto di Fisica dell'Università - Pavia

È stato dimostrato da VAN HOVE [1] che per un campo scalare neutro in interazione scalare con un certo numero di sorgenti ferme ed infinitamente pesanti lo spazio hilbertiano degli stati stazionari del campo interagente con le sorgenti è ortogonale allo spazio hilbertiano degli stati stazionari del campo libero. Questo teorema di ortogonalità (a proposito del quale v. anche [2]) rende evidentemente priva di senso, in generale, l'applicazione della teoria delle perturbazioni al problema considerato.

In questa lettera ci proponiamo di far vedere come un analogo teorema di ortogonalità valga anche nel problema di un elettrone in interazione col campo elettromagnetico, ove ci si metta nelle approssimazioni non relativistica e di dipolo ed inoltre si trascuri il termine dell'hamiltoniano contenente il quadrato del potenziale vettore. Sono queste, com'è noto [3], delle condizioni che permettono, grazie alla trasformazione canonica di Bloch e Nordsieck, di risolvere esattamente il problema detto.

Rinormalizzata la massa ed eseguita la trasformazione di Bloch e Nordsieck, l'equazione di Schrödinger del nostro problema si scrive, nella rappresentazione in cui $\boldsymbol{X}$ e le Q sono diagonali [4]:

$$(1) \qquad \left\{ -\frac{\hbar^2}{2m_f} \Delta_X + \frac{1}{2} \sum_k \left(-\frac{\partial^2}{\partial Q_k^2} + Q_k^2 \right) \hbar c |k| \right\} \psi(\boldsymbol{X}, Q, t) = i\hbar \frac{\partial \psi}{\partial t}.$$

Le autofunzioni della (1) sono:

$$(2) \qquad \psi_{n_{k_1} \cdots n_{k_j} \cdots; \, \boldsymbol{p}}(X, Q) = \exp\left[\frac{i}{\hbar} \boldsymbol{P} \cdot \boldsymbol{X} \right] \prod_k h_{n_k}(Q_k),$$

[1] L. VAN HOVE: *Physica*. **18**, 145 (1952).

[2] A. LOINGER: *Nuovo Cimento*. **9**, 1080 (1952); **10**, 356 (1953).

[3] Vedi, ad esempio, G. MORPURGO: *Suppl. al Nuovo Cimento*. **8**, 109 (1951). Per tutto quel che riguarda il metodo di Bloch e Nordsieck rinviamo a questa rassegna e alla bibliografia in essa citata (e, in particolare, alla memoria di PAULI e FIERZ in *Nuovo Cimento*, **15**, 167 (1938)).

[4] Le notazioni da noi usate sono quelle della rassegna [3].

ove le $h_{n_k}(Q_k)$ sono le consuete funzioni (normalizzate) associate ai polinomi di Hermite.

L'equazione di Schrödinger del problema elettrone + campo e.m. disaccoppiati è:

$$(3) \qquad \left\{ -\frac{\hbar^2}{2m_0} \Delta_x + \frac{1}{2} \sum_k \left(-\frac{\partial^2}{\partial Q_k^2} + Q_k^2 \right) \hbar c \, |k| \right\} \varphi(x, Q, t) = i\hbar \frac{\partial \varphi}{\partial t} ,$$

(rammentiamo che $X = x - \hbar \sum_k Q_k \gamma_k$; $\gamma_k = \frac{2e}{m_f} \frac{1}{\hbar c \, |k|} \left(\frac{\pi \hbar}{c \, |k|} \right)^{1/2} e_k$; ove e_k è il versore di polarizzazione).

Le sue autofunzioni sono:

$$(4) \qquad \varphi_{m_{k_1}, \dots m_{k_j}, \dots; \, p}(x, Q) = \exp \left[\frac{i}{\hbar} p \cdot x \right] \prod_k h_{m_k}(Q_k) .$$

Vogliamo ora mostrare che lo spazio dei vettori di stato (2) è ortogonale allo spazio dei vettori di stato (4).

Poichè il prodotto scalare di uno qualsiasi dei vettori di stato (2) per uno qualsiasi dei vettori di stato (4) differisce solo in un numero finito di fattori dal prodotto scalare dei corrispondenti stati di vuoto [5], è sufficiente dimostrare l'ortogonalità di questi ultimi. Avremo pertanto da calcolare l'integrale

$$\int \exp \left[\frac{i}{\hbar} P \cdot \left(x + \hbar \sum_k Q_k \gamma_k \right) \right] \prod_k h_0(Q_k) \exp \left[-\frac{i}{\hbar} p \cdot x \right] \prod_k h_0(Q_k) \, d_3 x \prod_k dQ_k ,$$

il quale si può trascrivere

$$\int \exp \left[\frac{i}{\hbar} (P - p) \cdot x \right] d_3 x \prod_k \int \exp \left[i P \cdot Q_k \gamma_k \right] h_0^2(Q_k) \, dQ_k ;$$

ma è:

$$\prod_k \int \exp \left[i P \cdot Q_k \gamma_k \right] h^2(Q_k) \, dQ_k = \prod_k \exp \left[-\frac{1}{4} (P \cdot \gamma_k)^2 \right] =$$

$$= \exp \left(-\frac{e^2 P^2}{3\pi m_f^2 \hbar c^3} \int_0^\infty \frac{d \, |k|}{|k|} \right) = 0 ; \quad \text{c. v. d.}$$

Ovviamente, l'interesse del presente problema (come anche dei problemi studiati in [1,2]) è essenzialmente di carattere matematico, se non altro perchè la validità dell'hamiltoniano della (1) è verosimilmente limitata al primo ordine in e^2 (vedi [3], p. 137). Malgrado ciò, il risultato ottenuto ci sembra egualmente non privo di un certo interesse, in quanto esso rafforza il sospetto (insorto in seguito alle conclusioni di [1,2]) che le difficoltà cui dà luogo l'applicazione dei metodi perturbativi ai problemi di elettrodinamica quantistica (e, più generalmente, ai problemi della teoria quantistica dei campi) siano dovute, almeno in parte, all'esistenza di teoremi di ortogonalità analoghi a quelli validi pei casi semplici studiati.

[5] Escludiamo gli stati stazionari a energia infinita.

On the Non Local Interaction and on the Statistical Interpretation of the Cut-off Operators.

G. Wataghin

Istituto di Fisica dell' Università - Torino
Istituto Nazionale di Fisica Nucleare - Sezione di Torino

Recently several valuable contributions to the theory of non local fields were made [1]. The purpose of the present remarks is to show the possibility of an approximate description of non local interactions, starting from a local hamiltonian formalism and using the covariant interaction representation. The equation of interaction representation can be transformed in a way as to obtain the non adiabatic formalism proposed by Tamm [2]. The stationary Schrödinger equation, used successfully by Tamm, Dancoff and M. Lévy, is suitable to analyse the statistical significance of the cut-off operators obtained covariantly from a set invariant form-factors.

Let us start from the well known equation of the interaction representation (Tomonaga):

$$(1) \qquad i\hbar \frac{\delta \Psi}{\delta \sigma} = H\Psi ,$$

where H indicates a local, invariant, hamiltonian density. H depends on free field operators. In the approximation here considered, we shall assume for these free fields the validity of the usual local equations of motion and of the usual quantum-commutation relations. In the case of the charge-symmetrical pseudoscalar interaction between meson and nucleon fields:

$$H = ig \sum \bar\psi \gamma^5 \tau^r \psi \phi^r .$$

Generally, H can be an invariant density:

$$H = \sum \Gamma_{\lambda_1 \ldots \lambda_n} \Phi_{\lambda_1}(x) \ldots \Phi_{\lambda_n}(x) ,$$

[1] Markov, Yukawa, McManus, Peierls, Rayski, C. Bloch. Kristensen, Möller. Pauli.
[2] I. Tamm: *Journ. of Phys. of Sov. Un.*, **9**, 449 (1945); Dancoff: *Phys. Rev.*, **78**, 382 (1950).

where Φ_{λ_k} are the components of different interacting fields, Γ_{λ_k} are operators depending on spin an charge coordinates λ_k, and x is the four-vector $(x_0 x_1 x_2 x_3)$. If, for example, Γ depends also on some of the differences $p' \quad p''$ of the momenta. H represents a non local interaction.

Introducing an invariant form factor $F(xx_1 \ldots x_n)$ depending on the differences between $n+1$ variables: $x_1 - x = \eta_1; \ldots, x_n - x = \eta_n$ one can define [3] a new hamiltonian density [4]:

$$(2) \quad H'(x) = \sum \Gamma_{\lambda_1 \ldots \lambda_n} \int \Phi_{\lambda_1}(x_1) \ldots \Phi_{\lambda_n}(x_n) F(xx_1 \ldots x_n) \, \mathrm{d}x_1 \ldots \mathrm{d}x_n =$$

$$= \sum \Gamma_{\lambda_1 \ldots \lambda_n} \int \Phi_{\lambda_1}(x + \eta_1) \ldots \Phi_{\lambda_n}(x + \eta_n) F(\eta_1 \ldots \eta_n) \, \mathrm{d}\eta_1 \ldots \mathrm{d}\eta_n .$$

Instead of chosing one universal F, we shall assume that $F(xx_1 \ldots x_n, \lambda_1 \ldots \lambda_n)$ depends also on other parameters. We shall need to decompose covariantly every field operator in positive and negative frequency parts, e.g.

$$\Phi^+_{\lambda_1}(x + \eta_1) = \frac{1}{(2\pi)^4} \int \mathrm{d}^4 p_1 \, a_{\lambda_1}(p_1) \, \delta(p_1^2 + m^2) \Phi^+_{\lambda_1}(p_1) \exp\left[ip_1(x + \eta_1) \right] .$$

Let $\mathcal{G}(p_k \lambda_k \varepsilon_k)$ be the Fourier transform of $F(\eta_k \lambda_k \varepsilon_k)$, which we introduce now in the integrands of (2). Then one has:

$$(3) \quad H'(x) \quad \sum \Gamma^{\varepsilon_1 \ldots \varepsilon_n}_{\lambda_1 \ldots \lambda_n} \int \mathrm{d}p_1 \ldots \mathrm{d}p_n \exp\, i(p_1 \quad \ldots \, p_n)x \, |\mathcal{G}(p_k, \lambda_k, \varepsilon_k) \Phi^\pm_{\lambda_1}(p_1) \ldots \Phi^\pm_{\lambda_n}(p_n).$$

where $\Gamma^{\varepsilon_1 \ldots \varepsilon_n}_{\lambda_1 \ldots \lambda_n}$ are new constant operators depending on the signs: $\varepsilon_k \quad$ of p_{k_μ} and on the annihilation or creation operators $a^{\varepsilon_k}_{\lambda_k}$ and:

$$(4) \qquad \mathcal{G}(p_k, \lambda_k, \varepsilon_k) = \int \exp\left[i(p_1\eta_1 + \ldots + p_n\eta_n) \right] F(\eta_k, \lambda_k, \varepsilon_k) \, \mathrm{d}\eta_1 \ldots \mathrm{d}\eta_n .$$

Instead of defining F, we can chose $\mathcal{G}$. And the operators $\mathcal{G}$ can depend explicitly not only on the invariants formed with p_k, but also on the parameters as spins, isotopic spins, and signs of the frequency of the interacting fields. If $\mathcal{G}$ is Lorentz invariant so is also F. Let us consider a term of (3), and, in chosing $\mathcal{G}$, assume the prescription suggested previously [3]: one introduces the total momentum $P_\mu \quad \sum_\sigma p'^{(\sigma)}_\mu$ of the ingoing particles and the four-velocity: $u_\mu = P_\mu / \sqrt{P_\mu P^\mu}$. then one can put:

$$(5) \qquad \mathcal{G} \quad \prod_{k=1}^{n} \bar{\mathcal{G}}(p_{k\mu} u^\mu, p_{k\mu} p_k^\mu .$$

[3] G. WATAGHIN: *Nuovo Cimento*. **8**, 592 (1951); **9**, 208 (1952).
[4] See also R. ASCOLI: *Nuovo Cimento* (to be publihed).

In the center' of mass system of ingoing particles the components u_μ are (1, 0, 0, 0) and $\bar{\mathcal{G}}$ can be chosen in a way that for $|\boldsymbol{p}_k| \to \infty$, it tends to 0 as $|\boldsymbol{p}_k|^{-4}$ and for $|\boldsymbol{p}_k| = 0$, $\bar{\mathcal{G}} = 1$. This last condition is necessary in order to obtain in the limit of slowly varying fields the usual local theory. Usually we shall have $p_\mu p^\mu = m^2$; in some cases $p^{(k)}$ can denote a difference between two momenta.

In some cases the vector u_μ in $\bar{\mathcal{G}}$ is the same for all elements of H' and $F(\eta_k \lambda_k \varepsilon_k)$ vanishes rapidly outside the domain D_{I}:

$$2(\eta_{k\mu} u^\mu)^2 - \eta_{k\mu} \eta_k^\mu \lesssim l^2 \qquad\qquad (k = 1, \ldots, n).$$

The chief difficulty of the proposed method consists in the condition (DIRAC. BLOCH, TOMONAGA) of commutability of $H'(x)$ and $H'(x')$ in a pair of points x and x' satisfying: $|\boldsymbol{x} - \boldsymbol{x}'| > |x_0 - x_0'|$. If the absolute value of the interval between these two events is greater than the linear dimension l of the interaction domain D_{I}, this condition is fulfilled.

We think that, although for a problem of initial values given in a pair of points sufficiently near to each other (e.g. given in the same domain D_{I}), the interaction representation is incompatible with the introduction of formfactors, an approximate description with form factors of the type specified above can be valid for certain classes of problems, e.g. for stationary collision problems threated with the non adiabatic method.

As shown recently by CINI [5] one can obtain covariantly from the equation (1) the Schrödinger stationary equation of the Tamm-Dancoff method. This method has a great advantage of permitting to solve the statistical equilibrium problem independently from the question of propagation and quantization of free fields. The conservation laws do hold exactly in the same way as in local theories.

From (3) one can see that every matrix-element of the hamiltonian operator in the Schrödinger representation is now modified by the introduction of $\bar{G}$ factors (5). The introduction of such invariant factors $\bar{\mathcal{G}}$ for each ingoing and outgoing particle in every matrix element of interaction matrix H', does not alter the hermitian character of H'. It is also compatible with the usual quantization of free fields as adopted in the T.D. formalism. Let us consider the collision of two particles in the center of mass system, which is supposed at rest in the stationary state considered in the Tamm-Dancoff method. Then the $\bar{G}$ factors appear in matrices corresponding to transitions between states for which the space component of the total momentum of ingoing (or outgoing) particles is $= 0$. They become in this case particularly simple and, in the case of high energy collisions, give rise to a spherical simmetrical distribution $\left[\bar{\mathcal{G}} = \bar{\mathcal{G}}(p_0, m^2)\right]$ of outgoing particles.

The following statistical interpretation of the « cut-off » factors $\bar{\mathcal{G}}$, suggested in earlier papers [6] seems plausible: the $\bar{\mathcal{G}}$ factors define the *statistical weight* of the states in the C-system of ingoing particles considered in the definition of $\bar{\mathcal{G}}$. This statistical weight of a non degenerated state is $= 1$, in the limit of low energies and is $= \bar{\mathcal{G}}(p_0, m^2)$ in the case: $|\boldsymbol{p}| \gg h/l$ where l is a universal constant.

[5] M. CINI: *A covariant formulation of the non adiabatic method*, in *Nuovo Cimento* (to be published).

[6] *Nature*. **142**, 393 (1938); *C. R.*. **207**, 358. 421 (1938).

If in a collision there is a competition between several possible results, the states with lower momenta and higher multiplicity or higher masses of created particles acquire greater probability.

The $\bar{\mathcal{G}}$ factors must satisfy the condition: if $\boldsymbol{p} = 0$,

$$(6) \qquad\qquad \bar{\mathcal{G}}(m, m^2) = 1 .$$

This condition can be considered as *an equation which determines the possible masses* of the elementary particles. The statistical factors $\bar{G}$ can depend on spin and charge variables. Therefore one can expect to have different mass equations of the type (6) for different spins and charges. Examples of such mass equations will be discussed in a forthcoming paper.

LIBRI RICEVUTI E RECENSIONI

M. Villa — *Repertorio di Matematiche*, Cedam, Padova, 1951.

È ovvio che un buon insegnante non deve conoscere solo le nozioni che espone ai suoi allievi, ma questi devono inquadrarsi in una visione ampia e profonda di tutta la materia del suo insegnamento. Così, ad esempio, la trattazione della geometria euclidea, specie nei suoi fondamenti, non può riuscire veramente efficace se l'insegnante non conosce, almeno nelle linee generali, le geometrie non euclidee.

Perciò molto utile ai professori di matematica delle Scuole Medie (e in particolare ai giovani laureati che intendono prepararsi ai concorsi) il presente volume. che, sorto per iniziativa del professor Villa, raccoglie articoli di numerosi matematici italiani opportunamente coordinati dallo stesso prof. Villa.

Alcuni articoli del libro in esame si riferiscono ad argomenti che nelle loro parti elementari rientrano nel programma delle nostre scuole medie. Così G. Ricci e P. Buzano espongono in modo completo la teoria dei numeri; F. Conforto mette in chiara evidenza i rapporti fra la geometria euclidea e le geometrie non euclidee; G. Campedelli ed R. Calapso trattano rispettivamente dei metodi sintetici per risolvere problemi di geometria e problemi risolubili con la riga e il compasso; U. Cassina espone criticamente la teoria dell'equivalenza e le nozioni di lunghezza, di area e di volumi; S. Cherubino considera l'applicazione dell'algebra alla geometria; A. Agostini ricorda gli elementi fondamentali della trigonometria piana.

Altri articoli richiamano quelle nozioni di matematica svolte d'ordinario nei corsi universitari (alcune anzi rientrano nel programma delle ultime classi del liceo scientifico) indispensabili alla cultura di un insegnante di matematica delle scuole medie. Così A. Amato, G. Cimmino e C. Rimini espongono rispettivamente l'analisi algebrica dei nostri bienni, la teoria dei limiti e degli algoritmi finiti, il calcolo differenziale e integrale. M. Villa richiama invece la geometria analitica e la teoria generale delle trasformazioni geometriche; L. Campedelli la teoria delle curve e superfici; P. Buzano e C. Rimini la teoria dei vettori e dei calcoli approssimati; G. Cimmino gli elementi della teoria delle funzioni analitiche; G. Zappa i gruppi e le loro applicazioni alle equazioni algebriche. Importante l'articolo di F. Sibirani sulla probabilità e sulla matematica finanziaria, argomenti che rientrano nei programmi di matematica degli Istituti tecnici ma che non sono svolti in nessun corso fondamentale per la laurea in Matematica o in Matematica e Fisica. Chiude il libro un articolo di A. Agostini sulla storia delle matematiche. Manca la trattazione delle equazioni differenziali perchè non figurano nei programmi d concorso a cattedre di matematica nelle scuole medie. Però gli estensori di quei programmi hanno dimenticato che il professore di matematica nelle scuole medie superiori insegna anche la fisica e che per una conoscenza che non sia del tutto superficiale di questa disciplina, è necessaria la conoscenza delle equazioni differenziali. Ma non è qui il luogo di insistere su questa ed altre assurdità dei programmi di concorso [1].

---

[1] Mi limito ad osservare che sarebbe ora di rifare il programma di fisica per i concorsi nelle scuole medie, programma veramente antidiluviano.

Comunque è doveroso dar lode al VILLA ed ai suoi collaboratori che hanno arricchito la matematica italiana di un nuovo importante trattato. Naturalmente è spontaneo domandarsi perchè non si fa altrettanto per la fisica, cioè perchè non si prepara un libro che permetta di approfondire la fisica in relazione al suo insegnamento elementare (²). È ben vero che la redazione di questo libro offre notevoli difficoltà sia per la maggior complessità della fisica, sia per il suo rapido sviluppo, sia per la mancanza di un lavoro critico analogo a quello che i matematici hanno fatto per le parti elementari della loro scienza; sono certo però che i fisici italiani, volendo, possono superare questi ostacoli. Ritengo che ne avrebbe vantaggio non soltanto l'insegnamento della fisica nelle scuole medie.

DARIO GRAFFI

(²) Alcuni anni fa, per iniziativa del compianto prof. GIOVANNI GENTILE jr. si cominciò a redigere un trattato di fisica del tipo accennato nel testo. Di questo trattato è uscito però solo il 1º volume e non si ha notizia se verrà o no completato.

A. DAUVILLIER — *La physique cosmique*. Bibliothéque de Philosophie scientifique, pag. 846. Flammarion, Parigi, 1951.

La fisica cosmica è una scienza nuova di coordinamento e di sintesi che costituisce, oggi, l'appassionato oggetto di studio di molti scienziati che sentono il problema di una sistemazione logica e coerente di tutte le acquisizioni teoriche e sperimentali in ogni campo dello scibile.

La fisica cosmica non è geofisica nè astrofisica, è invece una scienza generale di universale portata che unisce, inquadra e comprende non solo quelle discipline, ma anche la fisica propriamente detta, la chimica cosmica e la stessa biologia.

In questo volume, della collana di «Filosofia Scientifica», Edizione Flammarion, l'autore che ha buona esperienza di lavoro nel campo della fisica, della geofisica ed astrofisica, presenta in forma discorsiva il risultato di suoi personali pensamenti e valutazioni e si sforza di dare una sistemazione di portata cosmica a leggi, fatti e fenomeni propri della fisica, della cosmologia, della geologia e della biologia.

Così egli affronta il problema dell'origine del sistema solare e in particolare del nostro pianeta, e propone una nuova ipotesi cosmogonica basata sulla generazione di coppie di pianeti gemelli, che fornirebbe la spiegazione di molte particolarità del sistema solare.

Altri importanti argomenti, come l'origine del rilievo terrestre, l'orogenesi, la glaciazione quaternaria ed il meccanismo delle glaciazioni, vengono dall'autore discussi e trattati con personali deduzioni.

Vengono poi i tre capitoli concernenti il magnetismo dei corpi celesti, il geomagnetismo e quello su i raggi cosmici; in essi l'autore espone più o meno succintamente i fatti cercando di coordinarli e tentandone una interpretazione, per quanto espressamente ed onestamente dichiari che la frammentarietà e l'incompletezza delle nostre conoscenze non può in questo campo certamente condurre a soluzioni definitive.

In due successivi capitoli sulla «Genesi della vita» e sul «Problema della evoluzione» l'autore espone alcune sue considerazioni sulle cause geochimiche e cosmiche che fornirebbero una spiegazione della formazione dei continenti e dell'apparizione della vita sul pianeta. In particolare l'apparizione della vita sulla Terra sarebbe il risultato di una concomitanza straordinariamente fortuita di condizioni fisico-chimiche favorevoli, e il fattore determinante dell'evoluzione sarebbe poi lo psichismo.

Il libro finisce con un capitolo su «Il valore sociale della Scienza» che praticamente si ridurrebbe a fornire un passatempo alle persone più intelligenti ed a risolvere il problema dell'alimentazione della schiatta umana!

M. GIORGI

H. GARTMANN - *Raumfahrt-Forschung*, R. Oldenbourg Ver ag, München, 1952, in-8°, pp. 200, fig. 57.

L'ing. GARTMANN ha raccolto in questo volume una serie di saggi sul problema del volo interplanetario aventi per autori alcuni dei pionieri tedeschi di questo campo di ricerche: dal prof. HERMANN OBERTH, che si occupa questa volta delle « stazioni spaziali », a WILLY LEY, del quale sono noti anche in Italia gli scritti di carattere divulgativo sui razzi, e che qui racconta brevemente la storia delle fantasie, dei progetti e degli esperimenti relativi ale possibilità di evasione dalla Terra.

Dopo che lo stesso CLARKE, organizzatore delle attività della British Interplanetary Society, si è dedicato alla compilazione di romanzi del genere « science fiction » ora di moda, i dubbi sulla serietà di alcune tra queste speculazioni sono cresciuti notevolmente. Bisogna riconoscere, però, che i membri degli analoghi gruppi tedeschi, affiliati di quella Federazione Astronautica Internazionale cui è dedicato l'ultimo capitolo del presente volume, manifestano un grado di preparazione tecnica tale da far apparire bene sviluppata, almeno, l'impostazione teorica di questi problemi dal punto di vista della fisica.

Particolarmente interessanti, infatti, risultano le applicazioni analitiche della meccanica celeste, al problema della navigazione interplanetaria, presentate dal prof. WERNER SCHAUB, e lo studio della fase preliminare costituita da una « sonda » percorrente un'orbita intorno alla Terra, sviluppato dagli ingegneri ENGEL e HANISCH tenendo conto delle possibilità attuali di un razzo a sei stadi da 220 tonnellate.

Meno sicure, invece, le considerazioni del dott. DIRINGSHOFEN sul comportamento del corpo umano in assenza di gravità, questione su cui solo ora si è cominciato a raccogliere dati sperimentali mediante il lancio di scimmie in razzi per alta quota.

V. SOMENZI

K. E. ZIMEN - *Angewandte Radioaktivität*, VIII+124 seiten mit 45 Textabbildungen und einer Tafel, Springer, Berlin 1952.

Questo volumetto di radioattività « applicata » dovuto alla penna di uno specialista e presentato da O. HAHN, raccoglie in poco più che un centinaio di pagine ciò che è strettamente necessario conoscere per poter lavorare con isotopi radioattivi.

La prima parte, di 56 pagine, contiene in un agile e scarno riassunto i fondamenti scientifici dei metodi, descritti poi per mezzo di esempi nella seconda parte (28 pagine). Le ultime quaranta pagine sono dedicate a tabelle di dati d'uso corrente e ad una aggiornata e accurata bibliografia.

Un singolare pregio di questa operetta consiste nel non perdere mai di vista lo scopo, che è quello di costituire una utile fonte di informazioni per chi si serve della radioattività come strumento di lavoro senza preoccuparsi degli aspetti e delle questioni fondamentali ch'essa presenta. Di conseguenza, i resultati dell'indagine scientifica sono presentati in modo rapido e dogmatico, sempre dal punto di vista sperimentale, facendo posto alla formula empirica che risponde alle esigenze pratiche assai più che alla descrizione dell'esperienza concettuale che mette in luce una difficoltà di principio o all'impostazione teorica del calcolo esatto di una determinata grandezza.

Naturalmente, nessuno potrà pretendere di trovare qui tutti i dati che gli servono per la progettazione e l'esecuzione delle sue esperienze; ma il chimico, il biologo, il medico, il tecnico e sotto certi aspetti anche il fisico, vi troveranno una guida chiara, e generalmente del tutto attendibile, per risolvere dubbi, chiarire possibilità e limiti dei vari metodi, progettare esperienze e misure in modo sensato.

Non manca tuttavia, qua e là, qualche frase che lascia perplessi, come alla pagina 16 dove si afferma che *la causa*

(Ursache) di una disintegrazione radio-
attiva è costituita dal fatto che l'energia
totale della particella emessa e del nucleo
residuo è minore dell'energia del nucleo
di partenza. E neppure manca qualche
errore, come alla pag. 28, ove dalla
fig. 14-3 si ricava che la velocità di una
particella α nell'aria resta costante fino
a un paio di centimetri dalla fine del
percorso; o alla pag. 53, ove a proposito
della reazione $C^{12}(\alpha, p)N^{15}$, endotermica
per 5 MeV, si afferma che per ottenerla
sono necessarie particelle α di almeno
5 MeV, senza tener conto che la soglia è
più elevata, dovendosi nel processo con-
servare la quantità di moto totale.

A parte questo, il libro indubbia-
mente è assai utile e consigliabile a chiun-
que si appresti a lavorare con radio-
isotopi.

M. AGENO

R. ROTHE – *Höhere Mathematik*
Teubner, Leipzig 1952; 4 voll. per
circa pagg. 1000 complessive;
in-16°.

La nuova edizione, fatta a cura di
W. SCHMEIDLER, di quest'opera già ben
nota, che trae origine dai corsi propedeu-
tici tenuti dal Prof. ROTHE alla Technische
Hochschule di Berlino, differisce dalla
precedente del 1949 per alcuni migliora-
menti e poche aggiunte, restando inalte-
rata nella sostanza.

Sull'Opera stessa — senz'altro consi-
gliabile come utile e pratico testo di con-
sultazione per ingegneri e per chiunque
applichi le scienze matematiche — ci limi-
tiamo perciò a riportare, oltre all'indica-
zione degli argomenti trattati e ad una
breve osservazione critica, le seguenti pa-
role della prefazione che chiaramente illu-
strano pregi e limiti del lavoro: ,

«... si è data molta importanza alle
relazioni tra la matematica pura e le sue
applicazioni e ai vari metodi della mate-
matica applicata, senza però trascurare le

cose più importanti della matematica
pura stessa ».

« Cresciuta dagli appunti per studenti
del Prof. ROTHE, l'Opera costituisce una
guida molto breve, con disposizione libera
della materia e con molti esempi, appli-
cazioni, esercizi. La brevità dello svolgi-
mento non facilita lo studio, anzi richiede
una collaborazione viva e coraggiosa che
certamente non può essere effettuata da
tutti senza sospiri e sudore. Ciò vale
soprattutto per gli esercizi, per i quali
sono dati solo una guida molto breve e i
risultati ».

Nonostante questo indirizzo essenzial-
mente pratico dell'Opera — o forse pro-
prio per questo — sarebbe talora deside-
rabile maggior rigore critico.

Per esempio, proprio in un'aggiunta
di questa edizione (vol. I, pag. 88), al
n. 11 del § 13, intitolato « Integrations-
grenzen bei neuen Veränderlichen», si dice:
« Sei $x = \varphi(t)$ und umgekehrt $t = \psi(x)$,
so wird die untere Grenze... $t_1 = \psi(x_1) =
= \psi(a)$, entsprechend die obere $t_2 =
= \psi(x_2) = \psi(b)$; also, ganz allgemein

$$F = \int_a^b f(x)\,dx =$$
$$= \int_{x_1}^{x_2} f(x)\,dx \; = \int_{t_1 = \varphi(a)}^{t_2 = \varphi(b)} f[\varphi(t)]\varphi'(t)\,dt \,. \;»$$

Ora, se si bada alla definizione di fun-
zione inversa data a pag. 15 (¹), ed al
fatto che per la sua esistenza non si pon-
gono condizioni, si ottengono sofismi di
tipo ormai classico, come il seguente:

$$\int_{-1}^{1} \frac{dx}{1 + x^2} = \frac{\pi}{2} \; ;$$

(¹) « Wenn in $y = f(x)$, x mit y vertauscht
wird, $x = f(y)$, so bildet die Gesamtheit der
Werte, die dadurch jedem Werte von x eines
Berciches zugeordnet werden können, die
Umkehrungsfunktion $y = g(x)$ ».

ponendo: $x = 1/t$:

$$\frac{\pi}{2} = -\int_{-1}^{1} \frac{dt}{1 + t^2} = -\frac{\pi}{2}.$$

È bensì vero che prima, a pag, 45, è dato il problema:

« Ist $y = f(x)$ für $a \leqslant x \leqslant b$ eindeutig, stetig und beständig zunehmend (oder beständig abnehmend), ohne streckenweise konstant zu sein, so hat die aus $x = f(y)$ sich ergebende Umkehrungsfunktion $y = g(x)$ in dem entsprechenden Bereiche dieselben Eigenschaften ».

Però tale teorema non serve se non si avverte che in seguito si considereranno funzioni inverse solo in tali ipotesi.

La materia contenuta nei primi tre volumi è — grosso modo, e astrazion fatta dal molto diverso rapporto tra teoria e pratica — quella che generalmente viene svolta nei due corsi d'Analisi Matematica delle nostre Facoltà di Scienze; ove però si aggiungano numerose applicazioni alla geometria, alla meccanica e in generale alla fisica.

Il quarto volume, costituito da tre quaderni staccati, è una varia e ricca raccolta d'esercizi.

Non ci risulta che sia stata ristampata la *Formelnsammlung zur höheren Mathematik* dello stesso Autore, che costituisce un utile complemento dell'Opera.

D. FÜRST